ESCUELA DE DOCTORADO
INTERNACIONAL DE LA USC

Wenceslao
Piedra Cascón

Tesis doctoral

Análisis de la precisión del flujo de trabajo digital en Odontología

Santiago de Compostela, 2025

PROGRAMA DE DOCTORADO EN CIENCIAS ODONTOLÓGICAS

TESIS DOCTORAL

Análisis de la precisión del flujo de trabajo digital en Odontología

Wenceslao Piedra Cascón

Directores:
Mercedes Gallas Torreira

Tutor:
Mercedes Gallas Torreria

PROGRAMA DE DOCTORADO EN CIENCIAS ODONTOLÓGICAS

SANTIAGO DE COMPOSTELA
2025

DECLARACIÓN DE CONFLICTO DE INTERESES Y FINANCIACIÓN

El doctorando Wenceslao Piedra Cascón, declara no tener ningún conflicto de interés en relación con la tesis doctoral titulada “Análisis de la precisión del flujo de trabajo digital en odontología”.

En Santiago de Compostela, a 1 de septiembre de 2025.

Fdo. Wenceslao Piedra Cascón

DEDICATORIA

A mi familia y amigos, por ser mi sostén constante, por acompañarme en los momentos difíciles y celebrar conmigo cada pequeño logro. Sin vuestro cariño, paciencia y apoyo incondicional, este camino habría sido imposible.

A mis directores de tesis, la profesora Mercedes Gallas y el profesor José Manuel Pose, por vuestra guía, confianza y exigencia, que me han permitido crecer tanto académica como personalmente.

A todos los co-autores de los artículos que conforman esta tesis, gracias por compartir vuestra experiencia y conocimiento, por la colaboración generosa y el compromiso científico que han hecho posible este trabajo.

Al profesor Carlos Oteo Calatayud por confiar en mí y a todos los profesores que me han formado a lo largo de estos años, por transmitirme no solo conocimientos, sino también valores y pasión por la Odontología y la investigación.

A todos vosotros, gracias por contribuir a que hoy sea quien soy, como profesional y como persona.

RESUMEN

Introducción: El flujo de trabajo digital aplicado en odontología ha permitido aumentar la predictibilidad de los tratamientos gracias a la integración de los diferentes archivos digitales que pueden obtenerse a través de herramientas digitales y que permiten digitalizar tridimensionalmente a un paciente. Para obtener una representación virtual del paciente siempre son necesarias tres fases: digitalización, diseño y fabricación. Durante la fase de digitalización se obtendrán registros de los tejidos del paciente mediante el uso de escáneres y tomografías computerizadas (TC/CBCT). Los diferentes archivos digitales se han de integrar mediante softwares CAD 3D para llevar a cabo el diseño de los dispositivos y/o restauraciones necesarias para ejecutar el tratamiento y finalmente materializarse mediante tecnologías de fabricación 3D, ya sean sustractivas o aditivas. A pesar de los avances en los últimos años en este campo de la odontología, aún no existe un flujo de trabajo digital completo y estandarizado, siendo por tanto un área de interés para la investigación en odontología. El presente trabajo analiza la precisión global del flujo de trabajo digital completo, desde el escaneado a la impresión 3D, determinando el carácter multifactorial de los factores que afectan a la precisión en el flujo de trabajo digital aplicado a odontología.

Material y métodos: Realizamos cuatro estudios experimentales *in vitro*. El primer estudio analizó la precisión de un escáner intraoral (PrimeScan; Dentsply Sirona) bajo 10 condiciones de iluminación ambiental diferentes. El segundo estudio, analizó el efecto de 12 algoritmos de alineación diferentes y el tiempo necesario para ejecutarlos en 6 *softwares* CAD 3D utilizando los archivos del grupo que obtuvo los mejores resultados de precisión en el primer estudio. El tercer y cuarto estudio determinaron la precisión en impresión 3D. Para ello se utilizaron dos impresoras 3D (NextDent 5100; 3D Systems y Sonic Mini 4K; Phrozen) y dos resinas de impresión (NextDent Model 2.0; NextDent y Aqua Gray 4K; Phrozen). El objetivo de los dos últimos estudios fue valorar la relación existente entre la tecnología de impresión 3D, la resina utilizada y el diseño del objeto 3D a imprimir, determinando, por tanto, la precisión en términos de exactitud y fiabilidad de los sistemas de impresión 3D.

Resultados: En el primer estudio, se analizó la precisión de un escáner intraoral (PrimeScan; Dentsply Sirona) bajo 12 condiciones de luz diferentes: 0, 500, 1.000, 2.000, 3.000, 4.000, 5.000, 6.000, 7.000, 8.000, 9.000, 10.000 luxes.

Se evidenció que existían diferencias estadísticamente significativas entre los diferentes grupos, así como una relación entre la luz ambiental del gabinete y la precisión obtenida por el escáner intraoral, concluyendo que la luz ambiental óptima para dicho escáner intraoral era de 1000 lx.

En la segunda investigación, se estudió el impacto en la precisión y el tiempo necesario para llevar a cabo 12 algoritmos de alineación diferentes que están incluidos en 6 *softwares* de diseño CAD 3D usados de forma rutinaria en odontología (Meshmixer; Autodesk, B4D; The Blender Foundation, Dental CAD App; Exocad, Medit Design; Medit Corp y NemoSmile; Nemotec). Los resultados del estudio demostraron que existe un impacto en la precisión de la alineación de mallas 3D en función del *software* seleccionado. Además, los mejores resultados se encontraron cuando se emplearon algoritmos de *best-fit* (BF), en comparación con algoritmos de alineación por superficies (SBF) o alineación por puntos (LBF). Por tanto, el algoritmo de alineación seleccionado tiene impacto tanto en la precisión como en el tiempo necesario para ser ejectuado, siendo el algoritmo de *best-fit* (BF) del *software* Medit Design el que obtuvo los mejores resultados.

En el tercer estudio, se analizó la precisión de dos tecnologías de impresión 3D diferentes (SLA-DLP vs SLA-LCD) utilizando una misma resina (NextDent Model 2.0; NextDent) para la fabricación de modelos de trabajo en odontología con diferentes diseños de zócalos y espesores de pared. Los resultados del estudio evidenciaron que a pesar de que ambas tecnologías de impresión 3D eran compatibles con la longitud de onda de la resina (405 nm), hubo diferencias estadísticamente significativas entre ambas tecnologías de impresión 3D, así como en el tipo de zócalo utilizado, encontrando que para la tecnología DLP el diseño de zócalo ideal para la resina utilizada era el diseño en panal de abejas con grosor de pared de 1 mm, mientras que para la tecnología LCD el diseño ideal era el zócalo ahuecado con espesor de pared 2 mm.

El cuarto estudio, estudió el impacto en la precisión obtenida en la fabricación de modelos dentales mediante una impresora 3D de tecnología SLA-LCD (Sonic Mini 4K, Phrozen) utilizando dos resinas diferentes (Aqua Grey 4K; Phrozen y NextDent Model 2.0). Los resultados del estudio demostraron que el tipo de resina utilizada tiene impacto sobre la precisión final de los modelos obtenidos, obteniendo el mejor resultado con la resina Aqua Gray 4K (Phrozen) y un diseño de zócalo ahuecado con un espesor de pared de 2 mm.

Conclusiones: La precisión global del flujo de trabajo digital depende de la precisión obtenida de forma individualizada en cada una de las tres fases del flujo digital: digitalización, diseño y fabricación. Durante la fase de digitalización con escáneres intraorales, se hace imprescindible analizar los luxes del gabinete dental para adaptarlos a la tecnología de escaneado utilizado, encontrando un rango óptimo en torno a los 1000 luxes para el sistema PrimeScan (Dentsply-Sirona). Durante la fase de diseño CAD siempre se hace imprescindible alinear mallas 3D entre sí, siendo necesario seleccionar aquellos *softwares* que integren algoritmos de alineación tipo *best-fit* (BF). Finalmente, la fabricación de modelos mediante impresión 3D está influenciada por el trinomio compuesto por el tipo de tecnología de impresión 3D, la resina 3D y el diseño del objeto 3D a imprimir. Los modelos fabricados mediante tecnologías SLA-LCD y SLA-DLP pueden obtener los mismos niveles de precisión si se utiliza la resina 3D adecuada a la longitud de onda de cada una de las tecnologías de impresión 3D, no existiendo, por tanto, una tecnología

superior a otra en términos de exactitud y fiabilidad.

RESUMO

Introdución: O fluxo de traballo dixital aplicado en odontoloxía permitiu aumentar a previsibilidade dos tratamentos grazas á integración dos diferentes arquivos dixitais que se poden obter a través de ferramentas dixitais e que permiten dixitalizar un paciente de forma tridimensional. Para obter unha representación virtual do paciente sempre son necesarias tres fases: dixitalización, deseño e fabricación. Durante a fase de dixitalización, obteranse rexistros dos tecidos do paciente mediante o uso de escáneres e tomografía computarizada (TC/CBCT). Os diferentes arquivos dixitais deberán integrarse mediante *software* CAD 3D para realizar o deseño dos aparellos e/ou restauracións necesarias para realizar o tratamento e que deberán materializarse mediante tecnoloxías de fabricación 3D, xa sexan substractivas ou aditivas. A pesar dos avances dos últimos anos neste campo da odontoloxía, aínda non existe un fluxo de traballo dixital completo e estandarizado, polo que é un ámbito de interese para a súa investigación en odontoloxía. O presente traballo analiza a precisión global do fluxo de traballo dixital completo, desde a dixitalización ata a impresión 3D, demostrando a natureza multifactorial dos factores que afectan á precisión no fluxo de traballo dixital aplicado á odontoloxía.

Material e métodos: Realizamos catro estudos experimentais in vitro. O primeiro estudo analizou a precisión dun escáner intraoral (PrimeScan; Dentsply Sirona) en 10 condicións de iluminación ambiental diferentes. O segundo estudo estudou o efecto de 12 algoritmos de aliñamento diferentes e o tempo necesario para executalos en 6 *softwares* CAD 3D utilizando os ficheiros do grupo que obtivo datos de mellor precisión no primeiro estudo. O terceiro e cuarto estudo abordarán a precisión na impresión 3D. Para iso utilizáronse dúas impresoras diferentes (NextDent 5100; 3D Systems e Sonic Mini 4K; Phrozen) e dúas resinas de impresión (NextDent Model 2.0; NextDent e Aqua Gray 4K; Phrozen). O obxectivo destes dous estudos foi valorar a relación existente entre a tecnoloxía de impresión 3D, a resina empregada e o deseño do obxecto 3D a imprimir, determinando polo tanto, a precisión en termos de exactitude e fiabilidade dos sistemas de impresión 3D.

Resultados: No primeiro estudo, a precisión do escáner intraoral (PrimeScan; Dentsply Sirona) analizouse en 12 condicións de luz diferentes: 0, 500, 1.000, 2.000, 3.000, 4.000, 5.000, 6.000, 7.000, 8.000, 9.000, 10.000 luxes.

Evidenciouse a existencia de diferenzas estatisticamente significativas entre os distintos grupos, así como unha relación entre a luz ambiental do consultorio e a precisión obtida polo escáner intraoral, concluíndo que a luz ambiental óptima para o escáner intraoral analizado era de 1003 lux.

Na segunda investigación, estudouse o impacto sobre a precisión e o tempo necesario para levar a cabo 12 algoritmos de aliñamento diferentes incluidos en 6 programas de deseño CAD 3D utilizados habitualmente en odontoloxía (Meshmixer, Blender, Exocad, Medit Design e Nemotec). Os resultados do estudo demostraron que existe un impacto na precisión do aliñamento das mallas 3D en función do *software* utilizado. Atopándose os mellores resultados a o empregar o *software best-fit* (BF) en comparación con algoritmos de aliñamento por superficies (SBF) ou aliñamento por puntos (LBF). Polo tanto, o algoritmo

de aliñamento empregado ten impacto tanto na precisión como no tempo necesario para ser executado, sendo o algoritmo *best-fit* (BF) do software Medit Design o que obtivo os mellores resultados.

No terceiro estudo, analizouse a precisión de dúas tecnoloxías de impresión 3D diferentes (SLA-DLP vs SLA-LCD) utilizando a mesma resina para a fabricación de modelos dentais/odontolóxicos con diferentes deseños de zócalos e grosores de parede. Os resultados do estudo evidenciaron que, aínda que ambas tecnoloxías de impresión 3D eran compatibles coa lonxitude de onda da resina, existían diferenzas estatisticamente significativas entre ambas tecnoloxías de impresión 3D, así como no tipo de zócalo empregado, descubrindo que para a tecnoloxía DLP o deseño de zócalo ideal para a resina utilizada foi o deseño de panal de abellas cun espesor de parede de 1 mm, mentres que para a tecnoloxía SLA-LCD o deseño ideal foi o zócalo oco cun espesor de parede de 2 mm.

O cuarto estudo estudou o impacto na precisión obtida na fabricación de modelos dentais/odontolóxicos mediante unha impresora 3D de tecnoloxía SLA-LCD utilizando dúas resinas diferentes. Os resultados do estudo mostraron que o tipo de resina empregada incidiu na precisión final dos modelos obtidos, obtendo o mellor resultado coa resina Aqua Gray 4K (Phrozen) e un deseño de zócalo oco cun espesor de parede de 2 mm.

Conclusións: A precisión global do fluxo de traballo dixital depende da precisión obtida individualmente en cada unha das tres fases do fluxo dixital: dixitalización, deseño e fabricación. Durante a fase de dixitalización con escáneres intraorais, é fundamental analizar os luxes da consulta dental para adaptalos á tecnoloxía de escaneado empregada, atopando un rango óptimo arredor dos 1003 luxos para o sistema PrimeScan (Dentsply-Sirona). Durante a fase de deseño CAD, é esencial aliñar as mallas 3D entre si, polo que é necesario seleccionar un *software* que integre algoritmos de aliñamento de tipo *best-fit* (BF). Finalmente, na fabricación de modelos por impresión 3D inflúe o trinomio composto polo tipo de tecnoloxía de impresión 3D, a resina 3D e o deseño do obxecto 3D a imprimir. Os modelos fabricados mediante tecnoloxías SLA-LCD e SLA-DLP poden obter os mesmos niveis de precisión se se utiliza a resina 3D adecuada para a lonxitude de onda de cada unha das tecnoloxías, polo tanto, non existe unha tecnoloxía superior a outra en termos de exactitude e fiabilidade.

ABSTRACT

Introduction: The digital workflow applied in dentistry has made it possible to increase the predictability of treatments thanks to the integration of the different digital files that can be obtained through digital tools, which makes it possible to digitize a patient three-dimensionally. To obtain a virtual representation of the patient, three phases are always necessary: digitization, design, and fabrication. During the digitization phase, records of the patient's tissues will be obtained through the use of scanners and computed tomography (CT/CBCT). The different digital files have to be integrated by 3D CAD software to carry out the design of the devices and/or restorations necessary to carry out the treatment, which must be materialized by 3D fabrication technologies, whether subtractive or additive. Despite the advances in recent years in this field of dentistry, a complete and standardized digital workflow does not yet exist and is, therefore, an area of interest for research in dentistry. This paper analyzes the overall accuracy of the complete digital workflow, from scanning to 3D printing, demonstrating the multifactorial nature of the factors affecting accuracy in the digital workflow applied to dentistry.

Materials and Methods: We conducted four experimental in vitro studies. The first study analyzed the accuracy of an intraoral scanner (PrimeScan; Dentsply Sirona) under ten different ambient lighting conditions. The second study studied the effect of 12 different alignment algorithms and the time required to run them in 6 different 3D CAD software using the files of the group that obtained the best accuracy data in the first study. The third and fourth studies dealt with 3D printing accuracy. Two different printers (NextDent 5100; 3D Systems and Sonic Mini 4K; Phrozen) and two different resins (NextDent Model 2.0; NextDent and Aqua Gray 4K; Phrozen) were used. In order to effectively assess the accuracy of each of the studies, the results were analyzed in terms of the accuracy and reliability obtained for each system.

Results: In the first study, the accuracy of the intraoral scanner (PrimeScan; Dentsply Sirona) was analyzed under 12 different light conditions: 0, 500, 1,000, 2,000, 3,000, 4,000, 5,000, 6,000, 7,000, 8,000, 9,000, 10,000 lux.

It was found that there were statistically significant differences between the different groups, as well as a relationship between the ambient light of the cabinet and the precision obtained by the intraoral scanner, concluding that the optimum ambient light for the intraoral scanner was 1003 lux.

In the second investigation, the impact on the accuracy and time required to perform 12 different alignment algorithms that are included in 6 3D CAD design software routinely used in dentistry (Meshmixer, Blender, Exocad, Medit Design, and Nemotec) was studied. The results of the study showed that the software used only has an impact on the accuracy of the alignment obtained, whereas if the algorithms are analyzed independently, they have an impact on both the accuracy and the time required to execute them, with the best-fit (BF) algorithms obtaining the best results.

In the third study, the accuracy of two different 3D printing technologies (SLA-DLP vs SLA-LCD) was analyzed using the same resin for the fabrication of dental models with different socket designs and wall thicknesses. The results of the study evidenced that although both 3D printing technologies were compatible with the wavelength of the resin, there were statistically significant differences between both 3D printing technologies, as well

as in the type of socket used, finding that forSLA- DLP technology, the ideal socket design for the resin used was the honeycomb design with wall thickness of 1 mm, while for LCD technology the ideal design was the hollowed socket with wall thickness 2 mm.

The fourth study studied the impact on the accuracy obtained in the fabrication of dental models by an SLA-LCD 3D printer using two different resins. The results of the study showed that the type of resin used had an impact on the final accuracy of the models obtained, obtaining the best result with the Aqua Gray 4K resin (Phrozen) and a hollow socket design with a wall thickness of 2 mm.

Conclusions: The overall accuracy of the digital workflow depends on the accuracy obtained individually in each of its phases. During the digitization phase with intraoral scanners, it is essential to analyze the fluxes of the dental office to adapt them to the scanning technology used, finding an optimum range of around 1003 luxes for the PrimeScan system (Dentsply-Sirona). During the CAD design phase, it is essential to align 3D meshes with each other, and it is necessary to select software that integrates best-fit (BF) alignment algorithms. Finally, the fabrication of models by printing is influenced by the combination of the type of 3D printing technology and the 3D resin. Casts manufactured by SLA-LCD and SLA-DLP technologies can obtain the same levels of accuracy if the appropriate 3D resin is used for each of the technologies, so there is no one technology superior to the other in terms of accuracy and reliability.

ABREVIATURAS

CAD	*(Computer aided-design*)
CAM	(*Computer aided-manufacturing*)
3D	(3 dimensiones)
BF	(*Best-Fit*)
LBF	(*Landmark Best-Fit* ó Alineación por puntos)
SBF	(*Section Best-Fit* ó Alineación por áreas/superficies)
LCD	(*Liquid Crystal Display*)
DLP	(*Direct Light Processing*)
SLA	(Estereolitografía)
LX	(Luxes)
CT	(*Computerized Tomography* ó Tomgrafía Computerizada)
CBCT	(Tomografía de Haz Cónico)
PDI	(Puntos de Interés)
ISO	(*International Organization for Standardization*)
NM	(Nanómetro)
UV	(Ultravioleta)
CMM	(*Coordinated Measured Machine* ó Máquina de coordenadas)

ÍNDICE

Tabla de contenido

1 ..... *13*

INTRODUCCIÓN **13**

1 INTRODUCCIÓN 14

2 ..... *25*

HIPÓTESIS y OBJETIVOS **25**

2 HIPÓTESIS y OBJETIVOS GENERALES y ESPECÍFICOS 26

3 ..... *27*

HERRAMIENTAS METODOLÓGICAS **27**

3 HERRAMIENTAS METODOLÓGICAS 28

4 ..... *35*

RESULTADOS: **35**

TRABAJOS PUBLICADOS **35**

4 RESULTADOS 36

TRABAJOS PUBLICADOS 36

5 ..... *75*

DISCUSIÓN **75**

5 DISCUSIÓN 76

6 ..... *85*

CONCLUSIONES **85**

6 CONCLUSIONES 86

7 ..... *87*

REFERENCIAS **87**

BIBLIOGRÁFICAS **87**

7 REFERENCIAS 88

8 ..... *108*

ANEXOS **108**

1
INTRODUCCIÓN

1 INTRODUCCIÓN

El flujo de trabajo digital, conocido como CAD-CAM por sus siglas en inglés (*computer-aided design* y *computer-aided manufacturing*), ha supuesto una revolución en la odontología debido a que ha permitido mejorar la eficiencia y predictibilidad de los tratamientos dentales/odontológicos, gracias a la posible implementación de registros intraorales y faciales del paciente, pudiendo llevar a cabo tratamientos planificados y guiados facialmente (1-8). Este aumento de la predictibilidad se debe a la utilización de una serie de herramientas digitales diseñadas y programadas cada una para un fin en específico (Tabla 1).

El flujo de trabajo digital consta de tres fases: digitalización, diseño y fabricación (9-14).

La fase de digitalización tiene como objetivo obtener un conjunto de datos del paciente que provienen de diferentes dispositivos de escaneado, tanto de tejidos duros como blandos, bien escáneres faciales (15-21), escáneres intraorales (22-33), tomografías computerizadas (34-35) y/o sistemas de la dinámica mandibular (36-42). Dependiendo del dispositivo o *hardware* utilizado, se pueden obtener archivos en formato *Joint Photographic Experts Group* (JPEG), *Digital Imaging and Communications in Medicine* (DICOM), *Standard Tesselation Language* (STL), *Tesselation with Polygonal Faces* (OBJ) y *Stanford Triangle Format* (PLY) (43). Cada uno de estos archivos tiene una naturaleza diferente, que además han de ser integrados y alineados entre sí para obtener una representación virtual del paciente, conocido como paciente virtual o paciente en 3-dimensiones (3D) (44).

La segunda fase, la fase de diseño 3D mediante el uso de *softwares* CAD (45-50). En esta fase se trabaja con los diferentes conjuntos de datos generados por los escáneres intraorales.o escáneres de laboratorio. La fase de diseño CAD comprende tanto la alineación de archivos para obtener el paciente virtual, como el diseño de los dispositivos y/o restauraciones/rehabilitaciones necesarias para llevar a cabo el tratamiento dental/odontológico propuesto, como pueden ser encerados diagnósticos, guías quirúrgicas, férulas de descarga o restauraciones protéticas (Fig.1A-D) (44).

Dependiendo del tipo de fabricación de los objetos 3D diseñados, se deberán importar en un *software* determinado ya sean para ser fabricados mediante tecnologías sustractivas, comúnmente conocido como fresado, o bien si se van a fabricar con tecnología aditiva, los objetos se deberán importar en un *software* conocido como *slicer* (50). Si se va a fabricar el objeto con tecnología sustractiva será necesario determinar la estrategia de fresado. Las tecnologías sustractivas, consisten en la obtención de un objeto físico mediante el fresado de un bloque sólido de un material específico, pudiendo ser éste un polímero, una cera, un metal o una cerámica. Por otra parte, la fabricación de los objetos mediante impresión 3D, será necesario determinar en el *slicer* la posición y orientación del objeto 3D a imprimir, la cantidad y morfología de soportes necesarios y los *parámetros* de impresión 3D, entre otros: altura de capa, tiempo exposición de la resina, velocidad de subida de la plataforma, velocidad de bajada de la plataforma y tiempo de descanso entre capa y capa (50).

En esta tesis se han analizado etapas específicas de cada una de las etapas del flujo de

trabajo digital. Para ello, nos hemos planteado una serie de preguntas que se detallan a continuación:

A) Escaneado intraoral: ¿La luz ambiental del gabinete clínico afecta a la precisión, en términos de exactitud y fiabilidad, de los escáneres intraorales? En caso afirmativo, ¿existe una condición de luz ambiental óptima?

B) *Softwares* CAD 3D: ¿Existen diferencias en términos de precisión a la hora de realizar alineaciones de mallas 3D? ¿Existe un protocolo de alineación ideal o es necesario individualizar los procedimientos de alineación en función del *software* CAD utilizado?

C) Impresión 3D: ¿Existen diferencias en términos de precisión entre una impresora 3D de tecnología DLP y LCD? En caso afirmativo, ¿existen diferencias en función de la resina 3D utilizada y la geometría del objeto a imprimir?

Para dar respuesta a estas preguntas de investigación, diseñamos 4 estudios científicos con objeto de abordar las tres fases del flujo digital. Así, para la fase de digitalización se analizó el impacto en la precisión de la luz ambiental del gabinete odontológico bajo 12 condiciones de luz ambientales direferntes usando el escáner intraoral PrimeScan®, Dentsply-Sirona (Artículo 1). Para la fase de diseño CAD se analizó la precisión de los procedimientos de alineación utilizando 6 *softwares* CAD 3D y 12 algoritmos de alineación (Artículo 2). Finalmente, para la fase de fabricación se estudió el impacto que tiene sobre los procedimientos de impresión 3D, la interrelación entre la tecnología de impresión 3D, la resina utilizada y el diseño del zócalo de modelo empleando el *software* B4D (Blender for Dental; The Blender Foundation) (Articulos 3 y 4).

1. Digitalización: Escáneres intraorales

El escáner intraoral es la piedra angular del flujo de trabajo digital, constituye la forma más sencilla de digitalizar/registrar en forma digital la situación intraoral del paciente de forma/manera directa. El primer sistema de escaneado se introdujo en odontología en el año 1973 por el Prof. Dr. Duret (Francia) (51,52), considerado el padre de la odontología digital. En 1971 presentó su tesis doctoral titulada *"Empreinte Optique"* ("Impresión óptica"), donde describía por primera vez la posibilidad de obtener registros digitales intraorales mediante un escáner óptico. Sin embargo, no fue hasta la década de los años 80 cuando Dentsply-Sirona introduce el sistema CEREC (del acrónimo en inglés *Chairside Economical Restoration of Esthetic Ceramics*) de la mano del Dr. Werner Mörmann y el ingeniero Marco Brandestini en 1985 (Suiza) (53). La principal innovación del sistema CEREC se basaba en el concepto *chairside* u odontología en el mismo día, en el que se realizaba la preparación dentaria, se realizaba el escaneado intraoral y el diseño y fabricación se realizaba directamente en clínica en una única visita, sin necesidad de provisionalización o de mandar el trabajo al laboratorio dental.

Los escáneres intraorales se basan en tecnologías de no-contacto, es decir, no necesitan estar en contacto con la superficie a escanear. Las tecnologías de escaneado intraoral se fundamentan en principios de interforometría y desplazamiento de fases, microscopía confocal, estereovisión pasiva y activa basada en triangulación y tomografía de coherencia óptica (54-57). Todos los escáneres intraorales del mercado emplean más de uno de los principios anteriormente mencionados pudiendo encontrar por tanto las siguientes tecnologías: *active wavefront*

sampling (muestreo activo de frente de onda), triangulación, confocal *parallel imaging (imagen paralela confocal)*, y estereofotogametría descritas brevemente a continuación:

- *Active Wavefront Sampling:* Técnica de adquisición de imágenes que se basa en el uso combinado de una cámara y un módulo de apertura desalineado respecto al eje óptico principal. Este módulo realiza un movimiento circular alrededor del eje óptico, provocando una rotación controlada del punto de interés (POI). A partir del análisis del patrón generado por cada punto durante el movimiento, es posible extraer y calcular información tridimensional relacionada con la distancia y la profundidad del objeto escaneado (56-57).

- Triangulación: se basa en el principio geométrico según el cual la posición del objeto a escanear se puede determinar conociendo la localización del mismo y los ángulos de observación desde dos puntos diferentes. Esta visión puede obtenerse de diferentes formas: 1) mediante dos sensores independientes, 2) mediante un único sensor asistido por un prisma, o bien, 3) registrando la escena desde diferentes posiciones en momentos sucesivos (56-57).

- Microscopía Confocal Paralela: tecnología patentada por Marvin Minsky en 1961, basada en la adquisición de imágenes enfocadas a distintas profundidades. (57,58) Esta tecnología permite identificar las zonas con mayor nitidez en la imagen para inferir la distancia al objeto, la cual se encuentra relacionada con la distancia focal del objetivo (57). La geometría tridimensional de la superficie escaneada puede reconstruirse mediante la combinación de imágenes capturadas sucesivamente con diferentes valores de enfoque, apertura y ángulos de observación alrededor del objeto (57).

- Estereofotogametría: permite estimar las coordenadas tridimensionales en los ejes -x, -y, -z a través del análisis algorítmico de imágenes, sin necesidad de proyectar luz activa sobre el objeto 3D a escanear. Esta tecnología se fundamenta en la captura pasiva de la luz reflejada por el objeto y en el procesamiento mediante un *software* especializado para reconstruir la geometría 3D (57).

1.1. Reconstrucción tridimensional de mallas 3D

Resumiendo, cada una de estas tecnologías obtiene imágenes de la situación intraoral de paciente, ya sea mediante fotografías o video. Los algoritmos implementados en los escáneres intraorales son capaces de reconocer PDI (puntos de interés) coincidentes entre diferentes imágenes. Estos puntos de interés son fácilmente identificables donde existen curvaturas pronunciadas, como pueden ser vertientes y fosas de sectores posteriores o bien límites físicos o diferencias de tonalidad en escala de grises en las imágenes. Una vez reconocidos los PDI, se genera una matriz de transformación para valorar la similitud entre todas las imágenes en términos de rotación y homogeneidad (57,58). Todos aquellos puntos considerados *outliers (valores atípicos)* de la matriz de confusión, son considerados como ruido y son eliminados. Una vez se han identificado y alineado los PDIs de las diferentes imágenes, se procede a una fase de integración de los datos, conocida como *stitching* o "cosido de la malla", de forma que se unen las diferentes imágenes entre sí, obteniendo un modelo tridimensional. Este proceso necesita además de la interpolación de los datos, donde se rellenan los espacios entre los puntos de interés con información adicional basada en el contorno y la superficie circundante identificada en las imágenes. Posteriormente, se suele aplicar un ajuste fino que refina la precisión de la malla, minimizando cualquier error de registro de los PDI. Este ajuste es crucial

para garantizar que el modelo final representa con precisión la geometría y topografía de la situación intraoral del paciente. En esta tesis se han trabajado con las mallas obtenidos del escáner intraoral PrimeScan® de Dentsply-Sirona (datos empresa) que utiliza *confocal parallel imaging* como tecnología de escaneado intraoral.

1.2. Precisión de los escáneres intraorales

En la literatura científica odontológica el estándar más utilizado para medir la precisión de los escáneres intraorales es la norma ISO 5725-1 (59). Según la Organización Internacional de Estandarización 5725-1 ISO, de sus siglas en ingles de *International Organization for Standardization*), se define la precisión de un escáner como la combinación de exactitud y fiabilidad (58-59). La exactitud hace referencia a la capacidad que tiene un escáner intraoral para reproducir digitalmente la situación intraoral de un paciente al tamaño real sin distorsión ni deformación. La fiabilidad de un escáner intraoral indica la repetibilidad de dicho escáner intraoral bajo unas mismas condiciones de escaneado.

En función de la tecnología de escaneado intraoral utilizada parecen existir diferencias en precisión (25,26,55,60-92). Además de las posibles diferencias entre las tecnologías de escaneado intraoral, se han identificado diferentes factores que afectan a la precisión de los escáneres intraorales siendo estos: la calibración, la luz ambiental del gabinete, la experiencia del operador, la extensión del escaneado intraoral, las características de los dientes y de las preparaciones dentales, así como restauraciones existentes, la cantidad y extensión de brechas edéntulas, el uso de matificadores de superficie como el óxido de titanio, los protocolos y técnicas de escaneado, el tipo de preparaciones dentales, la presencia de zonas edéntulas, la extensión del área a escanear, la distancia de escaneado y la temperatura ambiental (Tabla 2)

En la presente tesis abordamos el efecto que tiene la luz ambiental del gabinete dental en la precisión final de las mallas 3D.

1.3. Condición de luz ambiental del gabinete

La luz ambiental del gabinete odontológico es uno de los factores que tiene mayor importancia en relación a la precisión de los escáneres intraorales (24-32). Existen recomendaciones sobre la cantidad de iluminación que ha de tener un gabinete dental (24-32). En el año 1979, Viohl J estableció la iluminación ideal del gabinete en 500 luxes y la del sillón dental en 2.500 luxes (93). No fue hasta el año 2011 cuando el Estándar Europeo de Iluminación (EN 12464) recomendó 500 luxes para la iluminación general de la consulta, 1000 luxes para los gabinetes y 10.000 luxes en el sillón dental para tener mejor visibilidad a la hora de trabajar en la cavidad oral (94). Sin embargo, a pesar de estas recomendaciones, en la práctica clínica actual no se determina de forma sistemática la condición lumínica del gabinete dental mediante luxómetros.

En la literatura científica se han publicado varios artículos analizando las condiciones de luz óptima del gabinete para varios escáneres intraorales (27-34). En esta tesis, se ha analizado la precisión de un escáner intraoral con tecnología de microscopía confocal paralela (PrimeScan®; Dentsply Sirona) bajo 12 condiciones de luz ambiental, desde los 0-lux hasta los 10.000 lux. Para llevar a cabo una estandarización correcta de cada una de las condiciones de

luz ambiental se utilizó un luxómetro (LX1330B; Dr. Meter).

2. Diseño 3D: *Softwares* CAD

En odontología, se define un *software* CAD como una tecnología capaz de crear representaciones gráficas tridimensionales de dispositivos y/o restauraciones protésicas que pueden ser fabricados mediante tecnologías de fresado o de impresión 3D. En el ámbito dental/odontológico se utilizan los *softwares* CAD de forma rutinaria para realizar encerados diagnósticos, guías quirúrgicas para la colocación de implantes, férulas de descargas, cubetas individualizadas, ferulizaciones rígidas de impresión y restauraciones dentales.

En el mercado, existen *softwares* CAD diseñados específicamente para el sector dental y que denominaremos *softwares* CAD dentales, mientras que existen *softwares* libres *open-source* y que llamaremos *softwares* CAD no-dentales (44, 102-105). La diferencia entre ambos tipos de *softwares* radica en que los primeros presentan herramientas y flujos de trabajo optimizados para el sector dental, mientras que los segundos ofrecen total libertad de diseño, pero requieren de una mayor curva de aprendizaje para poder ser utilizados con solvencia y predictibilidad en odontología. Se han descrito en la literatura artículos para el diseño de dispositivos que requieren poca o baja precisión ya que van a ser rebasados en boca o bien servirán como pruebas intermedias de prótesis como son las planchas base y rodillos y ferulizaciones rígidas para la toma de impresión a implantes (43).

La importancia de la elección del *software* CAD a utilizar radica no sólo se debe basar en aquello que es capaz de diseñar dicho programa, sino en la facilidad de uso o en motivos económicos. El principio por el que se rige la odontología digital es la alineación de mallas 3D, con el objetivo de integrar todos los archivos digitalizados del paciente en el mismo eje de coordenadas. Sin embargo, a pesar de la importancia de ello, no existe ningún artículo en la literatura científica que analice los diferentes algoritmos y protocolos de alineación de mallas entre los diferentes *softwares* CAD 3D disponibles en el mercado (Tabla 3). Este hecho es de vital importancia si queremos conseguir una representación virtual del paciente de forma precisa. En esta tesis se han analizado 6 softwares CAD, 5 dentales y 1 no dental. Entre los 6 *softwares* CAD se han comparado 12 algoritmos de alineación diferentes, incluyendo algoritmos de *best-fit* (BF), alienación por superficies (SBF) y alineación por puntos (LBF).

3. Fabricación: Impresión 3D

Según el glosario de términos digitales se define la impresión 3D como una tecnología de fabricación aditiva de un objeto físico en 3 dimensiones (3D) mediante un proceso de fabricación capa a capa (95). La tecnología aditiva permite obtener geometrías complejas en menor tiempo y con un menor gasto de material si las comparamos con tecnologías sustractivas como es el fresado (96-104).

La Organización Internacional de Estandarización (ISO) junto con la Sociedad Americana de Pruebas y Materiales (ASTM) de sus siglas en inglés, *American Society for Testing and Materials*- definieron 7 categorías de impresión 3D diferentes: *vat-polymerization* (polimerización de resina), *material jetting* (inyección de material), binder jetting (inyección

de aglomerantes), *material extrusion* (extrusión de material), *powder bed fusion* (fusión de partículas en cama de polvo), *sheet lamination (laminación por capas)* y *direct energy deposition* (deposición directa de energía) (101). Además, en cada una de estas tecnologías se pueden utilizar un tipo determinado de materiales, ya sean polímeros (resinas), metales (cromo-cobalto y titanio), ceras y cerámicas (103-105).

3.1. Tecnologías de polimerización de resina o *vat-polymerization.*

De todas las tecnologías de impresión 3D, las tecnologías de *vat-polymerization* son la más utilizada en clínicas y laboratorios dentales. La tecnología de estereolitografía (SLA) fue desarrollada inicialmente por Hideo Kodama en Japón en 1981 (106). A lo largo de los años 80, se sumaron nuevas patentes, entre ellas las de Yoji Marutani (también en Japón) y las de Jean Claude André, Alain Le Méhauté y Olivier de Witte en Francia (107). Sin embargo, fue el profesor Charles W. Hull quien llevó esta tecnología al mercado por primera vez en Estados Unidos (1986), al fundar la empresa 3D Systems (108,109). Esta fecha marcó el comienzo de la estereolitografía como una tecnología de impresión 3D con aplicaciones industriales.

Todas las impresoras 3D de tecnología SLA cuentan con los mismos componentes: 1. Plataforma de impresión 3D, 2. Batea, 3. Raíles del eje Z y 4. Fuente de iluminación UV. La tecnología SLA se puede subclasificar a su vez en función del tipo de fuente de iluminación que utiliza la impresora 3D para polimerizar la resina, entre las que se encuentran el láser (SLA-Láser), proyector (SLA-DLP) o una pantalla de cristal líquido (SLA-LCD, de sus siglas en inglés *Liquid Crystal Display*) (107-111).

En las tecnologías de impresión 3D de SLA la plataforma de impresión se sumerge en la batea que contiene la resina en estado líquido. Esta resina será polimerizada por una fuente de iluminación ultravioleta que puede ser un Láser (SLA-Láser), un proyector (SLA-DLP) o una pantalla LCD (SLA-LCD) (107-112).

En las impresoras SLA-Láser, un láser ultravioleta dibuja las secciones transversales del objeto a imprimir capa por capa (98-103, 113). Las impresoras láser emplean un láser ultravioleta que se dirige hacia la plataforma de impresión 3D mediante un conjunto de lentes y espejos motorizados llamados galvanómetros. Estos espejos orientan el láser hacia la superficie de la resina en estado líquida iniciando la polimerización de cada capa que se desea imprimir (104-106, 113).

Por otro lado, nos encontramos con las impresoras 3D de proyección que polimerizan la resina utilizando un proyector (SLA-DLP) (110,115), o bien aquellas impresoras que utilizan un panel LCD (SLA-LCD) (50, 115-117). La principal ventaja y diferencia de las tecnologías de impresión 3D por proyección radica en la capacidad de poder polimerizar un mayor número de modelos en el mismo tiempo en comparación con las impresoras SLA-Láser.

No obstante, el procedimiento mecánico de impresión 3D de las resinas son iguales independientemente de la tecnología 3D utilizada para polimerizar la resina. En líneas generales, una vez que se ha polimerizado una capa de resina, la plataforma de impresión 3D asciende una distancia determinada para separar la capa polimerizada del *film* de la batea. Posteriormente, la plataforma de impresión 3D desciende hasta quedarse a una distancia de la pantalla de la impresora 3D equivalente al grosor de capa, permitiendo que una nueva capa de resina no curada recubra la anterior. Este proceso se repite sucesivamente tantas veces sea

necesario hasta completar la fabricación del objeto en 3 dimensiones.

Otro de los elementos importantes en la impresión 3D es la resina 3D. Podemos definir las resinas 3D como monómeros y oligómeros en estado líquido que tienden a polimerizar a una determinada longitud onda. En líneas generales, existen resinas de dos longitudes de onda 405nm y 385nm. Es determinante conocer la longitud de onda apropiada para cada resina, ya que ha de estar en consonancia con la longitud de onda de la tecnología de impresión 3D.

Las características superficiales de los objetos 3D impresos, así como su precisión están determinados por factores como el tipo de fotoiniciador utilizado, las condiciones de exposición (longitud de onda, potencia, tiempo de exposición y velocidad de impresión), así como la presencia de colorantes, pigmentos u otros aditivos que absorben la radiación UV.

En el año 2021, Piedra-Cascón y cols. (50) publicaron una revisión narrativa sobre todos los posibles factores condicionantes de la precisión en impresión 3D. En dicha revisión, los autores establecieron el concepto de *Manufacturing Trinomial*, denominando de esta forma la posible existencia de una interrelación entre la impresora 3D, la tecnología de impresión 3D y la resina utilizada.

No obstante, es importante remarcar que la precisión final de los objetos fabricados mediante tecnologías de impresión 3D está afectada de forma multifactorial (118-123) por: la tecnología de impresión 3D (118,119), la orientación del objeto a imprimir en la plataforma de impresión (120-124), las características y localización de estructuras de soporte (118), las propiedades de las resinas (119), la elección del *software* de preparación de archivos (*slicer*) (132), la geometría del objeto a imprimir (119, 123, 124), los parámetros de impresión 3D (50) y los procedimientos de post-procesado (125-129).

En la presente Tesis Doctoral, los artículos 3 y 4 pretenden establecer evidencia científica en relación al concepto de *Manufacturing Trinomial* y cómo afecta la tecnología de impresión 3D, las propiedades de la resina seleccionada y la geometría del objeto a imprimir en la precisión final resultante tras el proceso de impresión 3D.

TABLAS

Tabla 1. Resumen de *hardware* y *software* y su función en el flujo de trabajo digital odontológico.

Dispositivo	Función
Tomografía Computerizada de Haz Cónico (CBCT)	Digitalizar maxilares, dientes, estructuras anatómicas y tejidos blandos extraorales
Cámara de fotografía y/o vídeo	Registros faciales e intraorales del paciente estáticos y/o dinámicos
Escáneres Faciales	Digitalización extraoral del paciente
Escáneres Intraorales	Digitalización de estructuras intraorales y extraorales
Escáneres de laboratorio	Digitalización de modelos y estructuras físicas
Sistemas de fotogametría de implantes	Registrar la posición tridimensional de implantes

CAD *software*	Diseño de dispositivos para el tratamiento del paciente
CAM *software*	Determinación de estrategias de fresado y parametrización de resinas y soportes en impresión 3D.

Tabla 2. Factores descritos que afectan a la precisión de las tecnologías de escaneado intraoral

Autores	Año	Tipo de Estudio	Material y Métodos	Escáner intraoral	Factor Influyente
Ender y cols. (63)	2013	*In vitro*	Tipodonto dentado	Lava C.O.S. CEREC AC BlueCam iTero	Tecnología de escaneado
Patzelt y cols. (73)	2014	*In vitro*	Tipodonto dentado con preparaciones dentarias	CEREC AC BlueCam Lava C.O.S. iTero Zfx IntraScan	Tecnología de escaneado Extensión de área de escaneado
Ender y cols. (61)	2016	*In vivo*	Pacientes completamente dentados	CEREC AC BlueCam CEREC Omnicam True Definition Lava C.O.S. iTero Trios	Tecnología de escaneado
Kim y cols. (76)	2016	*In vitro*	Tipodonto dentado	iTero Trios	Experiencia del operador
Park y cols. (80)	2016	*In vitro*	Tipodonto dentado con diferentes diseños de preparaciones	E4D FastScan iTero Trios Zfx IntraScan	Tecnología de escaneado Características de la superficie a escanear
Jeong y cols. (25)	2016	*In vitro*	Tipodonto dentado	CEREC Omnicam CEREC AC BlueCam	Tecnología de escaneado
Renne y cols. (66)	2017	*In vitro*	Tipodonto dentado	CEREC Omnicam Cerec AC BlueCam PlanScan iTero Trios 3	Tecnología de escaneado Extensión de área de escaneado
Carbajal-Mejía y cols. (81)	2017	*In vitro*	Tipodonto con preparaciones de diferente convergencia oclusal	Trios	Características de la superficie a escanear

Medina-Sotomayor y cols. (66)	2018	*In vitro*	Tipodonto dentado	Cerec Omnicam True Definition iTero Trios	Tecnología de escaneado
Malik y cols. (70)	2018	*In vitro*	Tipodonto desdentado parcial	Cerec Omnicam Trios 3	Tecnología de escaneado
Nedelcu y cols. (71)	2018	*In vivo*	Pacientes dentados	Cerec Omnicam True Definition Trios 3	Tecnología de escaneado
Mennito y cols. (74)	2018	*In vitro*	Tipodonto dentado	Cerec Omnicam Emerald PlanScan Trios 3 iTero Element True Definition	Tecnologia de escaneado
Arakida y cols. (24)	2018	*In vitro*	Tipodonto parcial	True Definition	Luz ambiental
Kim y cols. (91)	2019	*In vitro*	Tipodonto dentado con 1 preparación dentaria	Trios CS 3500 PlanScan	Distancia de escaneado
Park y cols. (86)	2020	*In vitro*	Tipodonto dentado con diferentes diseños de preparaciones	CEREC Omnicam E4D FastScan Itero Trios 2 Zfx IntraScan	Carácterísticas de la superficie a escanear
Nagy y cols. (88)	2020	*Cadáveres*	Maxilares dentados con 3 preparacines dentarias	Cerec Omnicam Trios 3 CS 3600 iTero Element iTero Element 2 Planmeca Emerald PlanScan	Tecnología de escaneado
Winkler y cols. (89)	2020	*In vivo*	Pacientes dentados	Trios 3 CS3600	Tecnología de escaneado
Roig y cols. (90)	2020	*In vitro*	Tipodonto parcialmente desdentado con dos implantes	Trios 3 CS 3600 True Definition	Tecnología de escaneado

Revilla-León y cols. (25, 26)	2020	*In vitro*	Tipodonto dentado	Trios 3 iTero 2 CEREC Omnicam	Luz ambiental Calidad de malla
Revilla-León y cols. (27)	2020	*In vivo*	Maxilar dentado	Trios 3	Luz ambiental
Revilla-León y cols. (28)	2021	*In vitro*	Tipodonto dentado	Trios 3	Luz ambiental
Wesemann y cols. (29)	2021	*In vitro*	Tipodonto dentado	Trios 3 CEREC Omnicam iTero Element CS3600 Planmeca Emerald GC Advaa	Luz ambiental
Jivanescu y col.s (30)	2021	*In vitro*	Tipodonto con una preparación en un molar	Planmeca PlanScan	Luz ambiental
Koseoglu y cols. (31)	2021	*In vivo*	Maxilares dentados	Medit i500	Luz ambiental
Ochoa-López y cols. (32)	2022	*In vitro*	Tipodontos con implantes	Trios 3 PrimesScan iTero 5D Medit i500 Medit i700 CS 3600 CS 3700	Luz ambeintal
Revilla-león y cols. (91)	2023	*In vitro*	Tipodonto dentado	Trios 4	Temperatura ambiente
Agustín-Panadero y cols. (92)	2025	*In vitro*	Tipodonto dentado	Trios 3	Humedad

Tabla 3. Revisión bibliográfica de *softwares* CAD para alineación de mallas tridimensionales

Autores	Año	Tipo de Estudio	Material y Método	Software	Objetivo
Revilla-León y cols. (138)	2023	*In vitro*	Tipodonto mandibular	Geomagic Control X	Medir influencia diferentes algoritmos de alineación
Dede y cols. (139)	2023	*In vitro*	Prótesis sobre implantes	Geomagic Control X Medit Design	Comparación de softwares para saber cuál alinea mejor

Tabla 4. Revisión bibliográfica sobre precisión de impresión 3D de tecnologías *vat-polymerization*

Autores	Año	Variable analizada	Tipo de Medición	Impresora	Resina	Tecnología
Alharbi y cols. (121)	2016	Ángulo de orientación	Resistencia a fractura	DW028D; DWS	Temporis; DWS	SLA-DLP
Alharbi y cols. (127)	2016	Ángulo de orientación Soportes	Precisión	DW028D; DWS	Temporis; DWS	SLA-DLP
Unkovskiy y cols. (120)	2018	Ángulo de orientación Post-procesado	Resistencia a la fractura	Form 2; Formlabs	Dental SG; Formlabs	SLA-Láser
Reymus y cols. (123,128)	2020	Material Ángulo de orientación Post-procesado Envejecimeinto	Resistencia a fractura	D20II; Rapidshape	FreePrint Temp; Detax NextDent C&B; 3Dsystems 3Delta Temp; Deltamed Experimental	SLA-DLP
Arnold y cols. (133)	2019	Ángulo de orientación Post-procesado Espesor de capa Tipo de zócalo Soportes	Rugosidad superficial	Form 2; Formlabs	Grey V3; Formlabs	SLA-Láser
Revilla-León y cols. (103)	2023	Tipo de zócalo	Precisión	NextDent 5100	Model 2.0; 3DSystems	SLA-DLP
Maneiro-Lojo y cols. (114)	2024	Ángulo de orientación	Precisión	Photon Mono SE; Anycubic	Aqua Gray 4K; Phrozen	SLA-LCD

2

HIPÓTESIS y OBJETIVOS GENERALES y ESPECÍFICOS

2 HIPÓTESIS y OBJETIVOS GENERALES y ESPECÍFICOS

El flujo de trabajo digital en odontología comprende tres etapas fundamentales como son la digitalización, el diseño CAD y la fabricación. Se plantea la hipótesis de trabajo inicial de que la precisión global del flujo de trabajo digital depende de múltiples factores. Cada una de estas fases principales se compone, a su vez, de diversas subfases que pueden influir de forma significativa en la exactitud final del proceso, lo que convierte al flujo digital en un sistema inherentemente multifactorial

Objetivo principal

Evaluar el impacto de diferentes factores que afectan a la precisión del flujo de trabajo digital en las fases de digitalización, diseño CAD y fabricación mediante impresión 3D.

Objetivos secundarios

1. Analizar el efecto que tienen diferentes intensidades de iluminación ambiental del gabinete dental sobre un escáner intraoral que utilizada tecnología confocal.

2. Determinar la influencia de diferentes *softwares* CAD 3D y algoritmos de alineación en la precisión final de alineación, así como el tiempo de procesamiento de dicha alineación.

3. Evaluar el impacto de la tecnología de impresión 3D, la resina y el diseño del zócalo de los modelos en la precisión del proceso de impresión 3D.

3
HERRAMIENTAS METODOLÓGICAS

3 HERRAMIENTAS METODOLÓGICAS

A continuación, se describen brevemente los materiales y métodos utilizados en los cuatro artículos científicos que forman parte del compendio de esta Tesis Doctoral.

3.1. REVISIÓN Y ACTUALIZACIÓN DE LA LITERATURA

Se ha realizado una revisión de la literatura científica disponible hasta la fecha en relación a cada una de las fases del flujo de trabajo digital aplicado a odontología (Tabla 2, Tabla 3 y Tabla 4). El objetivo de esta revisión radica en la necesidad de comprender y analizar los hallazgos previos a los que habían llegado otros equipos de investigación en torno a flujo de trabajo digital en Odontología. Nos hemos centrado principalmente en aquellas áreas de investigación en las que no existe una evidencia científica clara todavía.

En la fase de digitalización, múltiples son los artículos en los que se analiza la precisión de escáneres intraorales sin encontrar una conclusión fehaciente de cuál es el escáner intraoral más apropiado. Esto nos hace pensar, que probablemente exista algún factor que no se está controlando en dichos estudios y que da lugar a una gran variabilidad de los resultados de dichos estudios (22-26). Tras la realización de la revisión hemos constatado que en la mayoría de artículos revisados sobre la precisión de escáneres intraorales, el factor luz ambiental del gabinete era un factor no controlado.

En la fase de diseño CAD, sólo existen dos artículos sobre la precisión de procedimientos de alineación de mallas 3D (138, 139). En uno de ellos, se analizaban los algoritmos de alineación del *software* Geomagic Control X (139), mientras que en el segundo estudio se comparaba el *software* Medit Design con Geomagic Control X (139). Es necesario remarcar que el *software* de la casa comercial Geomagic es un *software* no odontológico utilizado frecuentemente en el ámbito de la ingeniería debido a todas las posibilidades que ofrece dicho *software*, estando considerado el *gold standard* para realizar alineaciones y mediciones en estudios científicos del campo de la odontología. Sin embargo, también es necesario entender/*señalar* que no todos los *softwares* están programados de la misma manera y mucho menos, los resultados obtenidos en un estudio con un determinado *software* se pueden extrapolar al resto de *softwares* CAD, especialmente los diseñados para el sector odontológico.

En la literatura científica no existía previamente ningún estudio que comparase varios *softwares* CAD dentales y no dentales (pero de uso en odontología) y que además analizara la precisión de cada uno de los algoritmos de alineación y el tiempo necesario para procesar dichas alineaciones.

Por último, la literatura científica en relación a la precisión de modelos impresos 3D arroja resultados dispares no existiendo en ninguno de los artículos revisados (Tabla 4) resultados que expliquen la interrelación entre tecnologías de impresión 3D, resinas poliméricas y diseño de zócalos de los modelos fabricados mediante tecnologías aditivas.

3.2. DISEÑO DE LOS ESTUDIOS

La presente tesis doctoral está compuesta por cuatro estudios experimentales que comparten un enfoque metodológico común: el análisis *in vitro* de la precisión en las tres fases del flujo de trabajo digital en odontología. Este enfoque fue seleccionado con el objetivo de controlar estrictamente las variables involucradas en cada etapa del flujo digital y permitir una evaluación sistemática, reproducible y cuantitativa de los factores que afectan a la precisión global del proceso.

Todos los estudios se diseñaron como investigaciones experimentales, comparativas y transversales, en las que se modificaron de forma controlada determinadas variables independientes (condiciones de iluminación, *softwares* CAD de alineación, tecnología de impresión 3D, tipo de resina y diseño de zócalos de modelos) para analizar su impacto sobre las variables dependientes: exactitud, fiabilidad y/o el tiempo de procesamiento de alineación entre mallas 3D.

3.3. VARIABLES EVALUADAS

La variable principal analizada en cada uno de los estudios que conforman esta tesis doctoral es la precisión en las distintas fases del flujo de trabajo digital en odontología. No obstante, este término requiere un análisis detallado, ya que su definición varía según la entidad u organismo que lo establezca. En este contexto, se consideran las definiciones propuestas por el *Vocabulario Internacional de Metrología* (VIM, 2012) (140), la norma alemana DIN 55350-13:1987-07 (141) y la norma internacional ISO 5725-1:1994 (59).
Según el VIM (2012) (140), se distinguen los siguientes conceptos:

- **Exactitud** (*Trueness*): proximidad entre la media de un número infinito de mediciones repetidas y un valor de referencia.

- **Fiabilidad** (*Precision*): proximidad entre los valores obtenidos mediante mediciones repetidas sobre el mismo objeto o sobre objetos similares, bajo condiciones especificadas.

- **Precisión** (*Accuracy*): proximidad entre un valor medido y el valor verdadero del mensurando.

Por su parte, la norma DIN 55350-13:1987-07 (141) define:

- **Exactitud**: término cualitativo que describe la proximidad entre el valor esperado (media aritmética de múltiples resultados de ensayo) y un valor de referencia aceptado.

- **Fiabilidad**: término cualitativo que indica la proximidad entre resultados independientes obtenidos bajo las mismas condiciones. Depende exclusivamente de la distribución de errores aleatorios y no se relaciona directamente con el valor verdadero ni con el valor de referencia. Se expresa mediante la desviación estándar de los resultados.
En este caso, la precisión se entiende como la combinación de la exactitud y la fiabilidad.
Finalmente, la norma ISO 5725-1:1994 (59) establece definiciones similares:

- **Exactitud**: proximidad entre el valor medio de un conjunto amplio de resultados de ensayo y un valor de referencia aceptado.

- **Fiabilidad**: proximidad entre resultados de ensayo independientes realizados bajo condiciones repetibles.
  Así, tanto la norma DIN (141) como la ISO (59) consideran que el concepto de precisión implica la integración de la exactitud y la fiabilidad.

  Basándonos en estas definiciones, podemos concluir que la exactitud está relacionada con el error sistemático de la medición, la fiabilidad con el error aleatorio, que puede ser accidental, casual o indeterminado, y la precisión puede ser definida como el error total de la medición, es decir, la combinación del error sistemático (exactitud) y el aleatorio (fiabilidad).

  En los estudios de la presente Tesis Doctoral hemos utilizado las definiciones de precisión, exactitud y fiabilidad según la norma ISO 5725-1:1994, siendo éste el estándar utilizado en la literatura científica dental (59).

3.4. PROCEDIMIENTOS DE LABORATORIO PARA COMPARACIÓN DE MALLAS 3D

"Accuracy assessment (trueness and precision) of a confocal based intraoral scanner under twelve different ambient lighting conditions" y "Evaluation of the accuracy (trueness, precision) and processing time of different 3-dimensional CAD software programs and algorithms for virtual cast alignment"

El análisis de la precisión de un escáner intraoral se suele realizar mediante la medición de las discrepancias entre las mallas 3D obtenidas con dicho escáner intraoral y la malla 3D de referencia que comúnmente suele ser el modelo escaneado con un escáner extraoral de laboratorio, siendo éste considerado el *gold standard* en cuanto a tecnologías de escaneado se refiere (25). En el artículo 1 incluido en esta Tesis Doctoral titulado: "*Accuracy assessment (trueness and precision) of a confocal based intraoral scanner under twelve different ambient lighting conditions*" se llevaron a cabo los siguientes procedimientos para analizar la precisión del escáner intraoral PrimeScan® (Dentsply-Sirona). Los archivos generados por el escáner intraoral se exportaron en formato STL, que representa los datos registrados mediante una malla de triángulos. Cada triángulo está definido por tres vértices en coordenadas tridimensionales, pero debido a la naturaleza del formato es habitual que un mismo vértice aparezca duplicado múltiples veces en la malla. Además, cada escaneado intraoral generó un conjunto único de triángulos que, aunque representan el mismo modelo físico, no comparten una estructura de malla común. Para poder comparar los escaneados de forma consistente, se procedió a unificar los vértices coincidentes y reconstruir una malla triangular topológicamente conectada, definida como M (V, F), donde V es el conjunto de vértices unificados y F las caras triangulares generadas entre ellos. Este procesamiento de los datos escaneado se realizó utilizando el *software open-source* MeshLab, permitiendo así estandarizar las mallas antes de aplicar los algoritmos de comparación geométrica.

Por otra parte, en el artículo 2 de la presente Tesis Doctoral (*"Evaluation of the accuracy (trueness, precision) and processing time of different 3-dimensional CAD software programs and algorithms for virtual cast alignment"*), se seleccionó una de las mallas obtenidas con el escáner intraoral PrimeScan® (Dentsply-Sirona) correspondiente al grupo que presentó los mejores resultados bajo condiciones de 1000 lux. Esta malla fue duplicada 10 veces, de modo que todas compartieran la misma topología y se evitara que diferencias estructurales de la malla influyeran en los procedimientos de alineación.

En consecuencia, el protocolo de procesamiento de datos en este estudio difirió del utilizado en el artículo anterior, ya que se trabajó siempre con una malla de topología constante. El objetivo principal fue evaluar la precisión y fiabilidad de los procedimientos de alineación en distintos softwares CAD. El uso de la misma topología en cada alineación permitió eliminar posibles sesgos, dado que la variación en el número de vértices de las mallas puede afectar el comportamiento de los algoritmos de alineación e impedir una comparación objetiva entre programas CAD y entre distintos métodos de alineación.

A continuación, resumimos los procedimientos de laboratorio realizados en el artículo 2. Los archivos STL incluidos en el estudio representan mallas triangulares conectadas (M), compuestas por un conjunto de vértices tridimensionales $V = \{v_1, ..., vNV\}$ y un conjunto de caras triangulares $F = \{f_1, ..., fNF\}$, donde cada cara está definida por tres vértices distintos $fis = (a, b, c)$, con $a \neq b \neq c$ y $a, b, c \in [1, NV]$. Para calcular la precisión de alineación, cada malla triangular M(V, F) se transformó en una lista de puntos tridimensionales $P = \{p_1, ..., pNF\}$, donde cada punto representaba el centroide de una cara triangular, calculado como la media de las coordenadas de sus tres vértices: $pi = (vai + vbi + vci) / 3$. Una vez generadas las listas de puntos tanto del STL escaneado alineado (Pscan) como del STL de referencia (Pref), se calculó la distancia euclidiana tridimensional entre cada par de puntos más cercanos para cuantificar las desviaciones geométricas: $Dist (Pscan, Pref) = \sqrt{[(Pscan - Pref)^2]}$

Es importante señalar que los archivos STL generados por el escáner incluían regiones periféricas con artefactos o ruido (*outliers*) no presentes en el STL de referencia, ya que fueron eliminados en el procedimiento de preparación de archivos. Estas zonas fueron identificadas y eliminadas manualmente antes del análisis, con el fin de evitar sesgos en los resultados de precisión por un operador con 8 años de experiencia previa y calibrado (W.P.C)

3.5. PROCEDIMIENTOS DE LABORATORIO PARA MEDICIÓN MODELOS IMPRESOS 3D

"Influence of base designs on the manufacturing accuracy of vat- polymerized diagnostic casts using two different technologies" y "Impact of 3D resin and base designs on the accuracy of additively manufactured casts using a stereolithography technology"

Para la evaluación de la precisión de modelos impresos en 3D se han propuesto múltiples técnicas para llevar a cabo estas mediciones, entre las que se incluyen:

1. Mediciones con calibre entre pares de puntos identificables en el STL y el modelo impreso.
2. Escaneado del modelo impreso con escáner de laboratorio y comparación de mallas con el STL original.
3. Mediciones llevadas a cabo con máquina de coordenadas (CMM) entre pares de puntos previamente identificados. (102)

De los 3 métodos anteriormente mencionados el único que no introduce sesgos en las mediciones es el método en el que se emplea una CMM ya que se programa un *software* con el modelo que se desea medir, y la máquina, de forma autónoma realiza las mediciones entre los pares de puntos indicados mediante la punta de un palpador. Es por ello, que es un método objetivo y completamente reproducible. Los otros dos posibles métodos, tienen la capacidad de inferir errores ya sea por la acción humana de realizar mediciones con calibre o bien por los posibles sesgos que se pueden introducir en el sistema mediante el proceso de escaneado o de alineación 3D, como se evidencia en la presente Tesis Doctoral.

A continuación, se detallan los procedimientos de laboratorio llevados a cabo en los estudios que llevan por título *"Influence of base designs on the manufacturing accuracy of vat-polymerized diagnostic casts using two different technologies*" y "*Impact of 3D resin and base designs on the accuracy of additively manufactured casts using a stereolithography technology".*

En ambos estudios la precisión de los modelos impresos fue evaluada mediante una máquina de medición por coordenadas (CMM) (DEA Alpha Status; Hexagon AB) con un tamaño de palpador de 0.5mm. Estas mediciones se llevaron a cabo en el Departamento Dimensional del Laboratorio Oficial de Metroloxía de Galicia (LOMG) (Orense).

Cada modelo impreso en 3D tenía 11 cubos de 3x3x3mm colocados en su superficie. Se procedió a realizar la medición en las coordenadas X, Y y Z de los 11 cubos embebidos, junto con 36 mediciones adicionales distribuidos en la superficie del modelo. Se desarrolló un programa de medición específico a partir de los modelos CAD digitales correspondientes a cada diseño de zócalo, con el objetivo de automatizar el proceso de evaluación y mediciones.

Una vez recibidos los especímenes impresos, cada uno fue fijado de forma estable en la plataforma de medición de la CMM. La secuencia de medición se inició con la alineación del modelo físico respecto a su modelo CAD correspondiente. Para ello, se definieron 13 puntos de referencia en el CAD, ubicados en el centro geométrico de cada cara los cubos que actúan como elementos de referencia. Estos puntos fueron palpados en el modelo físico mediante la punta de palpación de la CMM, contactando con el centro de cada cara seleccionada para establecer una correspondencia espacial precisa entre el modelo digital y el impreso. El origen del sistema de coordenadas (0, 0, 0) se definió en el modelo CAD como el centroide del modelo maxilar, situado en la intersección entre el plano medio sagital y el plano transversal. Este punto de referencia fue utilizado de manera consistente durante todas las mediciones para garantizar una correcta alineación. Una vez completada la alineación inicial, el programa de medición registró automáticamente las coordenadas X, Y y Z de los puntos especificados. Cada punto fue medido una única vez, aprovechando la precisión del sistema CMM para asegurar la fiabilidad de los datos obtenidos.

7

El archivo STL del modelo digital fue convertido en un modelo CAD sólido mediante el software Metrolog X4 (v18; Metrologic Group), ya que la CMM requiere una superficie sólida en lugar de una malla para realizar una evaluación precisa.

3.6. ANÁLISIS ESTADÍSTICO

Los cuatro estudios *in vitro* permitieron evaluar posibles factores condicionantes de precisión (exactitud y fiabilidad) en el flujo de trabajo digital aplicado a la odontología en las fases de digitalización, diseño CAD y fabricación aditiva de modelos de estudio. En todos los estudios se fijó el nivel de significación estadística en $\alpha = 0.05$. Los softwares utilizados para análisis estadístico fueron IBM SPSS Statistics (IBM Corp., Armonk, NY, EE.UU.) y código propietario basado en Python (Python v3.8; Python, Delaware, USA).

Según las características de cada estudio, se aplicaron las siguientes pruebas estadísticas:

1. Accuracy assessment (trueness and precision) of a confocal based intraoral scanner under twelve different ambient lighting conditions:

- El análisis estadístico se realizó con IBM SPSS v25. Se comprobó la normalidad de las variables mediante la prueba de Shapiro-Wilk. Al no cumplirse el supuesto de normalidad en todos los grupos, se empleó la prueba de Kruskal-Wallis para comparaciones globales, seguida del test de Dunn con corrección de Bonferroni para comparaciones múltiples entre pares.

2. Evaluation of the accuracy (trueness, precision) and processing time of different 3-dimensional CAD software programs and algorithms for virtual cast alignment.

- El análisis estadístico se llevó a cabo con código Python propietario. Se comprobó la normalidad de las variables mediante la prueba de Shapiro-Wilk. Al no observarse distribución normal, se aplicaron pruebas no paramétricas: Kruskal–Wallis para comparaciones globales entre grupos y test de Dunn con corrección de Bonferroni para comparaciones múltiples entre pares.

3. ***Influence of base designs on the manufacturing accuracy of vat-polymerized diagnostic casts using two different technologies***

- En este estudio se aplicó la prueba de Shapiro-Wilk para determinar la distribución normal de las variables. Dado que no se cumplió el supuesto de normalidad, se emplearon pruebas no paramétricas: Kruskal-Wallis para la comparación global de grupos y U de Mann-Whitney para comparaciones por pares. Los resultados se expresaron como mediana y rango intercuartílico. Para el análisis estadístico se utilizó el software IBM SPSS Statistics v25.0.

4. Impact of 3D resin and base designs on the accuracy of additively manufactured casts using a stereolithography technology

- En este estudio se definieron como variables dependientes la exactitud y la fiabilidad. Para analizar los datos se aplicó la prueba de Shapiro-Wilk y, dado que no se cumplieron los requisitos de distribución normal de los datos, se emplearon pruebas no paramétricas: Kruskal-Wallis para comparaciones múltiples entre grupos y U de Mann–Whitney para comparaciones por pares. Para el análisis estadístico se utilizó el software IBM SPSS Statistics v25.0.

4

RESULTADOS:

TRABAJOS PUBLICADOS

4 RESULTADOS: TRABAJOS PUBLICADOS

4.1 ARTÍCULO 1.

Piedra-Cascón W, Addikhari RR, Özcan M, Krishnamurthy VR, Revilla-León M, Gallas Torreira M. Accuracy assessment (trueness and precision) of a confocal based intraoral scanner under twelve different ambient lighting conditions. J Dent. 2023; 134:104530.

DOI: 10.1016/j.jdent.2023.104530

Revista: Journal of Dentistry

Factor de Impacto (JCR 2024): 5.5

Cuartil: Q1

Categoría: Dentistry, Oral Surgery and Medicine

Posición: 9/271

Link:https://www.sciencedirect.com/science/article/abs/pii/S0300571223001161?via%3Dihub

Journal of Dentistry 134 (2023) 104530

Contents lists available at ScienceDirect

Journal of Dentistry

journal homepage: www.elsevier.com/locate/jdent

Accuracy assessment (trueness and precision) of a confocal based intraoral scanner under twelve different ambient lighting conditions

Wenceslao Piedra-Cascón [a], Riddhi R. Adhikari [b], Mutlu Özcan [c], Vinayak R. Krishnamurthy [d], Marta Revilla-León [e], Mercedes Gallas-Torreira [f,*]

[a] Department of Surgery and Medical-Surgery Specialities, Doctoral Programme in Dental Science, Stomatology Area, University of Santiago de Compostela, Spain. Affiliate Faculty Esthetic Dentistry Program, Complutense University of Madrid, Researcher at MovumTech, Madrid, Spain
[b] Graduate Research Assistant J. Mike Walker '66 Department of Mechanical Engineering, Texas A&M University, College Station, TX, USA
[c] Dental Materials Unit, Center for Dental and Oral Medicine, University of Zürich, Switzerland
[d] Assistant Faculty J. Mike Walker '66 Department of Mechanical Engineering, Texas A&M University, College Station, TX, USA
[e] Department of Restorative Dentistry, School of Dentistry, Graduate Prosthodontics, University of Washington, Seattle, Wash; Director of Research and Digital Dentistry Kois Center, Seattle, Wash; and Adjunct Professor, Department of Prosthodontics, Tufts University, Boston, MA, USA
[f] Department of Surgery and Medical-Surgery Specialities, Senior Lecturer in Planification and Management in Dental Clinics, Stomatology Area, Digital Dentistry Unit of the School of Dentistry, Faculty of Medicine and Dentistry, University of Santiago de Compostela, Spain

ARTICLE INFO

Keywords:
Accuracy
Ambient light scanning conditions
Digital impression
Intraoral scanner
Prosthodontics

ABSTRACT

Objectives: The ambient lighting condition has been identified as an important factor that influences the accuracy of intraoral scanners (IOSs). The purpose of this study was to evaluate the influence of 12 different ambient lighting conditions on the accuracy of a confocal based IOS (PrimeScan).

Materials and methods: A typodont was digitized using a laboratory scanner (L2i) to obtain a reference standard tessellation language (STL_R) file. A restorative dentist recorded the scans using an IOS (PrimeScan) under 12 different ambient lighting conditions where the luminosity was measured using a light meter (LX1330B Light Meter). Twelve groups were created, namely 0-, 500-, 1000-, 2000-, 3000-, 4000-, 5000-, 6000-, 7000-, 8000-, 9000-, and 10 000 lux groups. Ten STL files were recorded per group. The STL_R file was used as a reference with which to compare the distortion of the 120 STL files obtained using a software program (Meshlab). The normality Shapiro–Wilk test indicated that the distributions were not normal. Therefore, the nonparametric Kruskal–Wallis and pairwise multicomparison tests were used to analyze the data ($\alpha = 0.05$).

Results: The group with the 1000 lux lighting condition obtained the smallest median ±interquartile range (IQR) with scanning distortion values of 69.5 ± 97.4 μm, followed by the 8000 lux group with a median ±IQR of 166.5 ± 318.1 μm. The 0 lx group presented the highest distortion values with a mean ±IQR of 355.5 ± 488.0 μm ($p < 0.05$).

Conclusions: Ambient lighting conditions influenced the accuracy of the IOS tested. The highest accuracy values were obtained with 1000 lux. The lowest scanning accuracy was obtained with 0 lux.

1. Introduction

The ambient lighting condition has been identified as an important factor influencing the accuracy of digital scans performed using intraoral scanners (IOSs) [1–9]. A decrease in scanning accuracy of between 37% and 44% has been reported among different ambient lighting conditions, including no light (0 lux), natural light (500 lux), examination room light (1000 lux), and illuminance with the dental chair light (10,000 lux) [2,3]. Furthermore, the optimal ambient lighting condition varied among the different IOSs tested [1–3]. However, information on how the illuminance of ambient lighting influences the accuracy of dentate digital scans obtained with a confocal based IOS (PrimeScan; Dentsply Sirona, Bensheim, Germany) system is limited.

The ambient lighting conditions tested in previous studies [2–9]

Clinical SignificanceThe ambient lighting condition influence the accuracy of intraoral scanners (IOSs). The tested IOS (PrimeScan; Dentsply Sirona, York, USA) had significantly better scanning accuracy under 1000-lx illumination. Therefore, introducing a lux meter into the digital daily clinical practice is recommended.

* Corresponding author.
E-mail address: mercedes.gallas.torreira@usc.es (M. Gallas-Torreira).

https://doi.org/10.1016/j.jdent.2023.104530
Received 25 June 2022; Received in revised form 5 April 2023; Accepted 25 April 2023
Available online 26 April 2023

corresponds with the lighting recommendations for the dental practice of the European Standard for Illumination (EN 12,464), which recommended 500 lux for general illumination, 1000 lx in medical or examination rooms, and 10 000 lx for the operating cavity [10,11]. However, lux meters have yet to be systematically included in dental practice to standardize illuminance of the ambient lighting when performing a digital scan. Therefore, understanding how the scanning accuracy of an IOS is affected across different illuminance values will allow the development of scanning protocols to maximize scanning accuracy. This might popularize the implementation of those auxiliary instruments to standardize illuminance in the patient's mouth.

Different factors have been identified that influence scanning accuracy, including the scanning technologies [12–24], resolution at which the tooth is digitized [25,26], different fitting and smoothing algorithms that might be used to postprocess the data [27–33], IOS calibration [34], handling and learning curve [35–37], scanning conditions [35,38], surface characteristics, [39–42], and scanning protocol [43,44].

According to the International Organization for Standardization (ISO) 5725–1 [24], the accuracy of a scanner has been defined as the combination of trueness and precision [45]. Trueness relates to the ability of the scanner to reproduce a dental arch as close to its true form as possible without deformation or distortion, while precision indicates the difference among images acquired by repeated scanning under the same conditions [45].

The aim of the present *in vitro* study was to evaluate the influence of 12 different ambient lighting conditions, specifically the illuminance of the light (0-, 500-, 1000-, 2000-, 3000-, 4000-, 5000-, 6000-, 7000-, 8000-, 9000-, and 10 000 lux) on the scanning accuracy of a confocal based IOS (PrimeScan; Dentsply Sirona, Bensheim, Germany). The null hypothesis was that no significant difference would be found in the digital scan accuracy (trueness and precision) of the tested IOS system (PrimeScan; Dentsply Sirona, Bensheim, Germany) under the 12 different ambient lighting conditions evaluated.

2. Materials and methods

2.1. Experimental design

A dental simulator mannequin (NISSIN Type 2; Nissin, Kyoto, Japan) with a mandibular typodont set (Hard gingiva jaw model MIS2010-1-HD-M-32; Nissin, Kyoto, Japan) was selected. On the mandibular typodont, the second right premolar was missing to simulate a clinical situation. Three marker dots (Suremark SL-10; The Suremark Co, Mesa, Arizona, USA) were added onto the mandibular typodont using cyanoacrylate resin (Scotch Super Glue; 3 M ESPE) to aid future superimposition and 3D measurements. The markers were attached to the occlusal surfaces of the first left molar, first right premolar, and second right molar teeth. The reference typodont was then digitized as the reference model using a structured light laboratory scanner without scan powder (L2i; Imetric, Courgenay, Switzerland) to obtain a reference standard tessellation language (STL) file (Fig.1). The laboratory scanner had been previously calibrated by following the manufacturer's instructions. The manufacturer of this scanner reports a trueness of <5 μm and a precision of <10 μm.

To replicate the clinical environment, the interincisal opening was standardized to 50 mm. In addition, the mannequin was fixed on the head support of a dental chair, and the IOS was positioned on the left side of the chair. The same scanning protocol was performed in all test groups as follows: Digital scans were started occlusally on the mandibular left second molar. The tip of the scanner was tilted 60° in an oral direction and moved orally along the dental arch up to the lower right second molar. Then, the scanner was guided occlusally from the mandibular right second molar across the entire dental arch back to the mandibular left second molar. Finally, the scanner was tilted 60° in a buccal direction to complete the scans and moved buccally along the entire dental arch. The IOS (Primescan; Dentsply Sirona, Bensheim, Germany) and scanning software (Sirona Connect, v.5.1; Dentsply Sirona, Bensheim, Germany) were calibrated before performing the digital scans for each experimental group. A restorative dentist (W.P.C.) with 6 years of prior experience using IOSs recorded all the digital scans under different ambient lighting conditions, where the luminosity at the typodont of the mannequin was measured using a light meter (LX1330B Light Meter; Dr. Meter Digital Illuminance, Union City, USA).

2.2. Sample collection

Twelve groups were created based on the ambient light illuminance values evaluated (Table 1). For the 0-lux group, a room with no light and without windows was selected. For the 500-lux group, a room with natural window light was selected. For the remaining groups (from 1000 to 10,000 lux groups), a room with a dental chair (A-dec 500; A-dec Inc, Newberg, Oregon, USA) and no windows was used, where 2 main light sources were available, namely the room ceiling light and the chair light. The lighting in the room was 6 fluorescent tubes of 54 W, 5000 lm (GE F54W-T5–841-ECO; Ecolux High Output) with a white spectrum color temperature (4100 K) ceiling light. The light-emitting diode (LED) light of the chair had an intensity of 15 000 lux and 4100 K. For the 1000-lux or room light (RL), the chair light was turned off, and only the ceiling

Fig. 1. Reference STL with 3 markers on occlusal surfaces.

Table 1
Summary of different ambient lighting conditions tested mensured with a light meter (LX1330B Light Meter; Dr. Meter Digital Illuminance).

Group	Chair light	Room light	Windows
0 lux (ZL)	No	No	No
500 lux (NL)	No	No	Yes
1000 lux (RL)	No	Yes	No
2000 lux (CL-2) 3000 lux (CL-3) 4000 lux (CL-4) 5000 lux (CL-5) 6000 lux (CL-6) 7000 lux (CL-7) 8000 lux (CL-8) 9000 lux (CL-9) 10 000 lux (CL-10)	Yes. Variation in luminosity was achieved by changing the distance between the light of the chair and the typodont.	Yes	No

CL, chair light; NL, natural light; RL, room light; ZL, zero light.

light was used. For the remaining groups (from the 2000 lux to the 10,000 lux groups), both the chair light and the ceiling light was turned on, but the distance between the chair light and the mannequin was varied to adjust the luminosity at the typodont. The chair light was always oriented 45° from the mannequin.

Ten digital scans (10 STL files) were consecutively recorded for each ambient light illuminance tested. The control STL file was used as a reference digital model with which to compare the distortion of the 120 STL files obtained. The definition of trueness in the experiment was defined as the average absolute distance between the reference model and the scanned model; therefore, trueness was interpreted as the mean or median of the discrepancy between the control and the experimental groups. Precision was defined as the distances between the points of the reference model and the scanned model; hence, precision was interpreted as the standard deviation or the interquartile range of the discrepancy between the control and the experimental groups [44].

2.3. Statistical analysis

For the statistical analysis of the scanned models, the software package MeshLab was selected to accomplish the geometric preprocessing of the scanned models of the typodont, and MATLAB was used to postprocess the data before statistical analysis. Statistical software (IBM SPSS Statistics, v25 for Windows; IBM Corp) was used to perform all statistical analyses.

The STL file format represents the scanned data as a set of triangles, $\Delta_i = \{p_{i1}, p_{i2}, p_{i3}\}$, $i \in [1, n]$ that defines the surface of the dental model. $p_{ij} \in R^3$ was the j^{th} vertex of the i^{th} triangle ($j \in \{1, 2, 3\}$). Note that the lack of topological connectivity in the STL format results in the occurrence of each mesh vertex more than once in the mesh. Each scanning process resulted in a completely different set of triangles, all representing the same physical model. For this, the co-incident vertices of the triangle soup were unified to construct a topologically connected triangle mesh M(V,F). Here, $V = \{v_1, \ldots, v_n\}$, $v_i \in R^3$ was the set of unified vertices, and $F = \{(i, j, k)\}$, $i, j, k \in [1, n]$, $i \neq j \neq k$ described the triangular faces formed by the vertices. This was performed using MeshLab (Fig. 2A–C). To statistically analyze the scanned data, the same methodologies were used as those proposed by the authors in prior research [2].

The normality test Shapiro–Wilk test was conducted. The results indicated that the distributions were not normal; therefore, the nonparametric Kruskal–Wallis and pairwise multicomparison tests were used to analyze the data (α=0.05).

3. Results

The group with the 1000 lux lighting condition obtained the smallest median ±interquartile (IQR) scanning distortion values of 69.5 ± 97.4 µm, followed by the 8000 lx group with a median ±IQR of 166.5 ± 318.1 µm (Table 2). The 0 lux group presented the highest distortion values with a mean ±IQR of 355.5 ± 488.0 µm. In general, the median and IQR values were found to decrease from the 0 to 10,000 lux lighting conditions (Fig 3).

The Kruskal–Wallis pairwise multicomparison revealed significant differences among the different lighting conditions tested. All groups except for the 4000-, 5000-, 9000-, and 10,000 lux lighting conditions presented median ranks that were significantly different from the others ($p < 0.05$). Furthermore, the 4000 and 5000 lux groups presented comparable median value ($p = 0.368$). Similarly, the 9000 and 10,000 lux groups showed no significant difference in their median values ($p = 0.769$).

4. Discussion

Based on the results obtained in this study, significant differences in scanning accuracy were found among the different ambient light illuminance values evaluated. Consequently, the null hypothesis was rejected. Based on the results obtained, the ambient light illuminance of 1000 lux obtained the best trueness and precision values compared with that of the other ambient lighting conditions tested.

Based on the European Standard for Illumination (EN 12,464), 1000 lux illumination corresponds with the recommended ambient lighting condition for the medical or examination room. However, this is a recommendation, not a strict rule, which is followed by dental clinics. Based on the results of the present study, variations in illumination intensity significantly influenced the scanning accuracy of the IOS tested (PrimeScan), recording a 4.8 times lower accuracy between the best and the worst ambient lighting conditions tested. Furthermore, the second-best ambient lighting condition (8000 lux) obtained 2.39 times lower scanning accuracy compared with the best (1000 lux). Therefore, the introduction of a lux meter in the digital armamentarium to maximize scanning accuracy is highly recommended.

Previous *in vitro* and *in vivo* studies performed by the same authors have demonstrated the influence of ambient lighting conditions on the scanning accuracy of IOSs [2–5]. Furthermore, those reports concluded that depending on the IOSs selected, the optimal ambient lighting condition may differ [2–5]. Koseglu et al. [8] obtained results similar to those reported by Revilla-León et al. [2–5]. In another study, Wesseman et al. [6] found that after comparing 6 IOSs (TRIOS 3, Cerec Omnicam, CS3600, iTero Element, GC Advaa, and Planmeca Emerald), TRIOS 3 obtained the lowest 3D mean discrepancy under different ambient lighting conditions, these results being consistent with those obtained by Revilla-León et al. [2]. However, Jivanescu et al. [7] reported that ambient lighting conditions could not be a relevant external factor that affects intraoral scanning accuracy. The present study was developed with the same typodont and methodology as used in previous *in vitro* studies to allow the correct comparison of results [2,3]. The particular typodont used by this research team lacked the lower right second premolar to simulate a clinical situation in which it is necessary to scan the interproximal faces of adjacent teeth correctly, which is more challenging than scanning a complete dentition typodont. Therefore, our results might be comparable. The authors are unaware of available literature on the scanning accuracy of the selected IOS under 12 different ambient lighting conditions. The present IOS tested obtained

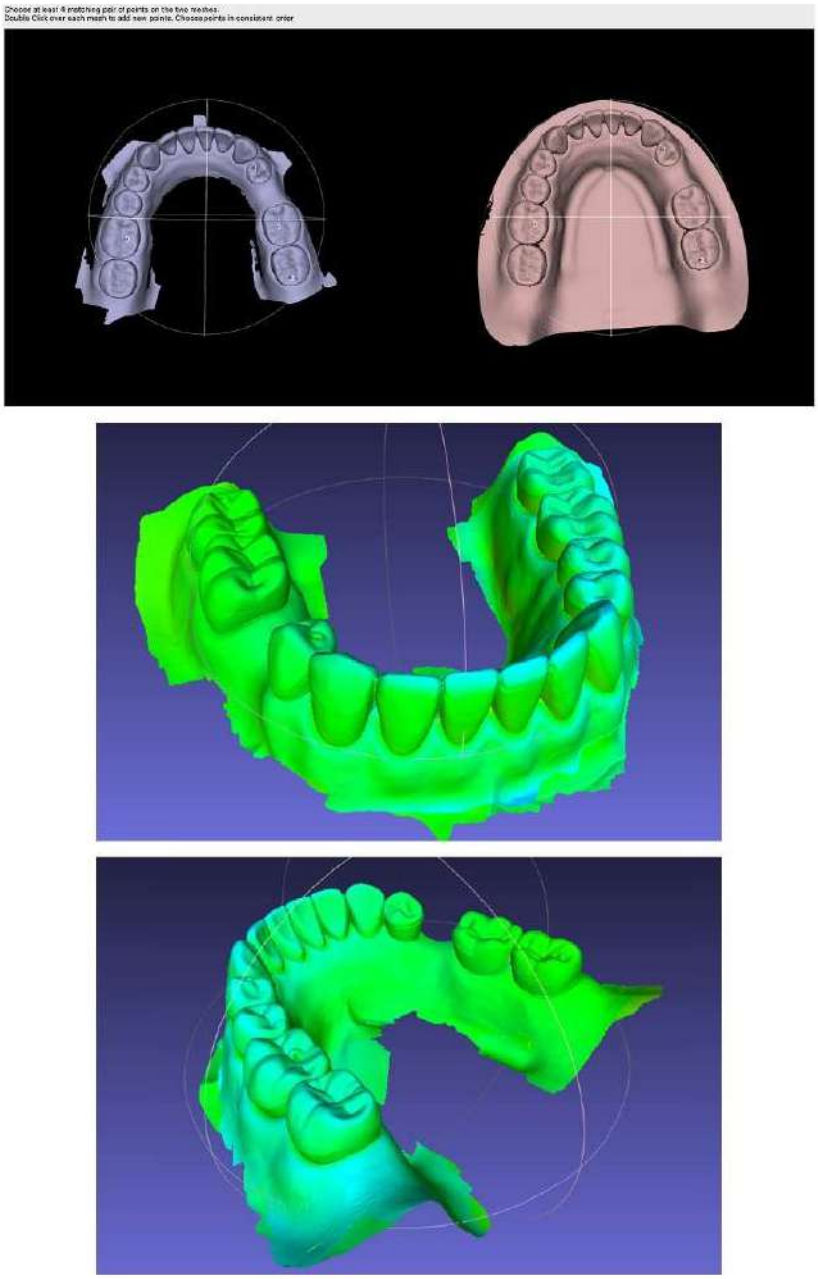

Fig. 2. A–C. (A) Typodont mesh alignment using iterative closest point algorithm in MeshLab. Pairs of correspondence points chosen. (B-C) Color coded signed distance field for treatment scan with respect to control mesh.

Table 2
Statistical aggregates of error of the IOS (PrimeScan; Dentsply Sirona) against lighting conditions tested. Values in micrometers.

Group	Trueness Median	Precision Interquartile range (IQR)
0 lux (ZL)	335.5	488.0
500 lux (NL)	322.6	482.5
1000 lux (RL)	69.5	97.4
2000 lux (CL-2)	315.1	468.8
3000 lux (CL-3)	293.3	452.0
4000 lux (CL-4)	309.0	473.3
5000 lux (CL-5)	308.8	466.9
6000 lux (CL-6)	304.5	463.9
7000 lux (CL-7)	195.7	330.7
8000 lux (CL-8)	166.5	318.1
9000 lux (CL-9)	195.5	338.1
10 000 lux (CL-10)	197.5	337.6

ZL, zero light, NL, natural light; RL, room light; CL, chair light.

the lowest distortion under 1000 lux illumination, with a trueness value of 69.5 μm and a precision value of 97 μm when performing a completely dentate arch digital scan. A previous study by the same authors, following the same methodologies, reported a trueness value of 191.85 μm for the Itero Element, 203.86 μm for the TRIOS 3, and 279.79 μm for the Cerec Omnicam, while precision values were 71.97 μm, 94.31 μm, and 247.06 μm, respectively. Therefore, the present IOS system recorded higher trueness values than these IOSs. However, a previous study tested six different ambient light illuminance conditions (0 lux, 100 lux, 500 lux, 1000 lux, 5000 lux and 10,000 lux) for the IOS tested in this research [9] and concluded that the optimal scanning ambient light illuminance for PrimeScan IOS was 10 000 lux, with a trueness of 65.6 μm and a precision of 46.8 μm but without significant differences with the 1000-lux group. In the present investigation, the 10 000-lux group obtained a trueness value of 197.5 μm and a precision of 337.6 μm. The differences found by this previous study could be explained because, in our study, the digital scans were performed on a dentate typodont, while, in their study, the scanned model was an edentulous typodont with metal scan bodies. Also, the authors stated that a zig-zag scanning pattern was performed, contrary to the scanning protocol used in our study. For these reasons, the results were not directly comparable with those of the present study. The different methodologies used made comparisons between the available studies difficult because of the complexity and area of the geometry analyzed (completely dentate arch or edentulous typodont with implants), superimposition software and method selected - best-fit algorithm or iterative closest point algorithm (ICP) - and/or reference model used. An ICP landmark-based algorithm needs a manual selection of different points to perform the alignment. As a manual procedure is required, a misalignment between 2 meshes is expected if compared with a best-fit algorithm, as demonstrated by Revilla-León et al. [46]. That is why in this study, a pre-alignment using an ICP algorithm was performed using the three metal markers, and then a best-fit algorithm was used to obtain the final global surface alignment.

Another factor that may have been considered is the operators' intraoral scanning experience level [35–37]. Scanning time and the number of images acquired by experienced and nonexperienced groups have been evaluated, and the more an intraoral scanning system is used the less time it takes to obtain the scan with fewer images. The level of operator experience may have a more significant impact on scanner precision than trueness [35–37].

Limitations of the present study included the *in vitro* environment in which the digital scans were performed and the digitized dentition corresponding to a typodont. Varying the substrate from *in vitro* to *in vivo* substrates will probably impact the nominal differences in the results, but ambient lighting will still be the factor influencing these values. Additional *in vivo* studies are recommended to fully understand the influence of lighting conditions on the accuracy of the tested intraoral digitizer. Also, only one scanner was used, and results should not be extrapolated to other IOSs. Further studies are needed to completely comprehend the influence of ambient light illuminance on the scanning accuracy of different IOS systems in different clinical settings and over different substrates.

5. Conclusions

Within the limitations of this *in vitro* study, the following conclusions were drawn:

1. Variations in the ambient lighting conditions had a significant influence on the scanning accuracy of the IOS tested.

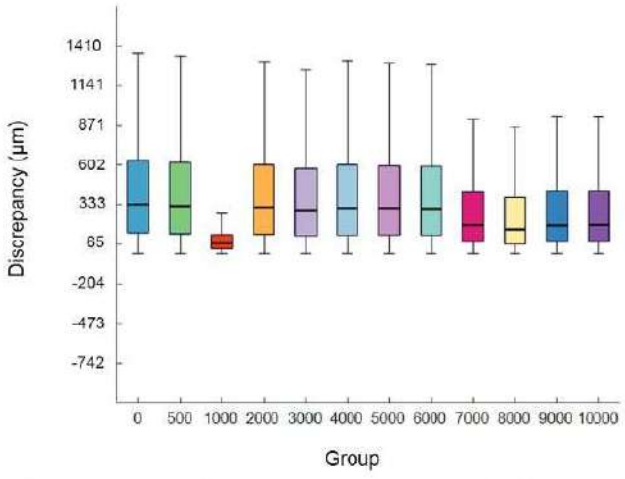

Fig. 3. Boxplot for trueness and precision of IOS tested (PrimeScan; Dentsply Sirona) among the different ambient light illuminance values evaluated (0-, 500, 1000, 2000, 3000, 4000, 5000, 6000, 7000, 8000, 9000, and 10,000 lx).

2. Ambient light illuminance influenced the scanning accuracy (trueness and precision) of the intraoral scanner tested (PrimeScan; Dentsply Sirona, Bensheim, Germany).
3. The optimal ambient light illuminance of the tested IOS was 1000 lux, obtaining the highest trueness and precision values; 0 lux obtained the lowest scanning accuracy values.
4. A lux meter is fundamental to maximizing the scanning accuracy of the IOS (PrimeScan; Dentsply Sirona, Bensheim, Germany) evaluated.

Funding

This research did not receive any specific grant from funding agencies in the public, commercial, or not-for-profit sectors.

CRediT authorship contribution statement

Wenceslao Piedra-Cascón: Conceptualization, Writing – original draft. **Riddhi R. Adhikari:** Formal analysis. **Mutlu Özcan:** Writing – review & editing. **Vinayak R. Krishnamurthy:** Formal analysis. **Marta Revilla-León:** Data curation. **Mercedes Gallas-Torreira:** Writing – review & editing.

Declaration of Competing Interest

The authors did not have any conflict interest, financial or personal, in any of the materials described in this study.

References

[1] T. Arakida, M. Kanazawa, M. Iwaki, T. Suzuki, S. Minakuchi, Evaluating the influence of ambient light on scanning trueness, precision, and time of intra oral scanner, J. Prosthodont. Res. 62 (2018) 324–329, https://doi.org/10.1016/j.jpor.2017.12.005.

[2] M. Revilla-León, P. Jiang, M. Sadeghpour, W. Piedra-Cascón, A. Zandinejad, M. Ozcan, et al., Intraoral digital scans-part 1: influence of ambient scanning light conditions on the accuracy (trueness and precision) of different intraoral scanners, J. Prosthet. Dent. 124 (2020) 372–378, https://doi.org/10.1016/j.prosdent.2019.06.003.

[3] M. Revilla-León, P. Jiang, M. Sadeghpour, W. Piedra-Cascón, A. Zandinejad, M. Ozcan, et al., Intraoral digital scans: part 2-influence of ambient scanning light conditions on the mesh quality of different intraoral scanners, J. Prosthet. Dent. 124 (2020) 575–580, https://doi.org/10.1016/j.prosdent.2019.05.004.

[4] M. Revilla-León, S.G. Subramanian, M. Ozcan, V.R. Krishnamurthy, Clinical study of the influence of ambient light scanning conditions on the accuracy (trueness and precision) of an intraoral scanner, J. Prosthodont. 29 (2020) 107–113, https://doi.org/10.1111/jopr.13135.

[5] M. Revilla-León, S.G. Subramanian, W. Att, V.R. Krishnamurthy, Analysis of different illuminance of the room lighting condition on the accuracy (trueness and precision) of an intraoral scanner, J. Prosthodont. 30 (2021) 157–162, https://doi.org/10.1111/jopr.13276.

[6] C. Wesemann, H. Kienbaum, M. Thun, B.C. Spies, F. Beuer, A. Bumann, Does ambient light affect the accuracy and scanning time of intraoral scans? J. Prosthet. Dent. (2020) 924–931, https://doi.org/10.1016/j.prosdent.2020.03.021.

[7] A. Jivanescu, A.B. Faur, R.N. Rotar, Can dental office lighting intensity conditions influence the accuracy of intraoral scanning? Scanning 27 (2021), 9980590 https://doi.org/10.1155/2021/9980590.

[8] M. Koseoglu, E. Kahramanoglu, H.K. Akin, Evaluating the effect of ambient and scanning lights on the trueness of the intraoral scanner, J. Prosthodont. 30 (2021) 811–816, https://doi.org/10.1111/jopr.13341.

[9] G. Ochoa-López, R. Cascos, J.L. Antonaya-Martín, M. Revilla-León, M. Revilla-León, N. Gómez-Polo, Influence of ambient light conditions on the accuracy and scanning time of seven intraoral scanners in complete-arch implant scans, J. Dent. 121 (2022), 104136, https://doi.org/10.1016/j.jdent.2022.104136 [Epub ahead of print].

[10] European lightening standard EN12464-1. Light and lighting - Lighting of work places - part 1: indoor work places (2011) 1–29.

[11] International organization for standardization. ISO 9680. Dentistry operating lights. Geneva: International Organization for Standardization; 2014. Available at: https://www.iso.org/standard/39276.html.

[12] S.B. Patzelt, S. Vonau, S. Stampf, W. Att, Assessing the feasibility and accuracy of digitizing edentulous jaws, J. Am. Dent. Assoc. 144 (2013) 914–920, https://doi.org/10.14219/jada.archive.2013.0209.

[13] T. Joda, F. Zarone, M. Ferrari, The complete digital workflow in fixed prosthodontics: a systematic review, BMC Oral Health 17 (2017) 124–131, https://doi.org/10.1186/s12903-017-0415-0.

[14] H. Khraishi, B. Duane, Evidence for use of intraoral scanners under clinical conditions for obtaining full-arch digital impressions is insufficient, Evid. Based. Dent. 18 (2017) 24–25, https://doi.org/10.1038/sj.ebd.6401224.

[15] W. Renne, M. Ludlow, J. Fryml, Z. Schurch, A. Mennito, R. Kessler, et al., Evaluation of the accuracy of 7 intraoral scanners: an *in vitro* analysis based on 3-dimensional comparison, J. Prosthet. Dent. 118 (2017) 36–42, https://doi.org/10.1016/j.prosdent.2016.09.024.

[16] V. Ruščinas, A. Gečiauskaitė, D. Jegelevičius, M. Vaitkūnas, Accuracy of digital implant impressions with intraoral scanners. A systematic review, Eur. J. Oral. Implantol 10 (2017) 101–120.

[17] P. Medina-Sotomayor, A. Pascual-Moscardó, I. Camps, Relationship between resolution and accuracy of four intraoral scanners in complete-arch impressions, J. Clin. Exp. Dent. 10 (2018) e361–e366, https://doi.org/10.4317/jced.54670.

[18] J. Abduo, M. Elseyoufi, Accuracy of intraoral scanners: a systematic review of influencing factors, Eur. J. Prosthodont. Restor. Dent. 26 (2018) 101–121, https://doi.org/10.1922/EJPRD_01752Abduo21.

[19] Y. Takeuchi, H. Koizumi, M. Furuchi, Y. Sato, G. Ohkubo, H. Matsumura, Use of digital impression systems with intraoral scanners for fabricating restorations and fixed dental prostheses, J. Oral. Sci. 60 (2018) 1–7, https://doi.org/10.2334/josnusd.17-0444.

[20] Y. Tomita, J. Uechi, M. Konno, S. Sasamoto, M. Iijima, I. Mizoguchi, Accuracy of digital models generated by conventional impression /plaster-model methods and intraoral scanning, Dent. Mater. J. 37 (2018) 628–633, https://doi.org/10.4012/dmj.2017-208.

[21] J. Malik, J. Rodriguez, M. Weisbloom, H. Petridis, Comparison of accuracy between a conventional and two digital intraoral impression techniques, Int. J. Prosthodont 31 (2018) 107–113, https://doi.org/10.11607/ijp.5643.

[22] R. Nedelcu, P. Olsson, I. Nyström, J. Rydén, A. Thor, Accuracy and precision of 3 intraoral scanners and accuracy of conventional impressions: a novel *in vivo* analysis method, J. Dent. 69 (2018) 110–118, https://doi.org/10.1016/j.jdent.2017.12.006.

[23] S.B. Patzelt, A. Emmanouilidi, S. Stampf, J.R. Strub, W. Att, Accuracy of full-arch scans using intraoral scanners, Clin. Oral. Investig. 18 (2014) 1687–1694, https://doi.org/10.1007/s00784-013-1132-y.

[24] A.S. Mennito, Z.P. Evans, A.W. Lauer, R.B. Patel, M.E. Ludlow, W.G. Renne, Evaluation of the effect scan pattern has on the trueness and precision of six intraoral digital impression systems, J. Esthet. Restor. Dent. 30 (2018) 113–118, https://doi.org/10.1111/jerd.12371.

[25] P. Medina-Sotomayor, A. Pascual-Moscardó, I. Camps, Relationship between resolution and accuracy of four intraoral scanners in complete-arch impressions, J. Clin. Exp. Dent. 10 (2018) 361–366, https://doi.org/10.4317/jced.54670.

[26] R. Nedelcu, P. Olsson, I. Nyström, A. Thor, Finish line distinctness and accuracy in 7 intraoral scanners versus conventional impression: an *in vitro* descriptive comparison, BMC Oral. Health 1 (2018) 18–27, https://doi.org/10.1186/s12903-018-0489-8.

[27] M. Zimmermann, A. Mehl, W.H. Mörmann, S. Reich, Intraoral scanning systems - a current overview, Int. J. Comput. Dent. 18 (2015) 101–129.

[28] T.F. Alghazzawi, Advancements in CAD/CAM technology: options for practical implementation, J. Prosthodont. Res. 60 (2016) 72–84, https://doi.org/10.1016/j.jpor.2016.01.003.

[29] T.V. Flügge, S. Schlager, K. Nelson, S. Nahles, M.C. Metzger, Precision of intraoral digital impressions with iTero and extraoral digitalization with iTero and a model scanner, Am. J. Orthod. Dentofacial. Orthop. 144 (2013) 471–478, https://doi.org/10.1016/j.ajodo.2013.04.017.

[30] P. Papaspyridakos, C.J. Chen, G.O. Gallucci, A. Doukoudakis, H.P. Weber, V. Chronopoulos, Accuracy of implant impressions for partially and completely edentulous patients: a systematic review, Int. J. Oral. Maxillofac. Implants. 29 (2014) 836–845, https://doi.org/10.1111/jopi.13211.

[31] G. De Luca Canto, C. Pachêco-Pereira, M.O. Lagravere, C. Flores-Mir, P.W. Major, Intra-arch dimensional measurement validity of laser-scanned digital dental models compared with the original plaster models: a systematic review, Orthod. Craniofac. Res. 18 (2015) 65–76, https://doi.org/10.1111/ocr.12068.

[32] G. Al-Jobuoi, A. Azari, An introduction to dental digitizers in dentistry: A systematic review, J. Chem. Pharm. Res. 7 (2015) 10–20.

[33] M.L. Aragón, L.F. Pontes, L.M. Bichara, C. Flores-Mir, D. Normando, Validity and reliability of intraoral scanners compared to conventional gypsum models measurements: a systematic review, Eur. J. Orthod. 38 (2016) 429–434, https://doi.org/10.1093/ejo/cjw033.

[34] R. Richert, A. Goujat, L. Venet, G. Viguie, S. Viennot, P. Robinson, et al., Intraoral scanners technologies: a review to make a successful impression, J. Health Eng. (2017) 1–9, https://doi.org/10.1155/2017/8427595.

[35] J. Kim, J.M. Park, M. Kim, S.J. Heo, I.H. Shin, M. Kim, Comparison of experience curves between two 3-dimensional intraoral scanners, J. Prosthet. Dent. 116 (2016) 221–230, https://doi.org/10.1016/j.prosdent.2015.12.018.

[36] J.H. Lim, J.M. Park, M. Kim, S.J. Heo, J.Y. Myung, Comparison of digital intraoral scanner reproducibility and image trueness considering repetitive experience, J. Prosthet. Dent. 119 (2018) 225–232, https://doi.org/10.1016/j.prosdent.2017.05.002.

[37] C.C.D. Resende, T.A.Q. Barbosa, G.F. Moura, L.D.N. Tavares, F.A.P. Rizzante, F. M. George, F.D.D. Neves, G. Mendonça, Influence of operator experience, scanner type, and scan size on 3D scans, J. Prosthet. Dent. 125 (2021) 294–299, https://doi.org/10.1016/j.prosdent.2019.12.011.

[38] B.M. Shearer, S.B. Cooke, L.B. Halenar, S.L. Reber, J.E. Plummer, E. Delson, et al., Evaluating causes of error in landmark-based data collection using scanners, PLoS One (2017) 1–37, https://doi.org/10.1371/journal.pone.0187452.

[39] T.F. Alghazzawi, K.H. Al-Samadani, J. Lemons, P.R. Liu, M.E. Essig, A. A. Bartolucci, et al., Effect of imaging powder and CAD/CAM stone types on the marginal gap of zirconia crowns, J. Am. Dent. Assoc. 146 (2015) 111–120, https://doi.org/10.1016/j.adaj.2014.10.006.

[40] J.W. Anh, J.M. Park, Y.S. Chun, M. Kim, A comparison of the precision of three-dimensional images acquired by two intraoral scanners: effects on tooth irregularities and scanning direction, Korean, J. Orthod. 46 (2016) 3–12, https://doi.org/10.4041/kjod.2016.46.1.3.

[41] P. Müller, A. Ender, T. Joda, J. Katsoulis, Impact of digital intraoral scan strategies on the impression accuracy using the TRIOS pod scanner, Quintessence Int. 47 (2016) 343–349, https://doi.org/10.3290/j.qi.a35524.

[42] J.M. Park, Comparative analysis on reproducibility among 5 intraoral scanners: sectional analysis according to restoration type and preparation outline form, J. Adv. Prosthodont. 8 (2016) 354–362, https://doi.org/10.4047/jap.2016.8.5.354.

[43] J.B. Carbajal Mejía, K. Wakabayashi, T. Nakamura, H. Yatani, Influence of abutment tooth geometry on the accuracy of conventional and digital methods of obtaining dental impressions, J. Prosthet. Dent. 118 (2017) 392–399, https://doi.org/10.1016/j.prosdent.2016.10.021.

[44] H. Li, P. Lyu, Y. Wang, Y. Sun, Influence of object translucency on the scanning accuracy of a powder-free intraoral scanner: a laboratory study, J. Prosthet. Dent. 117 (2017) 93–101, https://doi.org/10.1016/j.prosdent.2016.04.008.

[45] International Organization for Standardization. ISO 5725-1. Accuracy (trueness and precision) of measuring methods and results. Part-I: general principles and definitions. Berlin: International Organization for Standardization; 1994. Available at: https://www.iso.org/standard/11833.html.

[46] M. Revilla-León, A. Gohil, A.B. Barmak, A. Zandinejad, A.J. Raigrodsky, J.A. Pérez-Barquero, Best-Fit algorithm influences on virtual casts' alignment discrepancies, J. Prosthodont. (2022) 1–9, https://doi.org/10.1111/jopr.13537.

4.2 ARTÍCULO 2.

Piedra-Cascón W, Burgos-Artizzu XP, González-Martin O, Oteo-Morilla C, Pose-Rodriguez JM, Gallas-Torreira. Evaluation of the accuracy (trueness, precision) and processing time of different 3-dimensional CAD software programs and algorithms for virtual cast alignment. J Dent 2025; 155:105619

DOI: 10.1016/j.jdent.2025.105619

Revista: Journal of Dentistry

Factor de Impacto (JCR 2024): 5.5

Cuartil: Q1

Categoría: Dentistry, Oral Surgery and Medicine

Posición: 9/271

Link: https://linkinghub.elsevier.com/retrieve/pii/S0300-5712(25)00064-8

Journal of Dentistry 155 (2025) 105619

Contents lists available at ScienceDirect

Journal of Dentistry

journal homepage: www.elsevier.com/locate/jdent

Evaluation of the accuracy (trueness, precision) and processing time of different 3-dimensional CAD software programs and algorithms for virtual cast alignment

Wenceslao Piedra-Cascón [a,b,c,d,*], Xavier Paolo Burgos-Artizzu [e,f], Óscar González-Martín [g,h,i], Carlos Oteo-Morilla [j,i], Jose Manuel Pose-Rodriguez [k], Mercedes Gallas-Torreira [l]

[a] Doctoral Student, Doctoral Progamme in Dental Science, Stomatology Area, Department of Surgery and Medical-Surgery Specialitites. University of Santiago de Compostela, Spain
[b] Affiliate Faculty Esthetic Dentistry Program, Complutense University of Madrid, Spain
[c] Private practice, Oviedo, Spain
[d] Researcher at Movumtech. Madrid, Spain
[e] Faculty Member, Faculty of Computer Science, Multimedia and Telecommunications, Open University of Catalonia, Barcelona, Spain
[f] Researcher, MovumTech, Madrid, Spain
[g] Affiliate Faculty Member, Faculty of Restorative Dentistry and Biomaterials Sciences Harvard School of Dental Medicine, Boston, Mass, USA
[h] Affiliate Faculty Member, Faculty of Periodontology, Complutense University of Madrid, Madrid, Spain
[i] Private practice, Madrid, Spain
[j] Affiliate Faculty Member, Graduate in Esthetic Dentistry Program, Complutense University of Madrid, Madrid, Spain
[k] Associated Lecturer in Adult Comprehensive Dental Clinic. Stomatology Area, Department of Surgery and Medical-Surgery Specialities. Digital Dentistry Unit of the School of Dentistry, Faculty of Medicine and Dentistry. University of Santiago de Compostela, Spain
[l] Senior Lecturer in Planification and Management in Dental Clinics. Stomatology Area, Department of Surgery and Medical-Surgery Specialities. Digital Dentistry Unit of the School of Dentistry, Faculty of Medicine and Dentistry. University of Santiago de Compostela, Spain

ARTICLE INFO

Keywords:
Accuracy
Best fit
Alignment methods
Superimposition teheniques
Virtual casts

ABSTRACT

Objectives: This in vitro study aimed to evaluate the impact of different alignment algorithms and CAD software programs on alignment accuracy (trueness and precision) and processing time.
Methods: A mandibular typodont was digitized using a laboratory scanner (L2i) to obtain a reference standard tesselletion language (STLr) file. It was then scanned with an intraoral scanner (Primescan) and digitally duplicated ten times ($n = 10$). Each scan was aligned with the STLr using 42 combinations of 3D CAD software and alignment algorithms. The tested software programs included Blender for Dental, BlueSkyPlan, Dental CAD App (Exocad), Medit Design, NemoSmile, and Meshmixer. Alignment accuracy (trueness and precision) and processing time were recorded using Python software (v3.8). Statistical analysis was performed with a two-way ANOVA test ($\alpha = 0.01$) to identify overall differences, followed by a post hoc Tukey Honestly Significant Difference test ($\alpha = 0.05$) to establish rankings.
Results: Significant differences in alignment accuracy were observed based on the software and algorithm used, affecting both trueness ($p<.01$) and precision ($p<.01$). Processing time also varied significantly ($p<.01$). Post hoc analysis identified the optimal algorithm for each software, revealing variations in trueness, precision, and processing time among the optimal versions. Medit Design achieved the best overall performance by combining high accuracy with the fastest processing time, while Meshmixer exhibited the lowest accuracy due to its lack of advanced algorithms.
Conclusions: The choice of CAD software and alignment algorithm significantly influences alignment accuracy and efficiency. Best-fit and section-based provided the best results, offering valuable insights into the optimization of digital workflows in prosthodontics.
Clinical significance: Alignment protocols must be tailored to the specific CAD software program used, as no universal protocol was effective across all tested software. Optimizing alignment protocols reduces errors,

* Corresponding author: Doctoral Program in Dental Sciences University of Santiago de Compostela Rua Entrenïos, s/n, Santiago de Compostela 15782 Spain.
E-mail address: wpiedra@movumtech.com (W. Piedra-Cascón).

https://doi.org/10.1016/j.jdent.2025.105619
Received 26 May 2024; Received in revised form 3 February 2025; Accepted 6 February 2025
Available online 6 February 2025

enhances prosthodontic outcomes, and improves the reliability and efficiency of clinical and laboratory workflows, ultimately ensuring better patient care and treatment success.

1. Introduction

Prosthetic dental treatments have incorporated advanced 3-dimensional (3D) technologies, including facial scanners, intraoral scanners (IOSs), and cone beam computed tomography (CBCT), to obtain digital data from patients. These technologies facilitate the integration of patient data, enhancing the creation of virtual patients [1–7]. For this reason, computer-aided design (CAD) software programs are crucial when executing the superimposition procedures required [8–13]. The primary objective of alignment procedures is to achieve the highest degree of concordance, producing a close match to the reference mesh. Accurate alignment is a crucial step in digital dentistry, enabling the seamless integration of digital patient data into CAD software for the design and planning of dental treatment devices. This process is essential, as it significantly influences the clinical outcomes, highlighting its critical role in contemporary prosthetic dentistry. Misalignments in patient data can result in issues such as improper contact points, inadequate crown margin fit, occlusal discrepancies, or poor integration with the patient's face, all of which can compromise the effectiveness and functionality of the treatment [11–12].

The primary best-fit (BF) methods for aligning 3D files can be classified as BF, section-based best-fit (SBF), landmark-based best-fit (LBF), or a combination of these (LBF + BF, LBF + SBF, SBF + BF) [10–12]. The BF uses an iterative closest point (ICP) algorithm to align the entire datasets of 2-point clouds by iteratively minimizing the distance between corresponding points [13–15]. Every iteration includes 3 main steps known as correspondence, transformation calculation, and update transformation. The SBF is a computational method of aligning 2 data sets which need to be equal in both meshes [16–17] by constraining the alignment process to areas or regions designated manually by the operator. The LBF algorithm also involves the alignment of 2 datasets by the human selection of identifiable common points between each data set [13–15].

Most available dental CAD software programs offer multiple alignment algorithms [16–23]. Each implements a different number and type of these algorithms, and, unfortunately, manufacturers do not provide clear guidelines or recommendations on which of these algorithms should be used. Moreover, studies on the effect of each of these different algorithms and/or CAD software programs on alignment accuracy are scarce in the dental literature.

The aim of the present in vitro study was to measure the alignment accuracy (trueness, precision) and processing time of different algorithms and 3D CAD software programs. The null hypothesis was that no significant differences would be found in alignment accuracy nor in processing time.

2. Materials and methods

A mandibular typodont was digitized with a laboratory scanner to obtain a reference standard tessellation language file (STL_r) scanned with an IOS (Primescan; Dentsply-Sirona; Bensheim, Germany). The scan was manually aligned to the STL_r using six CAD 3D software programs with all their implemented algorithms (42 combinations). The process was repeated 10 times for each scan, resulting in 420 superpositions. Individual processing times were recorded. Once aligned, alignment accuracy (trueness and precision) was measured. A two-way ANOVA test ($\alpha = 0.01$) was performed to identify overall differences, followed by a post hoc Tukey Honestly Significant Difference test ($\alpha = 0.05$) to establish the performance of each alignment algorithm.

2.1. Data acquisition

A mandibular typodont (Hard gingiva jaw model MIS2010-I-HD-M-32; Nissin) was selected. Three metal markers (Suremark SL-10; Suremark) were fixed onto the mandibular typodont using cyanoacrylate resin (Scotch Super Glue; 3 M ESPE, Seefeld, Germany) to aid in reliable landmark selection for future superimposition procedures. The markers were attached to the occlusal surfaces of the first left molar, first right premolar, and second right molar teeth. The typodont was then digitized by using a desktop laboratory scanner (L2i; Imetric, Courgenay, Switzerland) without scan powder to obtain the reference standard tessellation language (STL_R) file (Fig. 1A). The laboratory scanner had been previously calibrated according to the manufacturer's recommendations. The manufacturer of this scanner specifies a trueness of <5 μm and a precision <10 μm.

The mandibular typodont was mounted on a dental simulator mannequin (NISSIN Type 2; Nissin, Kyoto, Japan). To reproduce the clinical environment, the interincisal opening was standardized to 50 mm. The typodont was digitized by a restorative dentist with extensive experience (a co-author of this study *initials omitted for review*) using a previously calibrated IOS scanner (Primescan; Dentsply Sirona, Bensheim, Germany) and scanning software program (Primescan; Dentsply Sirona, Bensheim, Germany) in a windowless room and with an ambient lighting condition of 1000 lux determined with a meter (LX1330B Light Meter; Dr. Meter Digital Illuminance, Union City, USA) (Fig. 1B) [2–3]. The scanning protocol was performed once as follows: digital scans were started occlusally on the mandibular left second molar. The tip of the scanner was tilted 60° in an oral direction and moved orally along the dental arch up to the mandibular right second molar. Then, the scanner was guided occlusally from the mandibular right second molar across the entire dental arch back to the mandibular left second molar. Finally, the scanner was tilted 60° in a buccal direction to complete the scans and moved buccally along the entire dental arch. The resulting STL scanned file was duplicated 10 times as STL_1, STL_2, ..., STL_{10}.

2.2. Digital scan alignment

Six different 3D CAD software programs were tested: B4D (Blender v.3.6.5; B4D, Queensland, Australia), BSP (BlueSkyPlan v.4.13; BlueSkyBio, Illinois, USA), DCA (DentalCAD v.3.2; Exocad, Darmstadt, Germany), MD (Medit Design v.2.1.4; Medit, Seoul, South Korea), NMS

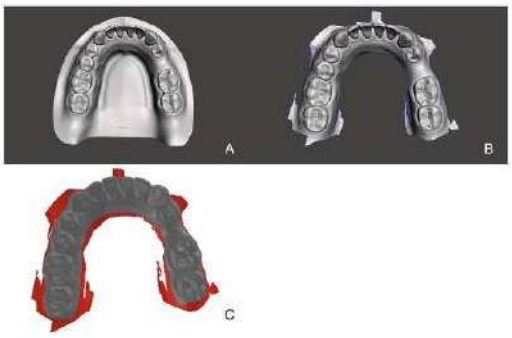

Fig. 1. A-C. A, Reference STL with 3 metal markers on occlusal surfaces. B, Test group STL. C, Test group boundary imperfections manually removal.

(NemoSmile v.24.0.0.3; Nemotec, Madrid, Spain), and MSH (Meshmixer v.3.5.474; Autodesk, California, USA).

Each of these software programs incorporated different algorithms, which were classified into 12 groups (Table 1). The number of implemented algorithms ranged from 3 to 11 (no single software was capable of performing all 12 algorithms). A total of 42 different software program and alignment algorithm combinations were available and tested (Table 2).

Each available 3D CAD software program and alignment algorithm combination was tested by the same operator, an expert clinician (and co-author of this study *initials omitted for review*) with 8 years of experience in 3D CAD software programs. Nonetheless, to incorporate intra-operator reliability, the process was repeated 10 times for each software program and algorithm combination, resulting in a total of 420 alignments. Each time, the STL_R file and digital scan were imported into the tested CAD software program (Fig. 2AD), the STL_R file was marked as the reference mesh, and the digital scan was aligned using the tested algorithm, with the resulting aligned STL files being stored.

2.3. Processing time

All 10 repetitions of each software/algorithm combination were performed consecutively using the same computer. The alignment procedures were performed on a system equipped with an MSI Intel Core i7–10870H CPU operating at 2.20 GHz, 32 GB of RAM, an NVIDIA GeForce RTX 3080 GPU, and running the Windows 11 Pro operating system. The time required to apply each algorithm was computed by using the creation time stamp in the metadata of each resulting STL file and reporting the mean elapsed time among all 9 pairs when using that software program and algorithm (Fig. 3AG).

2.4. Alignment accuracy

Proprietary python software code (Python v3.8; Python, Delaware, USA) was used to measure alignment accuracy (trueness and precision)

Table 1
Description of anatomic landmarks for each alignment algorithm group.

ALIGNMENT PROCEDURE	LANDMARKS AND SURFACES
BF	Entire dataset
LBF-3_o	3 markers attached to the occlusal surfaces.
LBF-6_o	3 occlusal markers + distobuccal of second left molar cusp, left canine cusp, and mesiobuccal cusp of first left molar
LBF-3_{xyz}	Occlusal marker on left first molar, gingival zenith of right first central incisor, and mesiolingual cusp of right first molar
LBF-6_{xyz}	3 markers + distobuccal cusp of left second molar, gingival zenith of right first central, and mesiolingual cusp of right first molar
SBF-3	First left molar, first right premolar, and second right molar teeth
SBF-6	First left molar, first right premolar, second right molar, second left premolar, left lateral incisor, and right lateral incisor
SBF-All	All teeth
LBF-3_o + BF	First alignment: 3 markers attached to occlusal surfaces. Second alignment: best-fit of pre-aligned entire data
LBF-3_{xyz} + BF	First alignment: Occlusal marker on left first molar, gingival zenith of right first central incisor, and mesiolingual cusp of right first molar Second alignment: best-fit of pre-aligned entire data
LBF-6_o + BF	First alignment: 3 markers + distobuccal of second left molar cusp, left canine cusp, and mesiobuccal cusp of first left molar Second alignment: best-fit of pre-aligned entire data
LBF-6_{xyz} + BF	First alignment: 3 markers + distobuccal cusp of left second molar, gingival zenith of right first central incisor, and mesiolingual cusp of right first molar Second alignment: best-fit of pre-aligned entire data

Table 2
Alignment errors for each alignment procedure performed on each 3D CAD software program tested.

Num	CAD Software	Alignment algorithm	Trueness (μm)	Precision (μm)	Processing time (seconds)
1	B4D	LBF-3o	110.70	70.79	196.0
2	B4D	LBF-3o + BF	67.35	55.52	230.0
3	B4D	LBF-3xyz	96.78	68.31	184.0
4	B4D	LBF-3xyz + BF	70.62	58.49	212.0
5	B4D	SBF-3	68.67	54.75	336.0
6	B4D	LBF-6o	99.78	65.90	98.0
7	B4D	LBF-6o + BF	67.04	54.59	124.0
8	B4D	LBF-6xyz	86.56	60.04	222.0
9	B4D	LBF-6xyz + BF	70.05	58.98	270.0
10	B4D	SBF-6	66.73	54.24	438.0
11	B4D	SBF-All	66.94	54.69	561.0
12	BSP	LBF-3o	161.80	83.04	66.0
13	BSP	LBF-3xyz	148.18	77.53	72.0
14	BSP	LBF-6o	128.92	62.10	66.0
15	BSP	LBF-6xyz	129.14	63.67	86.0
16	DCA	LBF-3o	105.60	69.72	160.0
17	DCA	LBF-3o + BF	70.09	57.07	167.0
18	DCA	LBF-3xyz	90.17	62.37	168.0
19	DCA	LBF-3xyz + BF	70.08	57.05	176.0
20	DCA	LBF-6o	79.00	59.34	184.0
21	DCA	LBF-6o + BF	70.09	57.05	203.0
22	DCA	LBF-6xyz	84.53	60.79	209.0
23	DCA	LBF-6xyz + BF	70.09	57.05	222.0
24	MD	SBF-All	71.09	56.59	130.0
25	MD	LBF-3o	70.44	56.46	40.0
26	MD	LBF-3xyz	70.53	56.53	55.0
27	MD	SBF-3	71.66	57.14	106.0
28	MD	BF	70.79	56.31	33.0
29	MSH	SBF-3	74.64	57.05	194.0
30	MSH	SBF-6	76.94	54.99	236.0
31	MSH	SBF-All	74.67	51.66	262.0
32	NMS	LBF-3o	84.88	60.20	68.0
33	NMS	LBF-3o + BF	76.62	66.55	88.0
34	NMS	LBF-3xyz	90.28	60.15	74.0
35	NMS	LBF-3xyz + BF	75.67	65.03	78.0
36	NMS	SBF-3	84.64	69.03	216.0
37	NMS	LBF-6o	92.73	62.95	80.0
38	NMS	LBF-6o + BF	76.75	66.76	102.0
39	NMS	LBF-6xyz	94.97	63.92	94.0
40	NMS	LBF-6xyz + BF	76.63	66.74	108.0
41	NMS	SBF-6	71.57	57.84	318.0
42	NMS	SBF-All	69.92	57.35	348.0

Software:
B4D (Blender; Blender for Dental, Queensland, Australia).
BSP (BlueSkyPlan; BlueSkyBio, Illinois, USA).
DCA (Dental CAD App; Exocad, Darmstadt, Germany).
MD (Medit Design; Medit, Seoul, South Korea).
NMS (NemoSmile; Nemotec, Madrid, Spain).
MSH (Meshmixer; Autodesk, California, USA).
Algorithms.
LBF: Landmark Based Fit algorithm (see Table 1 for more details).
SBF: Section Based Fit algorithm (see Table 1 for more details).
BF: Best Fit algorithm (see Table 1 for more details).

between each of the resulting aligned STL files ($N = 420$) and the reference mesh STL_{RL}.

The STL file format represented data as a connected triangular mesh (M) composed of a number (NV) of 3D vertices $V = \{v_1 \ldots v_{NV}\} \in \mathbb{R}^3$ and a number (NF) of Faces $F = \{f_1 \ldots f_{NF}\}$, where each face is a triangle composed by 3 distinct vertices $f_i = \{(a, b, c) \in [1, NV] \wedge a \neq b \neq c\}$. Vertices appear on more than one face, forming a connected mesh. No unreferenced vertices or duplicate or empty faces were present. To compute alignment accuracy, triangular meshes $M(V, F)$ were first

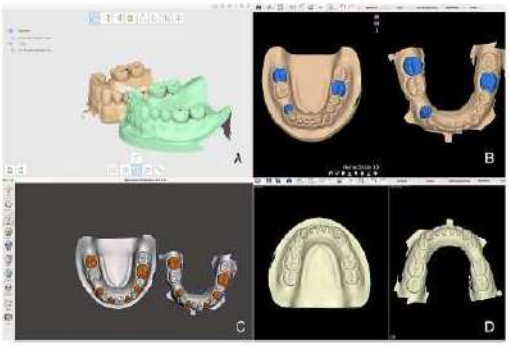

Fig. 2. A-D. Illustrative representations of different alignment algorithms performed in different CAD software programs. A) LBF-3_{xyz} Medit Design; Medit Link, B) SBF-3 NemoScan; Nemotec, C) SBF-6 Meshmixer; Autodesk, D) LBF-6_o NemoScan; Nemotec.

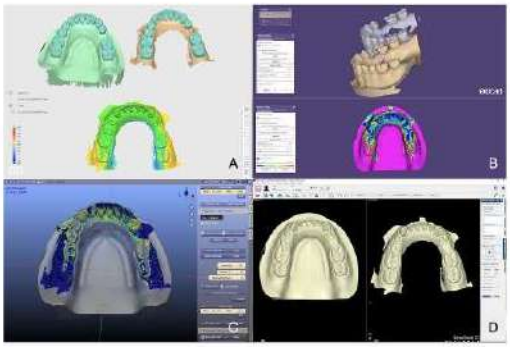

Fig. 3. A-D. Colored deviation maps between reference STL $_{Ile}$ and intraoral digital scan. A, SBF-All Medit Design; Medit. B, LBF-3_{xyz} DentalCAD App; Exocad GmbH. C, LBF-3_o + BF B4D; Blender Foundation. D, LBF-3_o NemoSmile 3D; Nemotec.

converted into a list of (NF) 3D points $P = \{p_1 \ldots p_{NF}\} \in \mathbb{R}^3$, each defined as the centroid position of each Face triangle $p_i = [v_{ai} + v_{bi} + v_{ci}/3]$.

Given the list of points from the aligned STL mesh (P^{scan}) and reference's STL_R (P^{ref}), Euclidean distance in three dimensions was computed between each pair of closest points: $Dist\left(p_{id}^{scan}, p_{id}^{ref}\right) = \sum_{d=1}^{3}\sqrt{\left(p_{id}^{scan} - p_{id}^{ref}\right)^2}/3$. Note: since the scanned STL presented imperfect outlier boundaries which were not present in the reference STL_R, these points were manually selected and removed beforehand (Fig. 1C).

Alignment accuracy was evaluated in accordance with ISO 5725–1 [24,25] and previous studies [2–4] using metrics of trueness and precision. Trueness was determined by calculating the mean difference between distances in the STL_T and the control groups, while precision was quantified as the standard deviation for each alignment technique.

2.5. Statistical analysis

The number of repetitions necessary for each group was estimated via power sampling to have a confidence interval of CI=95 % and a width for the interval of one. $N = 10$ was established in accordance with prior studies [2–4]. Once all metrics (trueness, precision and processing times) had been obtained, individual results were reported, as well as the averages of different groups. Then, significance tests were performed to compare the software and algorithms as independent factors. To establish whether any interactions occurred between the two and/or whether significant differences existed in each factor group, trueness, precision, and processing time were tested separately using a nonparametric type II two-way ART ANOVA (Aligned Rank Transform ANOVA). The nonparametric version of ANOVA was selected, since data were found to be nonhomoscedastic (Levene test, $p<.01$) and nonnormal (Kolmogorov–Smirnov test $p<.01$). Since not all software programs can perform all algorithms and the number each one is capable of performing varied greatly, we used different factorial balanced designs to test for the effect of each factor and the interactions between the two in different scenarios.

Finally, we conducted post hoc testing using the Turkey Honestly Significant Difference (HSD) to analyze the statistical results of algorithms from each software and to establish the performance of each software. All statistical analysis calculations were performed using proprietary python software code (Python v3.8; Python, Delaware, USA).

3. Results

The alignment accuracy and processing time of each of the 42 combinations of CAD software program and alignment algorithm is shown in Table 2. Mean trueness ranged from 67 to 162 µm, while mean precision ranged from 51 to 83 µm. Mean processing time ranged from 33 to 561 s. Fig. 4 shows a 2D visualization of the results from Table 2.

The average result for each of the algorithm groups (selecting only the software capable of performing that algorithm) is shown in Table 3. Mean trueness ranged from 70.51 to 106.68 µm, while mean precision ranged from 54.57 to 68.04 µm. Mean processing time ranged from 68 to 348 s. The algorithms that obtained the best results were those that incorporated best-fit (BF), followed by section-based (SBF), and finally, landmark-based (LBF).

To test the significance of the results of the different algorithms, a two-way ART ANOVA was performed on three different sets:

1) the four software programs (B4D, BSP, DCA, NMS) capable of performing landmark-based algorithms (LBF-3_{xyz}, LBF-6_{xyz}, LBF-3_o, LBF-6_o);
2) the four software programs (B4D, MD, MSH, NMS) capable of performing section-based algorithms (SBF-3 and SBF-All);
3) the three software programs (B4D, DCA, NMS) capable of performing best-fit algorithms (LBF-3_{xyz},+ BF, LBF-6_{xyz},+ BF, LBF-3_o,+ BF, LBF-5_o,+ BF).

In all cases, the software and algorithms had no interaction effect on each other in either trueness, precision, or time ($p>.05$). After removing that term, the algorithm used always showed a significant effect on trueness, precision, and time ($p<.01$) in all three scenarios. Finally, the software was also found to have a significant effect on trueness and precision in the last two scenarios (SBF and BF algorithms, $p<.01$).

The Turkey Honestly Significant Difference (HSD) post hoc test was then conducted. First, the optimal algorithm for each software was established. The optimal algorithm was defined as the fastest one (HSD processing time $p<.05$) among those with similar accuracy (trueness $p>.05$ and precision $p>.05$) compared with the overall best (lowest trueness and precision). Then, each optimal software/algorithm combination was ranked from best to worst, grouping together those not showing significant differences between them in some of the three metrics (trueness, precision or processing time) (Table 4).

MD using BF algorithm fared as the overall best combination, being faster than any other while reaching similar accuracy (trueness $p>.05$ and precision $p>.05$) compared with the optimal versions of three other

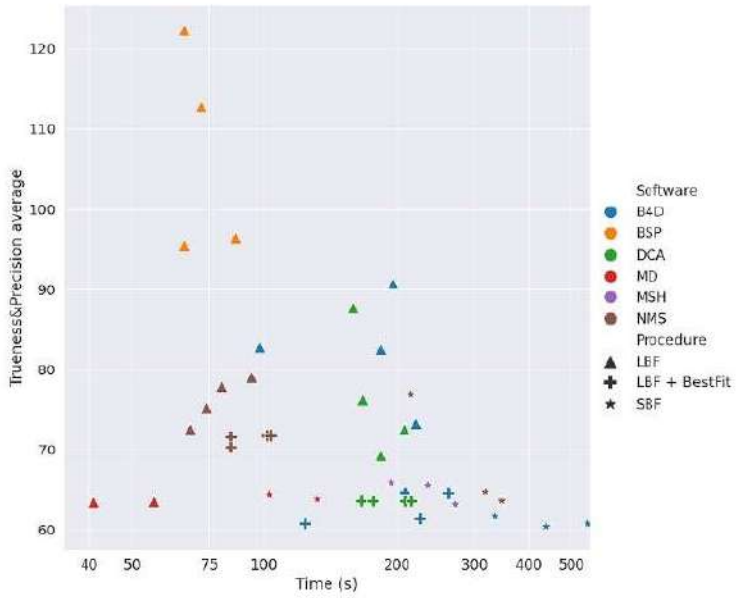

Fig. 4. Average alignment accuracy versus time required for each software program and alignment combination. X-axis: Time required (seconds). Y-axis: alignment accuracy (μm).

software programs (B4D, DCA, MSH). NMS reached similar Trueness ($p>.05$) but worse Precision ($p<.05$) and was slower ($p<.05$). Finally, MSH fared as the worst overall, reaching worse trueness ($p<.05$), precision ($p<.05$), and processing time ($p<.05$) because it did not implement either SBF or BF algorithms (Table 5).

4. Discussion

This study evaluated the accuracy, in terms of trueness and precision, of twelve different alignment algorithms and six software programs for virtual cast alignment. While previous authors have assessed the impact of various alignment algorithms, they did not test the same dataset among six dental and nondental CAD software programs with 12 alignment algorithms or measure the processing time required for each alignment [22].

Based on the results obtained in this study, the BF algorithms tested showed significant differences in both alignment error values (mean trueness and precision) and mean processing time; hence, the null hypothesis that no significant differences would be found in the alignment accuracy and the processing time among the reference and digital casts using the different alignment strategies tested was rejected. The SBF algorithms obtained lower discrepancies in trueness compared with the LBF algorithm methodologies. However, the processing time needed to perform the SBF algorithms was higher if compared with that of the LBF algorithms. SBF and LBF protocols need a human operator to select common landmark points or areas between the two 3D meshes. However, the errors introduced by manual procedures could be minimized by using a second-pass BF algorithm, thereby obtaining the highest alignment accuracy regarding trueness and precision.

Digital prosthetic treatments, including computer-aided dental implant planning, diagnostic waxing procedures, prosthetically driven devices, CAD designs, and three-dimensional virtual patient representations, require the highest alignment accuracy to facilitate the development of multidisciplinary diagnostics, treatment plans, and training simulations before clinical procedures. The present in vitro study revealed discrepancies of up to 95 μm in trueness and 31 μm in precision among the alignment algorithms tested in the selected CAD software programs, demonstrating that the algorithm selected affected the final outcome. While most dental CAD software programs allow users to select the alignment algorithm, there is a notable lack of scientific evidence guiding these choices, an oversight given the critical role alignment accuracy plays in treatment success. As far as we know, an established clinical threshold for virtual casts alignment in digital dentistry has not been published. Therefore, minimizing alignment errors is crucial to ensure a reliable digital workflow. Previous authors have reported accuracies in virtual cast alignments with trueness ranging from 150 μm to 200 μm and precision ranging from 1 μm to 37 μm, leading to an overall virtual cast alignment accuracy ranging from 149 μm to 237 μm [22]. Furthermore, studies that evaluated the impact of different alignment protocols on the superimposition accuracy of complete arch meshes are sparse. Moreover, disparities in research methodologies and differences among the data sets used in each study make comparisons challenging. Becker et al. [19] studied the alignment error discrepancies using LBF procedures by selecting 10 anatomic points and evaluated improvements when ICP methodologies were used in an open-source software program (Meshlab). The authors stated that LBF could produce alignment discrepancies higher than 0.5 mm and that ICP algorithms could successfully reduce initial alignment discrepancies when they were below 0.5 mm. The authors concluded that ICP algorithms could improve LBF procedures, consistent with the present study. Revilla-León et al. [22] assessed the following alignment algorithms: entire data set BF, 3 or 6 occlusal LBF, and 3 teeth SBF, concluding that LBF algorithms produced the highest alignment discrepancies compared with the entire BF and SBF. However, their results showed that both BF and SBF obtained the highest trueness and precision. Also, they reported statistically significant differences among 3 occlusal points LBF and 6 occlusal points LBF, while the results of the present study showed no significant differences in trueness ($p=.056$) or processing time ($p=.907$).

Table 3
Average alignment error for each alignment procedure group tested and the association of each alignment algorithm with its corresponding CAD software.

Alignment algorithm	CAD Software	Trueness (μm)	Precision (μm)	Processing time (seconds)
LBF-3o	B4D, BSP, DCA, MD, NMS	106.68	68.04	68.0
LBF-3o + BF	B4D, DCA, NMS	71.36	59.71	167.0
LBF-3xyz	B4D, BSP, DCA, MD, NMS	99.19	64.96	74.0
LBF-3xyz + BF	B4D, DCA, NMS	72.12	60.19	176.0
LBF-6o	B4D, BSP, DCA, NMS	100.11	62.57	89.0
LBF-6o + BF	B4D, DCA, NMS	71.29	59.47	124.0
LBF-6xyz	B4D, BSP, DCA, NMS	98.75	61.88	151.0
LBF-6xyz + BF	B4D, DCA, NMS	72.32	60.92	222.0
SBF-3	B4D, MD, MSH, NMS	74.90	59.49	205.0
SBF-6	B4D, MSH, NMS	71.75	55.39	318.0
SBF-All	B4D, MD, MSH, NMS	70.51	54.57	348.0

Software.
B4D (Blender; Blender for Dental, Queensland, Australia).
BSP (BlueSkyPlan; BlueSkyBio, Illinois, USA).
DCA (Dental CAD App; Exocad, Darmstadt, Germany).
MD (Medit Design; Medit, Seoul, South Korea).
NMS (NemoSmile; Nemotec, Madrid, Spain).
MSH (Meshmixer; Autodesk, California, USA).
Algorithms.
LBF: Landmark Based Fit algorithm (see Table 1 for more details).
SBF: Section Based Fit algorithm (see Table 1 for more details).
BF: Best Fit algorithm (see Table 1 for more details).

Table 4
Software and alignment algorithms performance, trueness, precision and processing time based on Turkey Honestly Significant Difference statistical test.

Performance	CAD Software	Alignment Algorithm	Trueness (μm)	Precision (μm)	Processing time (seconds)
Best Overall	MD	BF	70.79	56.31	33.0
Comparable accuracy but slower ($p<.05$)	B4D	LBF-6o + BF	67.04	54.59	124.0
	DCA	LBF-3xyz + BF	70.08	57.05	176.0
	MSH	SBF-All	74.67	51.66	262.0
Comparable trueness but worse precision and slower ($p < .05$)	NMS	LBF-3xyz + BF	75.67	65.03	78.0
Worse trueness and precision and slower ($p < .05$)	BSP	LBF-6o	128.92	62.10	66.0

Software.
B4D (Blender; Blender for Dental, Queensland, Australia).
BSP (BlueSkyPlan; BlueSkyBio, Illinois, USA).
DCA (Dental CAD; Exocad, Darmstadt, Germany).
MD (Medit Design; Medit, Seoul, South Korea).
NMS (NemoSmile; Nemotec, Madrid, Spain).
MSH (Meshmixer; Autodesk, California, USA).
Algorithms.
LBF: Landmark Based Fit algorithm (see Table 1 for more details).
SBF: Section Based Fit algorithm (see Table 1 for more details).
BF: Best Fit algorithm (see Table 1 for more details).

Table 5
Licensing for each CAD software program.

Software	Licensing
Medit Design	Free
Blender for Dental	One-time purchase
DentalCAD	Annual License
Nemosmile	Annual License
Meshmixer	Free
BlueSkyPlan	Freemium (Pay-per-use)

However, statistically significant differences were found in precision (p=.004) when LBF-3o and LBF-6o were compared. Moreover, no statistically significant differences were found in trueness (p=.296), precision (p=.134), and processing time (p=.077) when LBF-3_{xyz} and LBF-6_{xyz} alignment algorithms were compared.

Regarding SBF algorithms, all CAD software programs implementing the SBF algorithms performed similarly in selecting SBF-3 or SBF-6, except the NMS software program (NemoSmile), which performed better implementing an SBF-All algorithm (69.92 ± 57.35 μm) when compared with SBF-6 (71.57 ± 57.84 μm) and SBF-3 (84.64 ± 69.03 μm). The results reported by Revilla-León et al. [22] were partially consistent with the results of the present study, since BF algorithms were demonstrated to be the alignment procedure of choice with the fewest RMS errors. The discrepancies could be explained as differences in the reference extraoral scanners used to obtain the reference STL file, the IOS used for digitization, or the differences in the software programs and protocols tested in both studies. Dede et al. [23] compared a metrology-grade software program (Geomagic Control X) with a nonmetrology-grade freeware program (Medit Design) to measure RMS deviations in complete arch implant-supported frameworks. They concluded that no significant differences were present between the software programs when overall RMS values were considered. None of these studies measured the time needed to perform each alignment procedure.

The authors are unaware of previous studies on the alignment accuracy of 6 different dental and nondental CAD software programs used in clinical and laboratory practice, testing 12 different alignment procedures, and measuring the processing time needed to perform each alignment procedure. Regarding alignment accuracy, the ideal software program can be defined as one that achieves the highest alignment accuracy in the shortest time [13]. Most previous studies have focused solely on accuracy values, without considering the time required for alignment, which is crucial in daily clinical and laboratory routines. Independently of the CAD software program used, the algorithm affected trueness, precision, and time (p<.01). The results of the present investigation show that the best alignment algorithm was BF followed by the LBF in conjunction with a second-pass BF for performing cast alignment procedures. Finally, the CAD software program used had an impact on trueness and precision when section-based (SBF) and second-pass best-fit (BF) algorithms were used. A comparison between the best and fastest alignment algorithms for each software program tested was performed. Faster alternative alignment algorithms were defined as those reaching similar alignment accuracy according to Turkey Honestly Significant Difference testing (α=0.05) and requiring significantly less processing time. In absolute terms of accuracy, the best CAD software program was B4D, which obtained an accuracy of 66.73 ± 54.24 μm but required 438 s to perform the alignment using a SBF-6 alignment protocol. However, the faster alternative algorithm for the same software obtained an accuracy of 67.04 ± 54.59 μm and required 124 s. This means a reduction of 3.5 × of the time needed to perform the alignment, with no impact on the global accuracy alignment obtained.

Moreover, considering the fastest software program, the MD software program obtained its best alignment accuracy of 70.44 ± 56.46 μm in 40 s using the LBF-3o algorithm. However, the faster alternative algorithm obtained a mean trueness of 70.79 μm and mean precision of 56.31 μm, requiring 33 s with only a best-fit algorithm. The mean time spent on each software program and procedure combination showed considerable differences, with multipliers of 17 × between the fastest and slowest combination (33 s versus 561 s). Regarding the results of the present investigation, the differences in trueness between the best and the fastest software was similar (3.71 μm in trueness and 2.22 μm in precision), while the differences in the time required to perform the same alignment differed by 398 s.

The findings of this investigation suggest valuable guidance for clinicians and laboratory technicians in selecting the most appropriate alignment algorithm and protocol based on the CAD software used. An additional consideration is software licensing and pricing. Some of the CAD software tested in this study are free, such as Meshmixer and Medit Design, while others use a free or premium model (BlueSkyPlan) or require a paid annual license (Exocad and Nemotec) or a modular one-time purchase, (Blender for Dental). This distinction may impact the accessibility and selection of software by users. However, the findings of this study indicate no direct relationship between software cost and virtual cast alignment accuracy. Notably, Medit Design and Blender for Dental offered the best value for money, combining affordability with high alignment accuracy.

It must be taken into account that when alignments are made in CAD software, there are different methods of visual representation of the alignment performed. Medit, Exocad and Blender software provide a visual scale with a color map. In Medit, a green alignment means a discrepancy of 0 μm, blue −0.2, and yellow 0.5 mm, while in evoked and Blender software, a blue color means a discrepancy between 0 a 0.01 μm, a green color means a discrepancy between 0.04 and 0.05 μm, and a red color means a discrepancy up to 0.1 μm. However, Nemotec software does not provide visual information through a color map. Instead, this software offers the alignment error performed by RMS value, which is less intuitive for the user to understand the error obtained in the alignment. The more this value tends to zero, the better the alignment obtained. However, two software programs tested in this study, Meshmixer and BlueSkyPlan, do not provide any type of information, visual or numerical, about the alignment obtained.

The digital files used in this study were composed of a typodont digitized using two different noncontact optical scanners: a laboratory scanner (L2; Imetric 4D Imaging) and an IOS (Primescan; Dentsply Sirona). The intraoral scanner (IOS) used in this study demonstrated a reported accuracy in a previous investigation, achieving a trueness of 69.5 μm and a precision of 97.5 μm [3]. Also, the scanning protocol performed followed the manufacturer's recommendations and was additionally supported by findings from Piedra-Cascón et al. [3]. The combination of a laboratory scanner and the selected IOS was used to simulate a clinical situation.

Limitations of this study included the in vitro design and the evaluation of only a single intraoral scanner (IOS). Additionally, the laboratory scanner used had a specified trueness of <5 μm and a precision of <10 μm, which could have influenced the results. Potential scanning inaccuracies may also have arisen because of the metal markers attached to the occlusal surfaces of the typodont. Differences in the results regarding alignment procedure selection, accuracy, and processing time needed should be expected when aligning STL files with higher differences between the meshes, such as edentulous areas resulting in fewer common references for alignment. Further in vivo and in vitro studies are needed to evaluate alignment accuracy depending on the clinical situation.

5. Conclusions

Based on the findings of this in vitro study, the following conclusions were drawn:

1. The top performer alignment algorithm in terms of accuracy and processing time was the BF algorithm implemented by Medit Design software.
2. The worst performer alignment algorithm in terms of accuracy and processing time was the LBF-6o algorithm implemented by BlueSkyPlan software.
3. Section-based BF procedures significantly improved trueness compared with landmark-based BF methodologies but significantly increased the time required.
4. Incorporating second-pass best-fit algorithms into alignment procedures improved trueness and precision while not significantly impacting the required time.

Funding

This research did not receive any specific grant from funding agencies in the public, commercial, or not-for-profit sectors.

CRediT authorship contribution statement

Wenceslao Piedra-Cascón: Writing – original draft, Methodology, Conceptualization. **Xavier Paolo Burgos-Artizzu:** Writing – original draft, Software, Methodology, Formal analysis, Data curation. **Óscar González-Martín:** Writing – review & editing, Validation. **Carlos Oteo-Morilla:** Writing – original draft, Methodology, Conceptualization. **Jose Manuel Pose-Rodriguez:** Supervision, Conceptualization. **Mercedes Gallas-Torreira:** Writing – review & editing, Supervision, Project administration, Formal analysis.

Declaration of competing interest

The authors did not have any conflict interest, financial or personal, in any of the materials described in this study.

References

[1] T. Joda, U. Brägger, G. Gallucci, Systematic literature review of digital three-dimensional superimposition techniques to create virtual dental patients, Int. J. Oral Maxillofac. Implants 30 (2015) 330–337, https://doi.org/10.11607/jomi.3852.

[2] M. Revilla-León, P. Jiang, M. Sadeghpour, W. Piedra-Cascón, A. Zandinejad, M. Özcan, V.R. Krishnamurthy, Intraoral digital scans. Part 1: Influence of ambient scanning light conditions on the accuracy (trueness and precision) of different intraoral scanners, J. Prosthet. Dent. 124 (2020) 372–378, https://doi.org/10.1016/j.prosdent.2019.06.003.

[3] W. Piedra-Cascon, R.R. Adhikari, M. Özcan, V.R. Krishnamurthy, M. Revilla-Leon, M. Gallas-Torreira, Accuracy assessment (trueness and precision) of a confocal-based intraoral scanner under twelve different ambient lighting conditions, J. Dent. 134 (2023) 104530, https://doi.org/10.1016/j.jdent.2023.104530.

[4] W. Piedra-Cascon, M.J. Meyer, M.M. Methani, M. Revilla-Leon, Accuracy (trueness and precision) of a dual-structured light facial scanner and interexaminer reliability, J. Prosthet. Dent. 124 (2020) 567–574, https://doi.org/10.1016/j.prosdent.2019.10.010.

[5] S.P. Arunyanak, B.T. Harris, G.T. Grant, D. Morton, W.S. Lin, Digital approach to planning computer-guided surgery and immediate provisionalization in a partially edentulous patient, J. Prosthet. Dent. 116 (2016) 8–14, https://doi.org/10.1016/j.prosdent.2015.11.023.

[6] M. Revilla-León, D.E. Kois, J.M. Zeitler, W. Att, J.C. Kois, An overview of the digital occlusion technologies: intraoral scanners, jaw tracking systems and computerized occlusal analysis devices, J. Esthet. Restor. Dent. 5 (2023) 735–744, https://doi.org/10.1111/jerd.13044.

[7] W. Piedra-Cascón, J. Fountain, W. Att, M. Revilla-León, 2D and 3D patient representation of simulated restorative esthetic outcomes using different computer-aided design software programs, J. Esthet. Restor. Dent. 33 (2021) 143–151, https://doi.org/10.1111/jerd.12709.

[8] M. Revilla-León, J.A. Pérez-Barquero, B.A. Barmak, R. Agustín-Panadero, L. Fernández-Estevan, W. Att, Facial scanning accuracy depending on the alignment algorithm and digitized surface area location: an in vitro study, J. Dent. 110 (2021) 103680, https://doi.org/10.1016/j.jdent.2021.103680.

[9] M. Revilla-León, A. Zandinejad, M.K. Nair, A.B. Barmak, A.J. Feilzer, M. Özcan, Accuracy of a patient 3-dimensional virtual representation obtained from the superimposition of facial and intraoral scans guided by extraoral and intraoral

scanbody systems, J. Prosthet. Dent. 128 (2022) 984–993, https://doi.org/10.1016/j.prosdent.2021.02.023.
[10] K. Son, W.S. Lee, K.B. Lee, Effect of different software programs on the accuracy of dental scanner using three-dimensional analysis, Int. J. Environ. Res. Public Health 18 (2021) 8449, https://doi.org/10.3390/ijerph18168449.
[11] X. Garikano, X. Amezua, M. Iturrate, E. Solaberrieta, Evaluation of repeatability of different alignment methods to obtain digital interocclusal records: an in vitro study, J. Prosthet. Dent. 131 (2024) 709–717, https://doi.org/10.1016/j.prosdent.2022.07.014.
[12] M.G. Pérez-Giugovaz, S.H. Park, M. Revilla-León, Three-dimensional virtual representation by superimposing facial and intraoral digital scans with an additively manufactured intraoral scan body, J. Prosthet. Dent. 126 (2021) 459–463, https://doi.org/10.1016/j.prosdent.2020.07.012.
[13] P.J. Besl, N.D. McKay, A method for registration of 3-D shapes, IEEe Trans. Pattern. Anal. Mach. Intell. 14 (1992) 239–256, https://doi.org/10.1109/34.121791.
[14] H. Mora, J.M. Mora-Pascual, A. García-García, P. Martínez-González, Computational analysis of distance operators for the iterative closest point algorithm, PLoS. One 11 (2016) e0164694, https://doi.org/10.1371/journal.pone.0164694.
[15] S. Rusinkiewicz, M. Levoy, Efficient variants of the ICP algorithm, in: Proc Int Conf 3-D Digit Imaging Model, 2001, pp. 45–52, https://doi.org/10.1109/IM.2001.924423.
[16] S.D. Heintze, G. Zellweger, S. Sbicego, V. Rousson, C. Muñoz-Viveros, T. Stober, Wear of two denture teeth materials in vivo: 2-year results, Dent. Mater. 29 (2013) e191–e204, https://doi.org/10.1016/j.dental.2013.04.012.
[17] A. Mehl, W. Gloger, K.H. Kunzelmann, R. Hickel, A new optical 3-D device for the detection of wear, J. Dent. Res. 76 (1997) 1799–1807, https://doi.org/10.1177/00220345970760111201.
[18] S. O'Toole, C. Osnes, D. Bartlett, A. Keeling, Investigation into the accuracy and measurement methods of sequential 3D dental scan alignment, Dent. Mater. 35 (2019) 495–500, https://doi.org/10.1016/j.dental.2019.01.012.
[19] K. Becker, B. Wilmes, C. Grandjean, D. Drescher, Impact of manual control point selection accuracy on automated surface matching of digital dental models, Clin. Oral Investig. 22 (2018) 801–810, https://doi.org/10.1007/s00784-017-2155-6.
[20] A.K. Keeling, P.A. Brunton, R.J. Holt, An in vitro study into the accuracy of a novel method for recording the mandibular transverse horizontal axis, J. Dent. 42 (2014) 122–128, https://doi.org/10.1007/s00784-017-2155-6.
[21] H.L. Mitchell, R.G. Chadwick, Mathematical shape matching as a tool in tooth wear assessment: development and conduct, J. Oral Rehabil. 25 (1998) 921–928, https://doi.org/10.1046/j.1365-2842.1998.00324.x.
[22] M. Revilla-León, A. Gohil, A.B. Barmak, A. Zandinejad, A.J. Raigrodski, A.J. Pérez-Barquero, Best-Fit algorithm influences on virtual cast alignment discrepancies, J. Prosthodont. 32 (2023) 331–339, https://doi.org/10.1111/jopr.13537.
[23] D. Dede, G. Çakmak, M.B. Donmez, et al., Effect of analysis software program on measuring deviation in complete arch implant-supported framework scans, J. Prosthet. Dent. 16 (2023) S0022–S0391, https://doi.org/10.1016/j.prosdent.2023.06.028.
[24] International Organization for Standardization, ISO 5725-1: accuracy (Trueness and precision) of Measuring Methods and results. Part I: general principles and definitions, ISO, Geneva, 1994. http://iso.org/standard/11833.html, accessed 1 February 2024.
[25] A. Ender, A. Mehl, Accuracy of complete-arch dental impressions: a new method of measuring trueness and precision, J. Prosthet. Dent. 109 (2013) 121–128, https://doi.org/10.1016/S0022-3913(13)60028-1.

4.3 ARTÍCULO 3.

Piedra-Cascón W, Pérez-López J, Veiga-López B, Oteo-Morilla C, Pose-Rodriguez JM, Gallas-Torreira. Influence of base designs on the manufacturing accuracy of vat- polymerized diagnostic casts using two different technologies. J Prosthet Dent 2024; 132(2) 132:453.e1-e9

DOI: 10.1016/j.prosdent.2024.04.009

Revista: Journal of Prosthetic Dentistry

Factor de Impacto (JCR 2024): 4.8

Cuartil: Q1

Categoría: Dentistry, Oral Surgery and Medicine

Posición: 18/271

Link: https://linkinghub.elsevier.com/retrieve/pii/S0022-3913(24)00

ARTICLE IN PRESS

Clinical Implications

The optimal manufacturing accuracy of digital casts is achieved when the base designs are in accordance with the specific polymer material and 3D printing technology. In this study, solid cast base designs obtained inferior outcomes using the tested 3D printers and polymer resin material.

Stereolithography (SLA) can be defined as an additive manufacturing (AM) technology for the fabrication of 3-dimensional (3D) objects in a layer-by-layer building process.[1–3] AM technologies have been classified into 7 families: fused deposition modeling, vat-polymerization, material jetting, binder jetting, sheet lamination, powder-based fusion, and direct energy deposition.[4,5] Of these, vat-polymerization technologies have become popular for the manufacture of a wide range of digital dental devices, including diagnostic casts.[6] Vat-polymerization SLA-AM technologies can be categorized according to the type of light source used during the 3D printing process: laser (SLA-Laser), direct light processing (SLA-DLP), and liquid crystal display (SLA-LCD).[1,7–9]

Different factors have been identified that can impact the manufacturing accuracy of 3D printed devices, including intraoral scanning processes,[10] geometries of the design,[11,12] technology and printer,[13,14] polymer material,[15–17] print orientation,[18,19] slicer software program,[20] printing parameters,[3,21–28] support structures,[11,13,14,29–31] and postprocessing procedures.[32,33] In addition, human decisions can influence the final accuracy of AM diagnostic casts, including printer calibration, ambient temperature, and storage conditions of the 3D printing material. The accuracy of AM diagnostic casts has been previously investigated,[34–39] and clinically acceptable values for manufacturing discrepancies have been reported to range from 100 μm to 300 μm.[25,34,36,37] According to the International Organization for Standardization (ISO) 5725–1 standard, the accuracy of a 3D printer is defined by trueness and precision.[40] Trueness relates to the printer's ability to replicate the digital design as closely as possible to its real form contained in a standard tessellation language (STL) file, while precision refers to the manufacturing reliability of the device under the same conditions.[40]

Previous studies have reported on the accuracy of diagnostic casts fabricated using different AM technologies. As a result, generalizing the conclusions drawn in specific protocols should not be extrapolated as a basic truth, since the accuracy of dental 3D printing protocols relies on the manufacturing trinomial concept.[3] The manufacturing trinomial concept can be defined as the accordance between the additive manufacturing technology, 3D printer, and the resin material selected.[3] The manufacturing trinomial accuracy discrepancies using the same dataset, resin material, and post-processing procedures for two different 3D printing systems is lacking in the dental literature. Most of the studies about dental 3D printing available in the literature have only studied 3D printing systems and one 3D resin without taking into account the trinomial manufacturing concept. A systematic 3D printing workflow that includes the 3D printing parameters, supportive structures parameters, and post-processing procedures equal for different 3D printing systems based on the clinical applications of additive manufacturing dental casts needs to be studied.

The purpose of this in vitro study was to evaluate the influence of 3 different base designs for diagnostic casts (solid, honeycomb, and hollow) on the accuracy of 2 different vat-polymerization 3D printers, an SLA-DLP 3D printer (NextDent 5100; 3D Systems), and an SLA-LCD 3D printer (Sonic Mini 4K; Phrozen). The null hypothesis was that no significant differences would be found in the accuracy (trueness and precision) of the different base designs studied for the 3D printed casts in both vat-polymerization technologies.

MATERIAL AND METHODS

A maxillary diagnostic cast was digitized by using a dental laboratory scanner (Advaa Lab Scanner; GC) to obtain an STL file. Eleven 3×3×3-mm reference cubes were attached to the digital diagnostic casts using an open-source software program (Blender 3.3; The Blender Foundation) to aid in future measurements (Fig. 1A-E). Specimens were manufactured by using 2 vat-polymerization 3D printers: Nextdent 5100 (ND group) and Sonic Mini 4K (SM4K group). For each 3D printer group, three subgroups were created on the base design: solid (S group), honeycomb (HC group), and hollow (H group). Then, the HC and H groups were further categorized into 2 subgroups, distinguished by the wall thickness: 1 mm (HC1 and H1 subgroup) and 2 mm (HC2 and H2 subgroup) (N=100, n=10). The STL files associated with ND group were exported as ND-S, ND-HC1, ND-HC2, ND-H1, and ND-H2, while the STL files associated with SM4K group were exported as SM4K-S, SM4K-HC1 SM4K-HC2, SM4K-H1, and SM4K-H2 (Table 1). The same polymer printing material (NextDent Model 2.0; 3D Systems) was used for both vat-polymerization technologies (Table 2). Subsequently, the ND group specimens were processed through the NexDent 5100 slicing software program (3D Sprint; 3D Systems) and an open-source slicing software program (Chitubox v1.9.4; Chitubox) for specimens of SM4K group (Fig. 2A-B). All the specimens were manufactured horizontally (0-degree build position), with a

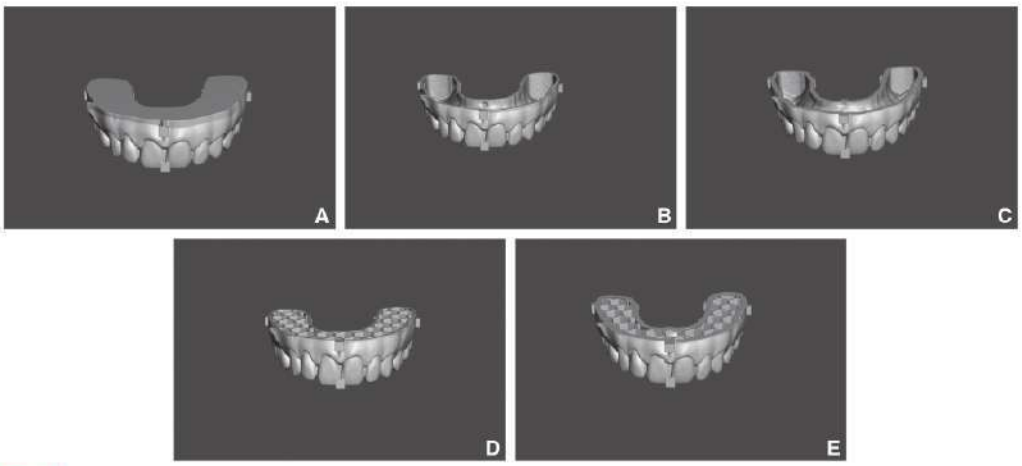

Figure 1. Digital design of maxillary virtual diagnostic cast of each group. A, Solid. B, 1-mm wall thickness hollow, C, 2-mm wall thickness hollow, D, 1-mm wall thickness honeycomb, E, 2-mm wall thickness honeycomb.

Table 1. Specimens groups categorization

3D Printer Group	Specimens Group	Final Group
ND*[1]	S*[3]	ND-S
	HC1*[4]	ND-HC1
	HC2*[5]	ND-HC2
	H1*[6]	ND-H1
	H2*[7]	ND-H2
SM4K*[2]	S	SM4K-S
	HC1	SM4K-HC1
	HC2	SM4K-HC2
	H1	SM4K-H1
	H2	SM4K-H2

*[1] ND: NextDent 5100 group
*[2] SM4K: Sonic Mini 4K group
*[3] S: Solid group
*[4] HC1: 1-mm wall thickness Honeycomb group
*[5] HC2: 2-mm wall thickness Honeycomb group
*[6] H1: 1-mm wall thickness Hollow group
*[7] H2: 2-mm wall thickness Hollow group

50-μm layer thickness (Fig. 2C). The polymer resin material was mixed for 2.5 hours using a specific oscillatory device (LC-3D Mixer; 3D Systems). Both printers had been previously calibrated according to the manufacturer's recommendations. The manufacturer reports the NextDent 5100 to have an XY resolution of 65 μm, whereas the manufacturer of the Sonic Mini 4K specifies an XY resolution of 35 μm (Table 3).

Consequently, identical postprocessing procedures, including rinsing and polymerization were achieved for all specimen groups by following the polymer material manufacturer's recommendations. The specimens were carefully removed from the building platforms using a spatula (iFixit; iFixit GmbH). Then, the 3D printed casts were submerged in a primary ultrasonic bath with 99% isopropyl alcohol (IPA) solvent (IPA 99%; Soluciones Químicas) for 3 minutes, followed by a secondary ultrasonic bath of clean 99% IPA solvent for an additional 2 minutes. Afterward, the specimens were thoroughly dried with compressed air and left in a dark room at room temperature for an additional 15 minutes. Finally, all the specimens were polymerized using an ultraviolet (UV) machine (LC-3DPrint Box; 3D Systems) for 10 minutes. A total of 100 specimens were manufactured (Fig. 3A-E).

A coordinate measured machine (CMM) (CMM DEA Alpha Status; Hexagon) was used to calculate the deviation between the digital casts and the vat-polymerized specimens. The position of the 11 reference cubes in 3 linear positions using the x-, y- and z- axes were computed with a 0.5-mm stylus scanning head under a light force of 0.1 N. Moreover, 36 additional points outside the cubes (Table 4) of the 3D printed diagnostic casts were also probed, and the discrepancy in the x-, y- and z- axes was calculated. A CMM cannot assess triangle meshes to determine differences between reference and test groups of virtual casts. Consequently,

Table 2. Specifications of polymer

Brand	Resin	Wavelength	Hardness	Flexural Modulus	ISO Standard
NextDent	Model 2.0 Gray	405 nm	≥80 shore D	≥1500 MPa	ISO 178

ISO, International Organization for Standardization.

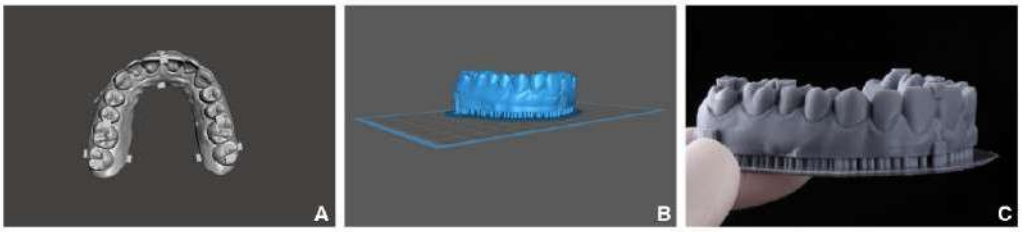

Figure 2. Digital diagnostic casts. A, Occlusal view. B, Support structures. C, 3D printed diagnostic cast with support structures.

Table 3. Specifications of 3D printers

Brand	Printer	Technology	Wavelength	Resolution XY	System Power
3D Systems	NextDent 5100	SLA-DLP	405 nm	65 μm	440 W
Phrozen3D	Sonic Mini 4K	SLA-LCD	405 nm	35 μm	40 W

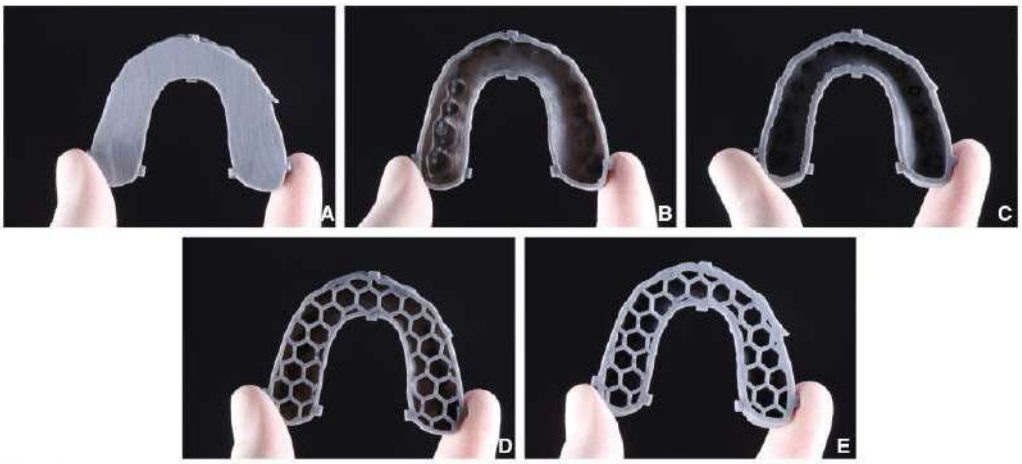

Figure 3. Cast base designs of additively manufactured specimens for each group. A, Solid. B, 1-mm wall thickness hollow. C, 2-mm wall thickness hollow. D, 1-mm wall thickness honeycomb. E, 2-mm wall thickness honeycomb.

the triangulation of the virtual cast was transformed into a CAD surface model utilizing a dedicated universal metrology 3D CAD software (Metrolog X4 v18; Metrologic). Following this, the CAD surface model was aligned with the STL file using the best-fit technique to evaluate accuracy deviations. Trueness in the experiment was defined as the average of the mean absolute dimensional discrepancies between the digital cast and the vat-polymerized specimens. Precision was determined by the standard deviation (SD) of the dimensional discrepancies between the virtual cast and the 3D-printed specimens.

The Kruskal-Wallis for independent samples and Mann Whitney U pairwise comparison tests were used to analyze data (α=.05) by using a statistical software program (IBM SPSS Statistics, v25; IBM Corp).

RESULTS

The median ±interquartile range (IQR) values for the x-, y- and z-axes and 3D discrepancies are presented in Table 5. Trueness and precision values are presented in Table 6. The Kruskal-Wallis test for independent samples revealed significant differences in accuracy (trueness and precision) among the tested 3D printers and digital cast base designs in terms of the x-, y-, and z-axes and the 3D discrepancy considering absolute discrepancies (all P<.001) (Table 6).

For x-axis discrepancy, the Mann-Whitney U pairwise comparison test for independent samples revealed significant differences in the global accuracy in the SM4K group between the H2 (19.00 ±29.50 μm) and H1

Table 4. Description of 36 additional points measured on additively manufactured specimens with coordinate measurement machine

Additional Point	Location
Dental 1	Tip of distobuccal cusp of right and left first molars
Dental 2	Tip of distobuccal cusp of right and left second molars
Dental 3	Tip of mesiolingual cusp of right and left first molars
Dental 4	Tip of mesiolingual cusp of right and left second molars
Dental 5	Tip of buccal cusp of right and left first premolars
Dental 6	Tip of lingual cusp of right and left first premolars
Dental 7	Tip of cusp of right and left canines
Dental 8	Distobuccal edge of right and left lateral incisors
Dental 9	Mesiobuccal edge of right and left lateral incisors
Dental 10	Distobuccal edge of right and left central incisors
Gingival Buccal 1	5 mm apically to buccal interdental papilla between right and left second and first molars on both right and left sides
Gingival Buccal 2	5 mm apically to buccal interdental papilla between first molar and second premolar on both right and left sides
Gingival Buccal 3	5 mm apically to buccal interdental papilla between first premolar and canine on both right and left sides
Gingival Buccal 4	5 mm apically to buccal interdental papilla between lateral and central incisors on both right and left sides
Gingival Palatal 1	5 mm apically to palatal interdental papilla between second and first molars on both right and left sides
Gingival Palatal 2	5 mm apically to palatal interdental papilla between first molar and second premolar on both right and left sides
Gingival Palatal 3	5 mm apically to palatal interdental papilla between first premolar and canine on both right and left sides
Gingival Palatal 4	5 mm apically to palatal interdental papilla between right and left central incisors

Table 5. Descriptive statistics of different groups tested (μm)

Discrepancy Measurement	3D Printer	Group	Median ±InterquartileRange	Percentile 25	Percentile 75
x-axis	NextDent	H2	9.90 ±15.40	3.50	18.90
		H1	9.60 ±18.00	3.20	21.20
		HC2	10.00 ±15.50	4.10	19.60
		HC1	8.20 ±14.70	3.30	18.00
		S	8.60 ±16.70	2.80	19.50
	Phrozen	H2	19.00 ±29.50	6.20	35.70
		H1	26.90 ±50.40	8.10	58.50
		HC2	23.90 ±43.40	5.70	49.10
		HC1	24.40 ±41.50	7.60	49.10
		S	26.60 ±55.70	9.00	64.70
y-axis	NextDent	H2	5.80 ±12.30	1.80	14.10
		H1	6.30 ±10.00	2.50	12.50
		HC2	5.40 ±10.40	1.90	12.30
		HC1	4.20 ±8.00	1.30	9.30
		S	4.80 ±10.00	1.80	11.80
	Phrozen	H2	8.70 ±18.90	2.80	21.70
		H1	14.60 ±22.30	6.70	29.00
		HC2	11.80 ±18.80	4.60	23.40
		HC1	11.20 ±19.10	4.30	23.40
		S	15.60 ±24.90	6.50	31.40
z-axis	NextDent	H2	11.10 ±19.30	4.50	23.80
		H1	12.10 ±13.60	5.50	19.10
		HC2	8.50 ±13.80	3.50	17.30
		HC1	9.20 ±14.30	3.90	18.20
		S	12.00 ±17.00	4.60	21.60
	Phrozen	H2	22.20 ±28.60	9.45	38.05
		H1	28.10 ±41.00	13.30	54.30
		HC2	22.80 ±29.70	9.30	39.00
		HC1	25.10 ±32.70	12.00	44.70
		S	29.50 ±36.10	14.50	50.60
3D Discrepancy	NextDent	H2	24.24 ±29.01	9.91	38.93
		H1	21.12 ±23.49	11.58	35.07
		HC2	19.69 ±23.00	9.82	32.81
		HC1	16.78 ±23.07	7.69	30.76
		S	20.14 ±26.78	8.89	35.66
	Phrozen	H2	37.73 ±42.21	19.79	62.00
		H1	52.50 ±60.26	26.41	86.67
		HC2	45.16 ±47.85	21.16	69.01
		HC1	45.36 ±55.95	21.22	77.18
		S	55.84 ±61.34	30.80	92.13

groups (26.90 ±50.40 μm) (P=.001), H2 (19.00 ±29.50 μm) and S groups (26.60 ±55.70 μm) (P<.001), and HC2 (23.90 ±43.40 μm) and S (26.60 ±55.70 μm) groups (P=.012). In the ND group, significant differences in trueness and precision were not observed (P>.05) (Fig. 4A). In the y-axis analysis, the Mann-Whitney U pairwise comparison test showed significant differences in the SM4K group between the H2 (8.70 ±18.90 μm) and H1 groups (14.60 ±22.30 μm)(P=.001), H2 (8.70 ±18.90 μm) and S groups (15.60 ±24.90 μm)(P<.001), H1 (14.60 ±22.30 μm) and HC2 (11.80 ±18.80 μm) groups (P=.007), HC2 (11.80 ±18.80 μm) and S groups (15.60 ±24.90 μm) (P=.009), H1 (14.60 ±22.30 μm) and HC1 groups (11.20 ±19.10 μm), and HC1(11.20 ±19.10 μm)

Table 6. Trueness and precision values obtained for different groups tested (μm)

	3D Printer	Group	Trueness	Precision
x-axis	NextDent	H2	13.19	12.69
		H1	14.20	13.71
		HC2	15.90	25.53
		HC1	13.12	14.30
		S	13.72	14.87
	Phrozen	H2	27.49	28.34
		H1	41.21	44.41
		HC2	33.42	34.24
		HC1	31.75	28.24
		S	39.18	36.15
y-axis	NextDent	H2	10.52	12.72
		H1	9.76	11.12
		HC2	11.51	16.89
		HC1	7.56	9.68
		S	8.92	11.21
	Phrozen	H2	14.26	15.21
		H1	21.07	20.65
		HC2	16.38	15.22
		HC1	16.92	18.60
		S	23.30	23.58
z-axis	NextDent	H2	15.32	13.34
		H1	14.15	11.38
		HC2	15.36	25.83
		HC1	12.47	11.50
		S	15.08	13.21
	Phrozen	H2	26.52	21.57
		H1	35.70	27.23
		HC2	26.59	20.72
		HC1	32.24	27.49
		S	35.04	25.76
3D Discrepancy	NextDent	H2	26.21	18.24
		H1	24.91	17.82
		HC2	28.35	37.70
		HC1	21.83	18.40
		S	24.79	20.03
	Phrozen	H2	45.15	33.51
		H1	64.51	48.92
		HC2	50.48	37.11
		HC1	52.54	38.37
		S	64.29	41.20

and S groups (15.60 ±24.90 μm) (both $P<.001$). In the ND group, significant differences were found between the HC1 (4.20 ±8.00 μm) and H2 groups (5.80 ±12.30 μm) ($P=.004$), and H1(6.30 ±10.00 μm) ($P=.020$) and HC2 (5.40 ±10.40 μm) ($P=.001$) groups (Fig. 4B). For the z-axis analysis, the Mann-Whitney U pairwise comparison test revealed significant differences in the SM4K group between the H2 (22.20 ±28.60 μm) and H1 groups (28.10 ±41.00 μm), H2 (22.20 ±28.60 μm) and S groups (29.50 ±36.10 μm), H1 (28.10 ±41.00 μm) and HC2 groups (22.80 ±29.70 μm), and HC2 (22.80 ±29.70 μm) and S groups (all $P<.001$). In the ND group, significant differences were found between the H2 group (11.10 ±19.30 μm) and HC2 (8.50 ±±13.80 μm) ($P=.047$) and HC1 groups (9.20 ±14.30 μm) ($P=.028$) (Fig. 4C). For the 3D discrepancy analysis, the Mann-Whitney U pairwise comparison test demonstrated significant differences in the SM4K group between the H2 (37.73 ±42.21 μm) and H1 groups (52.50 ±60.26 μm), H2 (37.73 ±42.21 μm) and S groups (55.84 ±61.34 μm) (both $P<.001$), H1 (52.50 ±60.26 μm) and HC2 groups (45.16 ±47.85 μm) ($P=.001$), HC2 (45.16 ±47.85 μm) and S groups ($P<.001$), H1 (52.50 ±60.26 μm) and HC1 groups (45.36 ±55.95 μm) ($P=.002$), and HC1 (45.36 ±55.95 μm) and S groups (55.84 ±61.34 μm) ($P<.001$). In the ND group, significant differences were found between the H2 (24.24 ±29.01 μm) and HC1 (16.78 ±23.07 μm) ($P=.012$) groups (Fig. 4D).

DISCUSSION

Based on the results, significant differences in the trueness and precision values on the x-, y- and z- axes and in the 3D, discrepancy were found among the groups tested, with the exception of the x- axis for the NextDent 5100 3D printer. Hence, the null hypothesis that no significant differences would be found in the accuracy (trueness and precision) of the different base designs studied for the 3D printed casts in both vat-polymerization technologies was rejected. According to the findings in the present study, the ND group exhibited the least mean 3D discrepancy manufacturing accuracy with the honeycomb 1-mm wall thickness base design, recording a trueness of 21.83 μm and a precision of 18.40 μm. Similarly, in the SM4K group, optimal manufacturing accuracy was achieved with the hollow 2-mm wall thickness cast base design, yielding a trueness of 45.15 μm and a precision of 33.51 μm.

In this in vitro experiment, the manufacturing trueness in the tested groups ranged from 21.83 μm to 64.51 μm. The precision ranged from 17.82 μm to 48.92 μm, all meeting the clinically acceptable manufacturing discrepancy. However, diverse clinical and laboratory scenarios exist. The determined manufacturing accuracies should not negatively influence the use of 3D printed casts for fabricating silicone indexes or thermoplastic matrices. However, the observed accuracy of both tested 3D printers also appears suitable for using AM casts as definitive casts. Nevertheless, this finding requires careful consideration, and additional studies are essential to evaluate the clinical impact of the definitive restorations produced and finalized on AM casts. The success of printed casts for definitive restorations relies not only on their accuracy but also on their surface texture.

Each 3D printer was calibrated according to the manufacturer's recommendations to use the same polymer resin (NextDent Model 2.0; 3D Systems) and the same supporting structures. Printing procedures for ND group were performed by experienced dental laboratory technicians with experience in digital production protocols, while those for the SM4K group were carried out by a clinician (W.P.C) with 6 years of 3D printing experience. All specimens were digitally prepared by the same operator (W.P.C), while the 3D printing procedures were performed by trained operators in each 3D printer. For the ND group specimens were 3D printed by J.P.L, while in SM4K group specimens were manufactured by W.P.C. All specimens were postprocessed using the recommended UV polymerization machine (LC-3DPrint Box; 3D Systems) by the same operator (W.P.C).

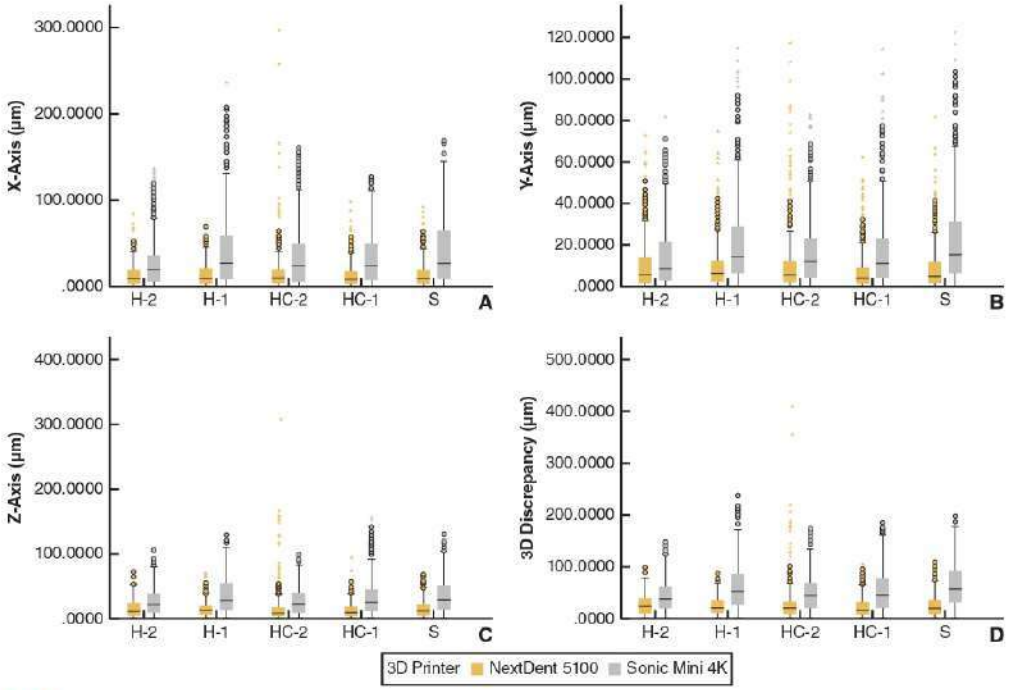

Figure 4. Accuracy (trueness and precision) discrepancies measured among groups tested. A, x-axis. B, y-axis. C, z-axis. D, 3D discrepancy (µm).

The authors are unaware of a previous in vitro study using the same resin polymer material and same support structures in two different 3D printing systems, an open and closed 3D printing system to validate the manufacturing trinomial.

Previous studies have analyzed the accuracy of 3D printed casts reporting trueness values ranging from 82 µm to 289 µm and precision values ranging from 20 µm to 284 µm. Most of those studies did not report the base design selected. Studies that reported the impact of the base design on the manufacturing accuracy of AM diagnostic casts are sparse. Rungrojwittayakul et al[35] compared a solid and hollow base design manufactured using 2 vat-polymerization technologies, SLA-DLP/CLIP (Carbon M2; Carbon) and SLA-DLP (MoonRay S100; Sprintray). The study reported that solid base designs exhibited the highest accuracy, with trueness ranging from 48 µm to 87 µm and precision values between 44 µm and 57 µm. Comparisons with the results of the present investigation are difficult because of variations in the manufacturing trinomial, print orientations, support structures, layer thicknesses, and measurement methods.

Different methods have been used to assess the accuracy of casts manufactured using vat-polymerization technologies, encompassing both manual and digital procedures. In manual measurements, digital calipers have been used to gauge the discrepancies between stone and 3D printed casts. Conversely, digital measurements have involved superimposition procedures for obtaining linear and angular measurements and commonly used root mean square (RMS) values.[19,39] However, the standard method of conducting these measurements is a coordinate measuring machine (CMM).[38]

The Revilla-León et al study[38] can be compared with the present investigation, where the dataset, manufacturing trinomial, printing parameters, postprocessing procedures, and measuring methods were equal for one of the groups tested in the present investigation (ND group), except for print orientation. In the present study, the print orientation was set horizontally, while, in their investigation, all specimens were positioned vertically on the build platform. As stated by different authors, 3D print orientation could affect the accuracy of the 3D printing casts.[18,19] Revilla-León et al[38] tested solid, honeycomb, and hollow models with variations in wall thickness of the base design (1 mm and 2 mm) using an SLA-DLP 3D printer (NextDent 5100; 3D Systems). They reported that solid models had the best accuracy with a trueness value at 63.73 µm and a precision of 45.42 µm. In our study, solid models obtained a trueness of 24.79 µm and precision of 20.03 µm. Conversely, the

results of the present study showed that casts manufactured by the NextDent 5100 3D printer exhibited fewer distortions and that, notably, the optimal cast base design was the honeycomb with a 1-mm wall thickness, obtaining a trueness of 21.83 µm and a precision of 18.40. This means a difference up to 42 µm in trueness and 27 µm in trueness using the same 3D printer. This finding differed from that of Revilla-León et al,[18] likely because of a different print orientation and different support structure parameters and location.

Vat-polymerization 3D printers have been broadly categorized as open and closed systems. Open systems provide flexibility in customizing printing parameters and their interrelation with printing zones. In contrast, closed systems do not allow for changes in printing parameters. In the present study, the NextDent 5100 printers represent a closed system, while the Sonic Mini 4K printer represents an open system. Theoretically, polymer materials and 3D printers with compatible wavelengths can be used interchangeably. However, the present investigation revealed that despite the compatibility of wavelengths between the resin material and the UV light source of 3D printers, variations in accuracy should be expected because of the need for adaptation in the manufacturing trinomial. A potential explanation for the differences in trueness and precision between both 3D printers may be attributed to variations in the power of the printers. Maneiro-Lojo et al[19] reported a manufacturing accuracy using an open-source SLA-LCD printer (Photon Mono SE; Anycubic) ranging from 92 µm to 131 µm. In the present study, the SLA-LCD group obtained a manufacturing accuracy ranging from 11.64 µm to 78.66 µm. Discrepancies between the studies could be attributed to variations in printing parameters, support structure parameters, and postprocessing procedures.

Limitations of the present study included that only 1 resin polymer was tested in both vat-polymerization printers. Further studies are needed to explore the manufacturing trinomial, evaluating diverse polymer materials using the SLA technologies employed in this study. This will contribute to optimizing the accuracy of 3D printed casts, making them applicable in more complex scenarios.

CONCLUSIONS

Based on the findings of this in vitro study, the following conclusions were drawn:

1. The type of 3D printing technology affected manufacturing accuracy using the same resin polymer material.
2. The tested base designs affected the accuracy of the digital casts manufactured with vat-polymerization technologies.
3. The honeycomb design with a 1-mm wall thickness had the highest accuracy in casts produced using SLA-DLP technology, while the hollow design with a 2-mm wall thickness had the highest accuracy in casts manufactured with SLA-LCD technology.
4. The highest manufacturing accuracy for SLA-DLP specimens ranged from 3.43 µm to 40.23 µm, while for SLA-LCD specimens the manufacturing accuracy ranged from 11.64 µm to 78.16 µm.

REFERENCES

1. Hull C.W. Apparatus for production of three-dimensional objects by stereolithography 1986. US Patent 4575330.
2. Glossary of digital dental terms, 2nd edition. American College of Prosthodontists and ACP Education Foundation. *J Prosthodont*. 2021;30:172–181.
3. Piedra-Cascón W, Krishnamurthy VR, Att W, Revilla-León M. 3D printing parameters, supporting structures, slicing, and post-processing procedures of vat-polymerization additive manufacturing technologies: A narrative review. *J Dent*. 2021;109:103630.
4. ISO 17296–2:2015. Additive manufacturing general principles part 2: overview of process categories and feedstock. https://www.iso.org/standard/61626.html?browse=tc. Accessed December 12, 2023.
5. ASTM, Committee F42 on Additive Manufacturing Technologies. West Conshohocken, Pa. 2009 Standard terminology for additive manufacturing general principles and terminology. ISO/ASTM52900–15. Accessed January 11, 2023.
6. Revilla-León M, Ozcan M. Additive manufacturing technologies used for processing polymers: Current status and potential application in prosthetic dentistry. *J Prosthodont*. 2019;28:146–158.
7. ISO 17296e2. Additive manufacturing general principles part 2: Overview of process categories and feedstock. 2015. Available at: https://www.iso.org/standard/61626.html?browse=tc.
8. Hornbeck L. Digital micromirror device 2009. US Patent No. 5061.049.
9. Holt P.M. Maskless photopolymer exposure process and apparatus 2012. US Patent 8.114.569 B2.
10. Piedra-Cascón W, Adhikari RR, Ozcan M, et al. Accuracy assessment (trueness and precision) of a confocal based intraoral scanner under twelve different ambient lighting conditions. *J Dent*. 2023;134:104530.
11. Ide Y, Nayar S, Logan H, et al. The effect of the angle of acuteness of additive manufactured models and the direction of printing on the dimensional fidelity: clinical implications. *Odontology*. 2017;105:108e115.
12. Wu D, Zhao Z, Zhang Q, et al. Mechanics of shape distortion of DLP 3D printed structures during UV post-curing. *Soft Matter*. 2019;15:e151e6159.
13. Puebla K, Arcaute K, Quintana R, Wicker RB. Effects of environmental conditions, aging, and build orientations on the mechanical properties of ASTM type I specimens manufactured via stereolithography. *Rapid Prototyp J*. 2012;18:3746388.
14. Braian M, Jimbo R, Wennerberg A. Production tolerance of additive manufactured polymeric objects for clinical applications. *Dent Mater*. 2016;32:853e861.
15. Alharbi N, Osman R, Wismeijer D. Effect of build direction on the mechanical properties of 3D printed complete coverage interim dental restorations. *J Prosthet Dent*. 2016;155.760e767.
16. Reymus M, Fabritius R, Keßler A, et al. Fracture load of 3D-printed fixed dental prostheses compared with milled and conventionally fabricated ones: the impact of resin material, build orientation, postcuring and artificial aging – An in vitro study. *Clin Oral Investig*. 2020;24:701e710.
17. Revilla-León M, Umorin M, Ozcan M. Piedra-Cascón W. Color dimensions of additive manufactured interim restorative dental material. *J Prosthet Dent*.. 2020.123:754e760.
18. Revilla-León M, Jordan D, Methani MM, et al. Influence of printing angulation on the surface roughness of additive manufactured clear silicone indices: An in vitro study. *J Prosthet Dent*. 2021;125:462–468.
19. Maneiro Lojo J, Alonso Pérez-Barquero J, García-Sala Bonmatí F, et al. Influence of print orientation on the accuracy (trueness and precision) of diagnostic casts manufactured with a daylight polymer printer. *J Prosthet Dent* 2023.
20. Reymus M, Fabritius R, Keßler A, et al. Fracture load of 3D-printed fixed dental prostheses compared with milled and conventionally fabricated ones: the impact of resin material, build orientation, postcuring and artificial aging – An in vitro study. *Clin Oral Investig*. 2020;24:701e710.
21. Arnold C, Monsees D, Hey J, Schweyen R. Surface quality of 3D-printed models as a function of various printing parameters. *Materials (Basel)*. 2019;12:19.
22. Park GS, Kim SK, Heo SJ, et al. Effects of printing parameters on the fit of implant-supported 3D printing resin prosthetics. *Materials (Basel)*. 2019;12:2533.

23. Zhang ZC, Li PL, Chu FT, Shen G. Influence of the three dimensional printing technique and printing layer thickness on model accuracy. *J Orofac Orthop*. 2019;80:194e204.
24. Lotlin WA, English JD, Borders C, et al. Effect of print layer height on the assessment of 3D-printed models. *Am J Orthod Dentofacial Orthop*. 2019;156:283e289.
25. Favero CS, English JD, Cozad BE, et al. Effect of print layer height and printer type on the accuracy of 3-dimensional printed orthodontic models. *Am J Orthod Dentofacial Orthop*. 2017;152:557e565.
26. Reymus M, Lümkemann N, Stawarczyk B. 3D printed material for temporary restorations: Impact of print layer thickness and post-curing method on degree of conversion. *Int J Comput Dent*. 2019;22:231e237.
27. Chockalingam K, Jawahar N, Chandrasekhar U. Influence of layer thickness on mechanical properties in stereolithography. *Rapid Prototyp J*. 2006;12:106e113.
28. Scherer M, Al-Haj Husain N, Barmak AB, et al. Influence of the layer thickness on the flexural strength of aged and nonaged additively manufactured interim dental material. *J Prosthodont*. 2023;32:68–73.
29. Cho HS, Park WS, Choi BW, Leu MC. Determining optimal parameters for stereolithography processes via genetic algorithm. *J Manuf Syst*. 2000;19:18e27.
30. Alharbi N, Osman RB, Wismeijer D. Factors influencing the dimensional accuracy of 3D-printed full-coverage dental restorations using stereolithography technology. *Int J Prosthodont*. 2016;29:503e510.
31. Unkovskiy A, Bui PH, Schille C, et al. Objects build orientation, positioning, and curing influence dimensional accuracy and flexural properties of stereolithographically printed resin. *Dent Mater*. 2018;34:e324ee333.
32. Mostafavi D, Methani MM, Piedra-Cascón W, et al. Influence of the rinsing postprocessing procedures on the manufacturing accuracy of vat-polymerized dental model material. *J Prosthodont*. 2021;30:610–616.
33. Mostafavi D, Methani MM, Piedra-Cascón W, et al. Influence of polymerization postprocessing procedures on the accuracy of additively manufactured dental model material. *Int J Prosthodont*. 2023;36:479–485.
34. Etemad-Shahidi Y, Qallandar OB, Evenden J, et al. Accuracy of 3-dimensionally printed full-arch dental models: A systematic review. *J Clin Med*. 2020;9:3357.
35. Rungrojwittayakul O, Kan JY, Shiozaki K, et al. Accuracy of 3D printed models created by two technologies of printers with different designs of model base. *J Prosthodont*. 2020;29:124–128.
36. Kim SY, Shin YS, Jung HD, et al. Precision and trueness of dental models manufactured with different 3-dimensional printing techniques. *Am J Orthod Dentofacial Orthop*. 2018;153:144–153.
37. Dietrich CA, Ender A, Baumgartner S, Mehl A. A validation study of reconstructed rapid prototyping models produced by two technologies. *Angle Orthod*. 2017;87:782–787.
38. Revilla-León M, Piedra-Cascón W, Arangoneses R, et al. Influence of base design on the manufacturing accuracy of vat-polymerized diagnostic casts: An in vitro study. *J Prosthet Dent*. 2023;129:166–173.
39. Morón-Conejo B, López-Vilagran J, Cáceres D, et al. Accuracy of five different 3D printing workflows for dental models comparing industrial and dental desktop printers. *Clin Oral Investig*. 2023;27:2521–2532.
40. ISO 5725–1. Accuracy (trueness and precision) of measuring methods and results. Part-I: general principles and definitions. Available at: https://www.iso.org/obp/ui/#iso:std:iso:5725:-1:ed-1:v1:en.

Corresponding author:
Wenceslao Piedra-Cascón
s/n Rua Entremíos
Santiago de Compostela 15782
SPAIN
Email: wpiedra@movumtech.com

Acknowledgments
The authors thank Tecnica Dental Studio VP and Dental Astur dental laboratories for their support with NextDent technologies.

CRediT authorship contribution statement
Wenceslao Piedra-Cascón: Idea, conceptualization, protocol development, results interpretation, Phrozen manufacturing procedures and contributed to the manuscript writing. **Javier Pérez-López**: NextDent manufacturing procedures. **Beatriz Veiga-López**: NextDent manufacturing procedures. **Carlos Oteo-Morilla**: Statistical analysis and contributed to the manuscript writing. **Jose Manuel Pose-Rodríguez**: Contributed to the protocol development and results interpretation. **Mercedes Gallas-Torreira**: Contributed to revision of the manuscript. All authors discussed the evolution and commented on the manuscript at all stages.

https://doi.org/10.1016/j.prosdent.2024.04.009

4.4 ARTÍCULO 4.

Piedra-Cascón W, Oteo-Morilla C, Pose-Rodriguez JM, Gallas-Torreira. Impact of 3D resin and base designs on the accuracy of additively manufactured casts using a stereolithography technology. J Prosthet Dent 2025; 14: S0022-3913(25)00282-3

DOI: 10.1016/j.prosdent.2025.03.033

Revista: Journal of Prosthetic Dentistry

Factor de Impacto (JCR 2024): 4.8

Cuartil: Q1

Categoría: Dentistry, Oral Surgery and Medicine

Posición: 18/271

Link: **https://linkinghub.elsevier.com/retrieve/pii/S0022-3913(25)00282-3**

ARTICLE IN PRESS

THE JOURNAL OF PROSTHETIC DENTISTRY

RESEARCH AND EDUCATION

Impact of 3D resin and base designs on the accuracy of additively manufactured casts using a stereolithography technology

Wenceslao Piedra-Cascón, DDS, MS,[a] Carlos Oteo-Morilla, DDS, MS, PhD,[b] Jose Manuel Pose-Rodriguez, DDS, MD, PhD,[c] and Mercedes Gallas-Torreira, DDS, PhD[d]

ABSTRACT

Statement of problem. Three-dimensional (3D) printed casts can be fabricated using a wide range of 3D polymer resins and designed with varying casts' base configurations. Nevertheless, the influence of different base designs, in conjunction with various 3D printing resins, on the final dimensional accuracy of casts manufactured through SLA-LCD 3D printing technology remains unclear.

Purpose. This study assessed the impact of 3D printing resins and base designs on the dimensional accuracy of diagnostic casts fabricated using a SLA-LCD vat-polymerization 3D printer. Two resins (NextDent Model 2.0 and Aqua Gray 4K) and 5 different base configurations were evaluated for their effect on trueness and precision.

Material and methods. A digital maxillary cast was modified into three base designs: solid (Group S), honeycomb (Group HC), and hollow (Group H). Honeycomb and hollow designs had subgroups with 1-mm (HC1, H1) and 2-mm (HC2, H2) wall thicknesses, resulting in 50 specimens (n=10 per subgroup). Eleven embedded precision cubes were used for accuracy assessment. A Sonic Mini 4K vat-polymerization printer was used for cast printing, and dimensional deviations were captured using a coordinate measuring device. Trueness was defined by the average dimensional discrepancy, and precision was indicated by the standard deviation. Statistical analysis included Kruskal-Wallis and Mann-Whitney U tests (α=.05).

Results. NextDent resin showed trueness falling between 44.8 5 μm and 64.5 μm and precision values varying between 33.5 5 μm and 48.9 μm, while Aqua Gray 4K resin ranged from 24.1 5 μm to 81.1 μm for trueness and 19.8 5 μm to 65.9 μm for precision. Significant differences (P<.001) were observed in all axes (x-, y-, z-axes) and 3D deviations, influenced by resin and base design.

Conclusions. Resin type and base design significantly affect the dimensional accuracy of 3D printed casts. Aqua Gray 4K with a 2-mm hollow base provided the highest accuracy, particularly when matched with the printer manufacturer. All casts met clinical standards. (J Prosthet Dent xxxx;xxx:xxx-xxx)

Additive manufacturing (AM) is a process where 3-dimensional (3D) objects are manufactured in a layer-by-layer building process.[1-3] According to the ASTM F42 Committee, AM technologies are divided in 7 categories: fused deposition modeling (FDM), vat-polymerization or stereolithography (SLA), binder jetting (BJ), material jetting (MJ), sheet lamination, direct energy deposition, and powder-based fusion.[4,5] SLA technology has gained popularity for fabricating a diverse array of dental devices, including diagnostics casts.[6] Ultraviolet (UV) light sources used in vat-polymerization 3D printing can be categorized into three types: laser (SLA-Laser), digital light processing (SLA-DLP), and liquid crystal display (SLA-LCD).[1,7-9]

This research did not receive any specific grant from funding agencies in the public, commercial, or not-for-profit sectors.
The authors declare that they have no known competing financial interests or personal relationships that could have appeared to influence the work reported in this paper.
[a]Doctoral student, Doctoral Program in Dental Science, Stomatology Area, Department of Surgery and Medical-Surgery Specialities, University of Santiago de Compostela (USC), Santiago de Compostela, Spain; Affiliate Faculty, Esthetic Dentistry Program, Complutense University of Madrid (UCM), Madrid, Spain; Private practice, Oviedo, Spain; and Researcher, Movumtech, Madrid, Spain.
[b]Affiliate Faculty Graduate, Esthetic Dentistry Program, Complutense University of Madrid (UCM), Madrid, Spain; and Private practice, Madrid, Spain.
[c]Associate Lecturer, Adult Comprehensive Dental Clinic, Stomatology Area, Department of Surgery and Medical-Surgery Specialities, Digital Dentistry Unit, School of Dentistry, Faculty of Medicine and Dentistry, University of Santiago de Compostela (USC), Santiago de Compostela, Spain.
[d]Senior Lecturer, Planning and Management in Dental Clinics, Stomatology Area, Department of Surgery and Medical-Surgery Specialities, Digital Dentistry Unit, School of Dentistry, Faculty of Medicine and Dentistry, University of Santiago de Compostela (USC), Santiago de Compostela, Spain.

Clinical Implications

The optimal dimensional accuracy of 3D-printed diagnostic casts is attained when the base design is specifically adapted to the chosen resin material. Notably, the same vat-polymerization technology can yield varying levels of accuracy depending on the properties of the 3D polymer resin used.

Multiple variables are known to have an impact on the accuracy of 3D printing, such as the intraoral scanning process,[10] the design's geometries,[11,12] the resin material,[13–15] printing technology,[16,17] the 3D printer,[16,17] the slicer software program,[18] the print build orientation,[19,20] the 3D printing parameters,[3,18,21–27] the support structures,[17,16,17,28,29,30] and the postprocessing procedures.[31,32] Furthermore, the accuracy of AM diagnostic casts is influenced by operator choices, namely 3D printer optimal calibration, the holding environment of the polymer material, the ambient temperature, and the digital base 3D designs. Additionally, the digital designer can select among solid, hollow, and honeycomb-based designs. Moreover, dental 3D printer manufacturers do not provide guidelines or recommendations on which wall thicknesses are appropriate in the hollow and honeycomb base designs for fabricating diagnostic casts. However, studies on the impact of different resin materials on additively manufactured diagnostic casts are scarce in the dental literature. Findings from previous studies assessing AM diagnostic casts' accuracy,[33–38] indicate that possible clinically acceptable manufacturing discrepancies oscillate between 100 µm and 300 µm.[24,33,35,36]

In accordance with the International Organization for Standardization (ISO) 5725–1 standard, the 3D printer's accuracy is determined by its trueness, which refers to how accurately the 3D printer can reproduce the true form of the digital design specified in the standard tessellation language (STL) file, and precision, that pertains to how consistently the 3D printer performs during the fabrication process under uniform conditions.[39]

Discrepancies in the accuracy of diagnostic casts produced through 3D printing have been investigated. However, many of these studies still need to consider the manufacturing trinomial concept (MTC),[3] encompassing the appropriate combination of printing technology, 3D printer, and polymer material.[3] This concept is essential for developing accurate dental 3D printing protocols. Conclusions from studies that overlook the MTC should not be universally generalized as truth. Additional 3D printing research that evaluates accuracy discrepancies within the framework of the MTC is still needed.

This in vitro study investigated how 2 different 3D printing polymers affected the diagnostic casts' accuracy using 3 distinct base designs (solid, honeycomb, and hollow) using a 3D printer with SLA-LCD technology (Sonic Mini 4 K; Phrozen). The initial hypothesis was that the 3D printed casts would not differ significantly in accuracy (measured by trueness and precision) across the different base designs when using 2 different resin polymer materials with the same 3D printer.

MATERIAL AND METHODS

A reference standard tessellation language (STL_r) file was generated by digitally scanning a maxillary diagnostic cast with a laboratory scanner (Advaa Lab Scanner; GC). Eleven reference cubes, each measuring 3×3×3 mm, were digitally incorporated into the cast design using an open-source software (Blender 3.3; The Blender Foundation) to enable precise readings (Fig. 1).

Three distinct base designs were developed for the cast: solid (S group), honeycomb (HC group), and hollow (H group). With honeycomb and hollow base designs being further classified into two subgroups according to wall thickness: 1 mm (subgroups HC1 and H1) and 2 mm (subgroups HC2 and H2), resulting in 50 specimens in total, with 10 specimens (n=10) per subgroup.

A single vat-polymerization 3D printer (Sonic Mini 4K; Phrozen) was used to fabricate all specimens with two different resin polymer materials, both compatible with the printer's wavelength: NextDent Model 2.0 (NDM) and Aqua Gray 4K (AG4K) (Table 1). All printing procedures were performed in a dedicated laboratory environment maintained at 23 °C and relative humidity of 50%. Temperature and humidity were monitored continuously using a digital hygrometer/thermometer (Model HT-1; Extech Instruments). The STL files were named according to the resin material and base design: NDM-S, NDM-H1, NDM-H2, NDM-HC1, and NDM-HC2 for the NextDent Model 2.0 group, and AG4K-S, AG4K-H1, AG4K-H2, AG4K-HC1, and AG4K-HC2 for the Aqua Gray 4K group.

All specimens were processed using an open-source slicing tool (Chitubox v1.9.5; Chitubox) (Fig. 2A, B). Each specimen was oriented horizontally on the build platform (0-degree angle) at a layer thickness of 50-µm, along with the same support structures for both resins (Fig. 2C, D). NextDent Model 2.0 resin was mixed for 2.5 hours, while Aqua Gray 4K was mixed for 5 minutes following manufacturers recommendations, using an oscillatory mixer (LC-3D Mixer; 3D Systems) to ensure homogeneity of the material. Manufacturer's recommendations were followed to calibrate the SLA-LCD Sonic Mini 4K 3D printer (Phrozen3D), with an XY resolution of 35 µm and a wavelength of 405 nm.

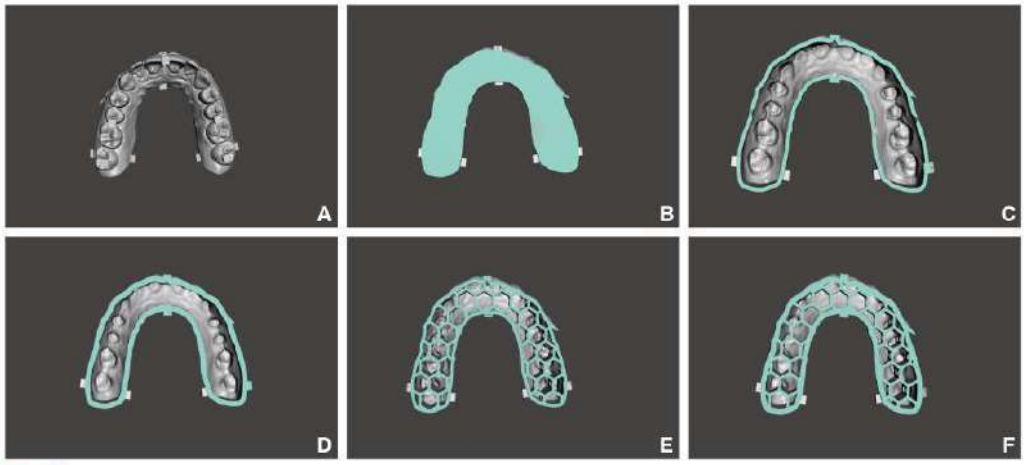

Figure 1. Digital design of maxillary virtual diagnostic cast of each group. A, Occlusal view. B, Solid. C, 1-mm wall thickness hollow, D, 2-mm wall thickness hollow, E, 1-mm wall thickness honeycomb, F, 2-mm wall thickness honeycomb.

Table 1. Specifications of polymer resin materials

Brand	Resin	Wavelength	Hardness	Flexural Modulus
NextDent	Model 2.0 Gray	405 nm	≥ 80 shore D	≥1500 MPa
Phrozen	Aqua Gray 4K	405 nm	80 shore D	1260–1520 MPa

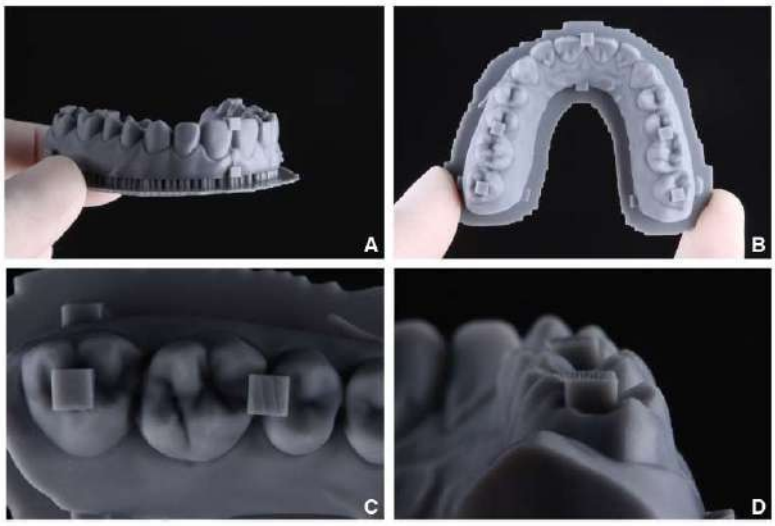

Figure 2. Additive manufactured diagnostic cast with reference cubes. A, Support structures. B, Global occlusal view. C, Sextant occlusal view. D, Lateral view.

Once printed, a spatula was used to remove the specimens from the build platform (iFixit; iFixit GmbH), which were subjected to a two-step cleaning process. First, the specimens were placed in an ultrasonic bath containing 99% isopropyl alcohol (IPA) (IPA 99%; EQM Soluciones Químicas) for 3 minutes, with a second

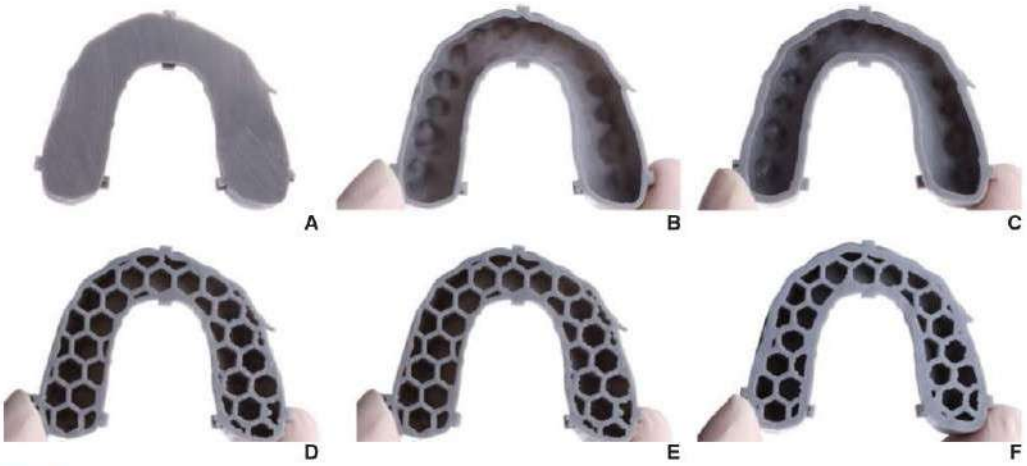

Figure 3. Additive manufacturing digital diagnostic cast base design for each group. A, Solid. B, 1-mm wall thickness hollow, C, 2-mm wall thickness hollow, D, 1-mm wall thickness honeycomb, E, 2-mm wall thickness honeycomb.

ultrasonic bath in fresh IPA for another 2 minutes. After being dried with compressed air, they were left at room temperature in a dark environment for 15 minutes to allow complete evaporation of the alcohol. A UV polymerization chamber was used to perform post-curing: 10 minutes for the NextDent Model 2.0 specimens and 6 minutes for the Aqua Gray 4K specimens, using the manufacturer-recommended curing devices (LC-3D Print Box; 3D Systems for NextDent, and Curing Station; Phrozen for Aqua Gray 4K). 50 specimens were successfully fabricated in total (Fig. 3).

Dimensional accuracy was measured using a coordinate measuring machine (CMM) (DEA Alpha Status; Hexagon AB). To assess accuracy, the X, Y, and Z coordinates of the 11 embedded cubes (each 3×3×3 mm) were measured, supplemented by 36 additional points on the cast surface (Table 2). A measurement program was developed using the CAD casts of the different cast base designs to automate the evaluation process. Upon receiving the printed specimens, each was securely fixed within the CMM's measurement volume. The measurement sequence began with an alignment of the physical specimen to its corresponding CAD cast. For alignment, 13 reference points were defined in the CAD, one at the geometric center of each fully intact cube face. These central points were palpated on the physical specimen using the CMM, with the stylus contacting the midpoint of each selected face to establish spatial correspondence between the digital and printed casts.

The coordinate system's origin (0, 0, 0) was defined in the CAD cast as the centroid of the maxillary cast, located at the intersection of the midsagittal plane and the

Table 2. Description of 36 additional points measured on additively manufactured specimens with coordinate measurement machine

Additional Point	Location
Dental 1	Tip of distobuccal cusp of right and left first molars
Dental 2	Tip of distobuccal cusp of right and left second molars
Dental 3	Tip of mesiolingual cusp of right and left first molars
Dental 4	Tip of mesiolingual cusp of right and left second molars
Dental 5	Tip of buccal cusp of right and left first premolars
Dental 6	Tip of lingual cusp of right and left first premolars
Dental 7	Tip of cusp of right and left canines
Dental 8	Distobuccal edge of right and left lateral incisors
Dental 9	Mesiobuccal edge of right and left lateral incisors
Dental 10	Distobuccal edge of right and left central incisors
Gingival Buccal 1	5 mm apically to buccal interdental papilla between right and left second and first molars on both right and left sides
Gingival Buccal 2	5 mm apically to buccal interdental papilla between first molar and second premolar on both right and left sides
Gingival Buccal 3	5 mm apically to buccal interdental papilla between first premolar and canine on both right and left sides
Gingival Buccal 4	5 mm apically to buccal interdental papilla between lateral and central incisors on both right and left sides
Gingival Palatal 1	5 mm apically to palatal interdental papilla between second and first molars on both right and left sides
Gingival Palatal 2	5 mm apically to palatal interdental papilla between first molar and second premolar on both right and left sides
Gingival Palatal 3	5 mm apically to palatal interdental papilla between first premolar and canine on both right and left sides
Gingival Palatal 4	5 mm apically to palatal interdental papilla between right and left central incisors

transverse plane. This reference point was consistently applied during CMM measurements to ensure alignment accuracy. Following initial alignment, the predefined measurement program automatically recorded the X, Y, and Z coordinates of all specified points (11 cube centers and 36 additional surface points) on the specimen. Each point was measured once, leveraging the CMM's to ensure reliable data.

The STL file of the digital cast was converted into a CAD cast using a software program (Metrolog X4 v18; Metrologic Group), as the CMM requires a solid surface cast rather than a mesh for accurate evaluation. Following measurement, a best-fit adjustment was performed using the eleven reference cubes to align the measured data with the CAD cast, using a local best-fit algorithm. This optimization minimized deviations between the digital and printed casts, enabling the calculation of absolute dimensional differences between the CAD design and the physical specimens.

In this experiment, trueness was determined by the average of the absolute dimensional differences between the digital and printed casts, while precision was characterized by the standard deviation of these differences. Statistical analysis was conducted through a Kruskal-Wallis test for independent samples, subsequently using the Mann-Whitney U pairwise comparisons (α=.05), using a statistical software program (IBM SPSS Statistics, v25; IBM Corp).

RESULTS

Table 3 shows the median values along with the ±interquartile range (IQR) for all axes (x-, y- and z-), along with 3D discrepancies. Table 4 presents the resulting trueness and precision. The 5 digital cast base designs were significantly different in the x-, y-, and z-axes and the 3D discrepancy as indicated by the Kruskal-Wallis' test for independent samples (all P<.001) independently of the 3D printer used. The Mann-Whitney U pairwise comparison test for independent samples identified significant differences between the AG4K and NDM resin groups in the x-, y-, and z-axes and in the 3D discrepancy (all P<.001), regardless of which cast base design was used (Table 4).

Table 3. Median dimensional discrepancies with interquartile ranges (IQR) of additively manufactured casts across different resin materials and base designs (µm)

Discrepancy Measurement	Resin Material	Group	Median ±Interquartile Range	Percentile 25	Percentile 75
x-axis	NDM	H1	26.90 ±66.60	8.10	58.50
		H2	18.80 ±410	6.00	35.00
		HC1	24.40 ±56.70	7.60	49.10
		HC2	23.90 ±54.80	5.70	49.10
		S	26.60 ±73.70	9.00	64.70
	AG4K	H1	11.80 ±34.50	3.70	30.80
		H2	8.20 ±20.50	3.10	17.40
		HC1	35.10 ±84.30	12.90	71.40
		HC2	13.80 ±38.00	4.60	33.40
		S	20.00 ±66.00	6.80	59.20
y-axis	NDM	H1	14.60 ±35.70	6.70	29.00
		H2	8.70 ±24.50	2.80	21.70
		HC1	11.20 ±27.70	4.30	23.40
		HC2	11.80 ±28.00	4.60	23.40
		S	15.60 ±37.90	6.50	31.40
	AG4K	H1	7.90 ±21.50	2.50	19.00
		H2	4.80 ±14.40	1.30	13.10
		HC1	14.2 ±37.50	5.20	32.30
		HC2	7.60 ±19.40	3.30	16.10
		S	14.40 ±32.20	4.20	28.00
z-axis	NDM	H1	28.10 ±67.60	13.30	54.30
		H2	22.20 ±47.00	9.50	37.50
		HC1	25.10 ±56.7	12.00	44.70
		HC2	22.80 ±48.30	9.30	39.00
		S	29.50 ±65.10	14.50	50.60
	AG4K	H1	16.90 ±39.50	4.60	34.90
		H2	9.90 ±22.50	4.60	17.90
		HC1	31.20 ±76.70	16.80	59.90
		HC2	12.60 ±38.90	4.10	34.80
		S	24.00 ±58.50	8.40	50.10
3D Discrepancy	NDM	H1	52.50 ±11.31	26.50	86.60
		H2	36.80 ±81.20	19.30	61.90
		HC1	45.40 ±98.40	21.20	77.20
		HC2	45.20 ±90.20	21.20	69.00
		S	55.80 ±123.00	30.80	92.20
	AG4K	H1	29.20 ±68.70	11.40	57.30
		H2	19.40 ±43.60	9.20	34.40
		HC1	61.70 ±148.90	32.70	116.20
		HC2	25.90 ±66.60	12.50	5410
		S	49.40 ±105.80	20.20	85.60

Table 4. Trueness and precision values obtained for different groups tested (μm)

	Resin Material	Group	Trueness	Precision
x-axis	NDM	H1	41.20	44.40
		H2	27.10	28.20
		HC1	31.70	28.20
		HC2	33.40	34.20
		S	39.10	36.10
	AG4K	H1	22.50	26.90
		H2	12.50	13.40
		HC1	48.00	45.70
		HC2	23.60	27.50
		S	35.10	36.10
y-axis	NDM	H1	21.00	20.60
		H2	14.20	15.10
		HC1	16.90	18.60
		HC2	16.30	15.20
		H1	23.30	23.50
	AG4K	H2	14.10	18.00
		HC1	10.40	14.40
		HC2	27.80	40.40
		S	11.90	13.10
		S	20.00	20.40
z-axis	NDM	H1	35.70	27.20
		H2	26.40	21.50
		HC1	32.20	27.40
		HC2	26.50	20.70
		S	35.00	25.70
	AG4K	H1	24.00	26.30
		H2	13.10	12.20
		HC1	46.10	44.60
		HC2	23.60	26.60
		S	32.60	29.10
3D Discrepancy	NDM	H1	64.50	48.90
		H2	44.80	33.50
		HC1	52.50	38.30
		HC2	50.40	37.10
		S	64.20	41.20
	AG4K	H1	39.80	37.90
		H2	24.10	19.80
		HC1	81.10	65.90
		HC2	39.00	37.00
		S	57.50	44.20

Considering the 3D printer, polymer resin materials, and cast base design, the following results were obtained in the x-, y-, and z-axes and the 3D discrepancy. For the x-axis discrepancy, the Mann-Whitney U pairwise comparison test for independent samples revealed significant differences between NDM-H1 (26.9 ±66.6 μm) and AG4K-H1 (11.8 ±34.5 μm) ($P<.001$), NDM-H2 (18.8 ±41 μm) and AG4K-H2 (8.2 ±20.5 μm) ($P<.001$), NDM-HC1 (24.4 ±56.7 μm) and AG4K-HC1 (35.1 ±84.3 μm) ($P<.001$), and NDM-HC2 (23.9 ±54.8 μm) and AG4K-HC2 (13.8 ±38 μm) ($P<.001$) but not for NDM-S (26.6 ±73.7 μm) and AG4K-S (20 ±66 μm) ($P=.549$) (Fig. 4A). For the y-axis analysis using the Mann-Whitney U pairwise comparison test, significant differences were detected between NDM-H1 (14.6 ±35.7 μm) and AG4K-H1 (7.9 ±21.5 μm) ($P<.001$), NDM-H2 (8.7 ±24.5 μm) and AG4K-H2 (4.8 ±14.4 μm) ($P<.001$), NDM-HC1 (11.2 ±27.7 μm) and AG4K-HC1 (14.2 ±37.5 μm) ($P<.005$), and NDM-HC2 (11.8 ±28 μm) and AG4K-HC2 (7.6 ±19.4 μm) ($P<.000$) but not for NDM-S (15.6 ±37.9 μm) and AG4K-S (14.4 ±32.2 μm) ($P>.999$) (Fig. 4B). In the case of the z-axis analysis using the Mann-Whitney U pairwise comparison test, significant differences were revealed between NDM-H1 (28.1 ±67.6 μm) and AG4K-H1 (16.9 ±39.5 μm) ($P<.001$), NDM-H2 (22.2 ±47 μm) and AG4K-H2 (9.9 ±22.5 μm) ($P<.001$), NDM-HC1 (25.1 ±56.7 μm) and AG4K-HC1 (31.2 ±76.7 μm) ($P<.001$), and NDM-HC2 (22.8 ±48.3 μm) and AG4K-HC2 (12.6 ±38.9 μm) ($P<.001$) but not for NDM-S (29.5 ±65.1 μm) and AG4K-S (24 ±58.5 μm) ($P=.222$) (Fig. 4C). Finally, the analysis of 3D discrepancy using the Mann-Whitney U pairwise comparison test highlighted significant differences between NDM-H1 (52.5 ±113.1 μm) and AG4K-H1 (29.2 ±68.7 μm) ($P<.001$), NDM-H2 (36.8 ±81.2 μm) and AG4K-H2 (19.4 ±43.6 μm) ($P<.001$), NDM-HC1 (45.4 ±98.4 μm) and AG4K-HC1 (61.7 ±148.9 μm) ($P<.001$), and NDM-HC2 (45.2 ±90.2 μm) and AG4K-HC2 (25.9 ±66.6 μm) ($P<.001$) but not for NDM-S (55.8 ±123 μm) and AG4K-S (49.4 ±105.8 μm) ($P=.061$) (Fig. 4D).

DISCUSSION

According to these findings, there was substantial variation in trueness and precision across the x-, y-, and z-axes, as well as 3D discrepancy between the tested groups. However, only the 3D discrepancy for solid cast

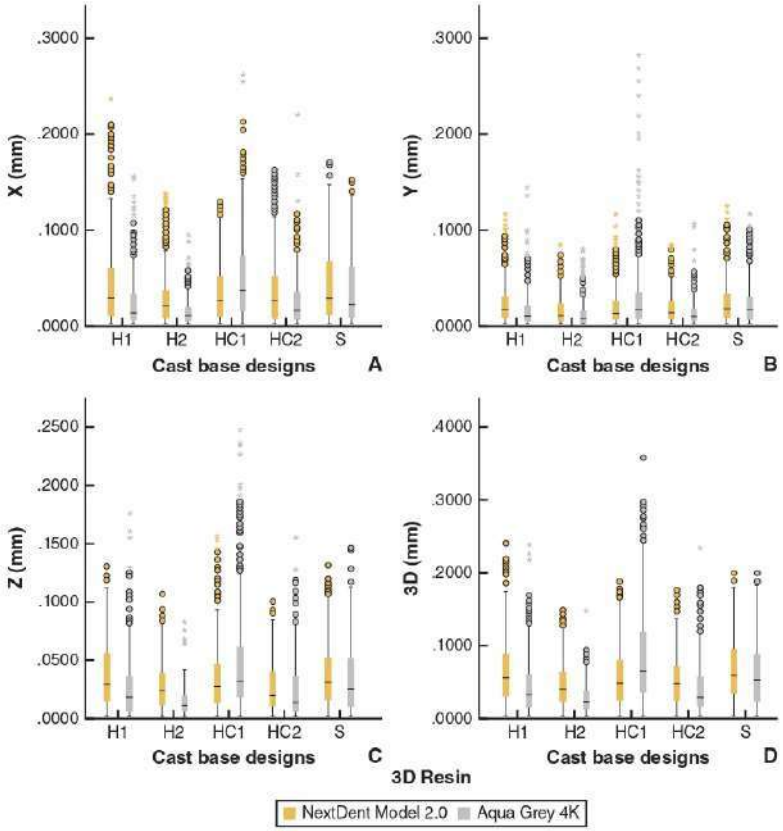

Figure 4. Measured discrepancies of material polymer groups tested. A, x-axis. B, y-axis. C, z-axis. D, 3D discrepancy.

base designs produced with NexDent Model 2.0 or Aqua Gray 4K resins were statistically similar. Consequently, the null hypothesis that accuracy (trueness and precision) would not vary significantly among the different base designs when using the same vat-polymerization technology and 2 different resin polymer materials was rejected. The findings revealed that the Aqua Gray 4K resin group achieved the highest manufacturing accuracy with a hollow base design featuring a 2-mm wall thickness, registering a trueness of 24.1 µm and a precision of 19.8 µm. Likewise, the NexDent Model 2.0 group attained optimal accuracy using the same hollow 2-mm wall thickness design, with a trueness of 44.8 µm and a precision of 33.5 µm.

The present in vitro study showed manufacturing trueness across the tested groups ranging from 24.1 µm to 81.1 µm, while precision oscillated between 19.8 µm and 65.9 µm, all within clinically acceptable limits. Despite the variety of clinical and laboratory conditions, these levels of manufacturing accuracy should not hinder the application of 3D printed casts in the production of thermoplastic devices or silicone indexes. Moreover, the accuracy observed in both 3D printing devices suggests they could be suitable for creating definitive casts, although this conclusion warrants further investigation, as the effectiveness of printed casts in permanent restorations depends on both dimensional accuracy and surface quality.

Calibration of the 3D printing device in this study was performed as indicated by the manufacturer's guidelines using 2 polymer resin materials (NextDent Model 2.0; 3D Systems and Aqua Gray 4K; Phrozen) and the same support structures. The printing process was conducted by a clinician (W.P.C.) with 7 years of experience in 3D printing. For postprocessing procedures, casts printed with NexDent Model 2.0 resin were polymerized with the recommended UV device (LC-3DPrint Box; 3D Systems), and casts printed using Aqua Gray 4K resin employed the

Phrozen polymerization machine (Curing Station; Phrozen) to obtain the optimal properties of the resins according to the manufacturer's recommendations. To the knowledge of the authors, this is the first in vitro study that employs the same 3D printing device and 2 different resin materials to validate the manufacturing trinomial and demonstrate that the same 3D printer can yield different accuracies depending on the resin polymer material used. The accuracy of 3D printed casts has been analyzed in previous studies, registering trueness values between 21.83 μm and 289 μm and precision values spanning from 17.82 μm to 284 μm. However, most studies compared different 3D printers and different resin polymer materials. Thus, a comprehensive comparison of data between different 3D printing systems is impossible. Also, none of the previous studies reported the cast base design selected. The impact that the cast base designs have on the manufacturing accuracy of 3D printing diagnostic casts has been studied.[34,37,40] Rungrojwittayakul et al[34] analyzed the differences between two different base designs (solid and hollow) fabricated with 2 distinct vat-polymerization technologies, SLA-DLP/CLIP (Carbon M2; Carbon) and SLA-DLP (MoonRay S100; Sprintray), reporting that the highest accuracy was achieved using solid base designs, with trueness values between 48 μm and 87 μm and precision values that ranged from 44 μm to 57 μm. Chen et al[35] evaluated two different 3D printing technologies: an SLA-Laser 3D printer (Form 3; Formlabs) and a DLP 3D printer (Straumann P30+; Rapidshape). Each printer was tested with a different resin polymer material: Model Resin V3 (Formlabs) for the Form 3 and P Pro Master Model (Institut Straumann AG) for the Straumann P30+. After printing, all casts were post-cured using the manufacturer-recommended curing machine for each 3D printer, reporting that casts with a hollow interior without a base (HB) exhibited significantly lower trueness (Form 3: 94.06 ±3.43 μm; Straumann *P30+*: 114.03 ±2.75 μm) and precision (Form 3: 66.65 ±3.06 μm; Straumann P30+: 29.78 ±1.90 μm) than designs with a base, such as hollow with perforated base (HWB) (Form 3: trueness 70.61 ±2.15 μm, precision 46.06 ±3.31 μm; Straumann P30+: trueness 98.06 ±2.20 μm, precision 24.38 ±2.36 μm) or solid (S) (Form 3: trueness 85.28 ±2.49 μm, precision 42.63 ±4.09 μm; Straumann P30+: trueness 98.01 ±4.95 μm, precision 20.96 ±0.95 μm). Their study underscores the necessity of a base for maintaining accuracy, attributing the HB design's inferior performance to insufficient structural support during layer-by-layer polymerization. While our study did not test a baseless design, the superior accuracy of the hollow base (H2) over solid and honeycomb configurations echoes Chen et al[35] finding that a base enhances stability, though our results further indicate that hollowing with an optimal wall thickness (2 mm) outperforms a solid structure in trueness, possibly due to reduced material-related distortions in the SLA-LCD process. These differences may also reflect the interplay between resin properties and printer technology, reinforcing the manufacturing trinomial concept's relevance in optimizing 3D printing outcomes. Moreover, differences in print orientations, layer thicknesses, support structures, manufacturing trinomial, 3D printer technologies, resin polymer materials and measurement approaches, make it challenging to compare previous investigations with the results presented here. Revilla-León et al[37] studied the same cast base designs as in the present study. They tested solid, honeycomb, and hollow casts with base designs featuring wall thicknesses of 1 mm and 2 mm using an SLA-DLP 3D printer (NextDent 5100; 3D Systems) and NextDent Model resin polymer material. They concluded that solid casts showed the highest accuracy values at 63.73 ±45.42 μm. Piedra-Cascón et al[40] studied the impact of the same base designs used by Revilla-León et al[37] but using two 3D printers, an SLA-DLP (NextDent 5100; 3D Systems and Sonic Mini 4K; Phrozen) with an identical polymer material (NextDent Model 2.0). The authors reported the best manufacturing accuracy for the NextDent 3D printer to be 21.83 ±18.4 μm. The possible reason for different manufacturing accuracies using the same 3D printer and polymer material could be that their study involved fabricating the specimens vertically in contrast with Piedra-Cascón et al,[41] where all the specimens were 3D printed horizontally; this could have influenced the final results. When a diagnostic cast is fabricated in a vertical orientation, it is probable that the increased hollowness leaves the walls unsupported, potentially leading to distortions. Piedra-Cascón et al[41] also reported that the Phrozen Sonic Mini 4K 3D printer, when paired with NextDent Model 2.0 polymer material, achieved its highest manufacturing accuracy with a trueness of 45.15 ±33.51 μm using a 2-mm hollow cast base design and printed horizontally. They reported statistically significant differences between Sonic Mini 4K and NextDent 5100 3D printers when the same NextDent Model 2.0 polymer material was used, with the NextDent 5100 3D printer being better than the Sonic Mini 4K. The study presented here aimed to provide insights into the accuracy of the Sonic Mini 4K printer using 2 different resins (NextDent Model 2.0; NextDent and Aqua Gray 4K; Phrozen). Using the same dataset as in previous studies,[37,40] the results revealed that the combination of Phrozen's 3D printer and resin achieved an accuracy of 24.1 ±19.8 μm similar to the results obtained using NextDent's 3D printing workflow.[40] These results show that not all resins can achieve the same level of accuracy even when their wavelength is compatible with the printer. This reinforces the need to understand the manufacturing trinomial concept applied to the 3D printing system used.[3]

Various approaches have been used to evaluate the accuracy of 3D printed casts produced with SLA technologies, including manual measurements using digital calipers, as well as digital techniques involving superimposition to obtain linear and angular measurements, often using root mean square (RMS) values.[20,39] Nevertheless, a coordinate measuring machine (CMM) is typically employed to perform such measurements.[38]

SLA 3D printers can be divided into open and closed systems, with the first providing flexibility in the customization of printing parameters and their interrelation with printing zones. In theory, when the wavelengths of polymer materials and 3D printing devices are compatible, they can be used interchangeably. Maneiro-Lojo et al[20] reported manufacturing accuracy ranging from 92 to 131 µm with an open-source SLA-LCD printer (Photon Mono SE; Anycubic) when using Aqua Gray 4K polymer material. In contrast, the current study found that the Sonic Mini 4K paired with the same Aqua Gray 4K resin achieved a manufacturing accuracy between 4.3 and 43.9 µm. The discrepancies between these studies could stem from differences in cast base designs, settings of the support structure, printing parameters, and postprocessing procedures. However, this investigation indicates that even when the wavelength of the resin materials and the 3D printer's UV light source are compatible, changes in accuracy are likely associated with the need for adjustments within the manufacturing trinomial concept.[3] Differences in accuracy between the two 3D polymer resin materials tested may also be attributed to differences in their formulations, including the types of photo-initiators used and the presence or absence of anti-sedimentation technology.

One of the main limitations of this study is the fact that only one 3D printer was tested with 2 resin polymer materials. Further research is necessary to investigate the manufacturing process using different 3D printing systems. This will help optimize the 3D printing workflow's accuracy, making it suitable for more complex applications.

CONCLUSIONS

Based on the findings of this in vitro study, the following conclusions were drawn:

1. The type of material polymer had an impact on the manufacturing accuracy with the same 3D printing technology.
2. The 2-mm wall thickness hollow design displayed the highest accuracy in casts produced using an SLA-LCD technology with Aqua Gray 4K resin material.
3. The highest manufacturing accuracy for Aqua Gray 4K specimens ranged from 4.3 to 43.9 µm.
4. The digital base designs impacted the manufacturing accuracy of the fabricated casts.
5. Solid casts were the least influenced by the printer/resin combination.

REFERENCES

1. Hull C.W. Apparatus for production of three-dimensional objects by stereolithography 1986, US Patent 4575330.
2. Glossary of Digital Dental Terms, 2nd Edition: American College of Prosthodontists and ACP Education Foundation. *J Prosthodont*. 2021;30:172–181.
3. Piedra-Cascón W, Krishnamurthy VR, Att W, Revilla-León M. 3D printing parameters, supporting structures, slicing, and postprocessing procedures of vat-polymerization additive manufacturing technologies: A narrative review. *J Dent*. 2021;109:103630.
4. ISO 17296-2:2015. Additive manufacturing general principles part 2: overview of process categories and feedstock. Last Accessed 01/08/2024.
5. ASTM, Committee F42 on Additive Manufacturing Technologies, West Conshohocken, Pa. 2009 Standard terminology for additive manufacturing general principles and terminology. ISO/ASTM52900-15. Last Accessed 01/08/2024.
6. Revilla-León M, Özcan M. Additive manufacturing technologies used for processing polymers: Current status and potential application in prosthetic dentistry. *J Prosthodont*. 2019;28:146–158.
7. Hornbeck L. Digital micromirror device 2009. US Patent No. 5061.049.
8. ISO 17296e2. Additive manufacturing general principles part 2: Overview of process categories and feedstock. 2015. Available at: https://www.iso.org/standard/61626.html?browse=tc.
9. Holt P.M. Maskless photopolymer exposure process and apparatus 2012. US Patent 8.114.569 B2.
10. Piedra-Cascón W, Adhikari RR, Özcan M, et al. Accuracy assessment (trueness and precision) of a confocal based intraoral scanner under twelve different ambient lighting conditions. *J Dent*. 2023;134:104530.
11. Ide Y, Nayar S, Logan H, et al. The effect of the angle of acuteness of additive manufactured models and the direction of printing on the dimensional fidelity: Clinical implications. *Odontology*. 2017;105:106e115.
12. Wu D, Zhao Z, Zhang Q, et al. Mechanics of shape distortion of DLP 3D printed structures during UV post-curing. *Soft Matter*. 2019;15:6151–6159.
13. Alharbi N, Osman R, Wismeijer D. Effect of build direction on the mechanical properties of 3D printed complete coverage interim dental restorations. *J Prosthet Dent*. 2016;155:760–767.
14. Reymus M, Fabritius R, Keßler A, et al. Fracture load of 3D-printed fixed dental prostheses compared with milled and conventionally fabricated ones: The impact of resin material, build orientation, postcuring, and artificial aging: An in vitro study. *Clin Oral Investig*. 2020;24:701–710.
15. Revilla-León M, Umorin M, Özcan M, Piedra-Cascón W. Color dimensions of additive manufactured interim restorative dental material. *J Prosthet Dent*. 2020;123:754–760.
16. Puebla K, Arcaute K, Quintana R, Wicker RB. Effects of environmental conditions, aging, and build orientations on the mechanical properties of ASTM type I specimens manufactured via stereolithography. *Rapid Prototyp J*. 2012;18:374–388.
17. Braian M, Jimbo R, Wennerberg A. Production tolerance of additive manufactured polymeric objects for clinical applications. *Dent Mater*. 2016;32:853–861.
18. Arnold C, Monsees D, Hey J, Schweyen R. Surface quality of 3D-printed models as a function of various printing parameters. *Materials (Basel)*. 2019;12:19.
19. Revilla-León M, Jordan D, Methani MM, et al. Influence of printing angulation on the surface roughness of additive manufactured clear silicone indices: An in vitro study. *J Prosthet Dent*. 2021;125:462–468.
20. Maneiro Lojo J, Alonso Pérez-Barquero J, García-Sala Bonmatí F, et al. Influence of print orientation on the accuracy (trueness and precision) of diagnostic casts manufactured with a daylight polymer printer. *J Prosthet Dent*. 2024;132:1314–1322.
21. Park GS, Kim SK, Heo SJ, et al. Effects of printing parameters on the fit of implant-supported 3D printing resin prosthetics. *Materials (Basel)*. 2019;12:2533.
22. Zhang ZC, Li PL, Chu FT, Shen G. Influence of the three-dimensional printing technique and printing layer thickness on model accuracy. *J Orofac Orthop*. 2019;80:194–204.
23. Lo Russo L, Guida L, Zhurakivska K, et al. Effect of print layer height on the assessment of 3D-printed models. *Am J Orthod Dentofacial Orthop*. 2019;156:283–289.
24. Favero CS, English JD, Cozad BE, et al. Effect of print layer height and printer type on the accuracy of 3-dimensional printed orthodontic models. *Am J Orthod Dentofacial Orthop*. 2017;152:557–565.
25. Reymus M, Lümkemann N, Stawarczyk B. 3D printed material for temporary restorations: Impact of print layer thickness and post-curing method on degree of conversion. *Int J Comput Dent*. 2019;22:231–237.

26. Chockalingam K, Jawahar N, Chandrasekhar U. Influence of layer thickness on mechanical properties in stereolithography. *Rapid Prototyp J*. 2006;12:106–113.
27. Scherer M, Al-Haj Husain N, Barmak AB, et al. Influence of the layer thickness on the flexural strength of aged and nonaged additively manufactured interim dental material. *J Prosthodont*. 2023;32:68–73.
28. Cho HS, Park WS, Choi BW, Leu MC. Determining optimal parameters for stereolithography processes via genetic algorithm. *J Manuf Syst*. 2000;19:18–27.
29. Alharbi N, Osman RB, Wismeijer D. Factors influencing the dimensional accuracy of 3D-printed full-coverage dental restorations using stereolithography technology. *Int J Prosthodont*. 2016;29:503–510.
30. Unkovskiy A, Bui PH, Schille C, et al. Objects build orientation, positioning, and curing influence dimensional accuracy and flexural properties of stereolithographically printed resin. *Dent Mater*. 2018;34:324–333.
31. Mostafavi D, Methani MM, Piedra-Cascón W, et al. Influence of the rinsing postprocessing procedures on the manufacturing accuracy of vat-polymerized dental model material. *J Prosthodont*. 2021;30:610–616.
32. Mostafavi D, Methani MM, Piedra-Cascón W, et al. Influence of polymerization postprocessing procedures on the accuracy of additively manufactured dental model material. *Int J Prosthodont*. 2023;36:479–485.
33. Etemad Shahidi Y, Qallandar OB, Evenden J, et al. Accuracy of 3-dimensionally printed full-arch dental models: A systematic review. *J Clin Med*. 2020;9:3357.
34. Rungrojwittayakul O, Kan JY, Shiozaki K, et al. Accuracy of 3D printed models created by two technologies of printers with different designs of model base. *J Prosthodont*. 2020;29:124–128.
35. Chen Y, Li H, Zhai Z, et al. Impact of internal design on the accuracy of 3-dimensionally printed casts fabricated by stereolithography and digital light processing technology. *J Prosthet Dent*. 2023;130:381.e1–381.e7.
36. Kim SY, Shin YS, Jung HD, et al. Precision and trueness of dental models manufactured with different 3-dimensional printing techniques. *Am J Orthod Dentofacial Orthop*. 2018;153:144–153.
37. Dietrich CA, Ender A, Baumgartner S, Mehl A. A validation study of reconstructed rapid prototyping models produced by two technologies. *Angle Orthod*. 2017;87:782–787.
38. Revilla-León M, Piedra-Cascón W, Arayonesers R, et al. Influence of base design on the manufacturing accuracy of vat-polymerized diagnostic casts: An in vitro study. *J Prosthet Dent*. 2023;129:166–173.
39. Morón-Conejo B, López-Vilagran J, Cáceres D, et al. Accuracy of five different 3D printing workflows for dental models comparing industrial and dental desktop printers. *Clin Oral Investig*. 2023;27:2521–2532.
40. ISO 5725-1. Accuracy (trueness and precision) of measuring methods and results. Part-1: General principles and definitions.
41. Piedra-Cascón W, Pérez-López J, Veiga-López B, et al. Influence of base designs on the manufacturing accuracy of vat-polymerized diagnostic casts using two different technologies. *J Prosthet Dent*. 2024;132:453.e1–453.e9.

Corresponding author:
Dr Wenceslao Piedra-Cascón
Rua Entremíos s/n
Santiago de Compostela 15782
SPAIN.
Email: wpiedra@movumtech.com

Acknowledgments
The authors thank Dental Astur dental laboratories for their support with NextDent technologies.

CRediT authorship contribution statement
Wenceslao Piedra-Cascón: Idea, conceptualization, protocol development, results interpretation, Phrozen manufacturing procedures and contributed to the manuscript writing. **Carlos Oteo-Morilla**: Statistical analysis and contributed to the manuscript writing. **Jose Manuel Pose-Rodríguez**: Contributed to the protocol development and results interpretation. All authors discussed the evolution and commented on the manuscript at all stages.

https://doi.org/10.1016/j.prosdent.2025.03.033

5
DISCUSIÓN

5 DISCUSIÓN

El objetivo de esta Tesis Doctoral ha sido la realización de una serie de cuatro estudios experimentales en los que se analizó el flujo de trabajo digital aplicado en odontología en cada una de sus fases: digitalización, diseño CAD y proceso de fabricación 3D. Como se ha demostrado en esta Tesis Doctoral, el flujo de trabajo digital es complejo y multifactorial, en las que, en cada una de sus etapas, existen una serie de subfases que afectan a la precisión global del flujo de trabajo. Por ese motivo hemos abordado un flujo de trabajo en específico, que es aquel que empieza con el escaneado intraoral del paciente, se diseñan los modelos con el diseño de zócalo deseado y se envían estos archivos a fabricar mediante tecnologías de fabricación aditiva, comúnmente conocidas como impresión 3D. En cada una de estas fases se evaluó la precisión en términos de exactitud y fiabilidad siguiendo la normativa ISO 5725-1:1994 (59).

El primer estudio que compone esta Tesis Doctoral analiza la precisión de un sistema de escaneado intraoral (PrimeScan®; Dentsply Sirona) bajo 12 condiciones de luz ambientales desde 0 lux, hasta los 10.000 luxes. Los resultados del estudio confirmaron que existe un impacto de la luz ambiental del gabinete sobre la precisión del dispositivo de escaneado intraoral utilizado. Los mejores valores de precisión se encontraron escaneando a 1000 lux, obteniendo una exactitud de 69.76µm y una fiabilidad de 97.4µm. Las diferencias entre este grupo y el resto de grupos estudiados mostraron diferencias en exactitud entre 97µm y 266µm mientras que en fiabilidad las diferencias entre grupos oscilaron entre 220,7µm y 390,6 µm. Estos valores dejan patente la importancia de controlar la luz ambiental del gabinete odontológico ya que, con el dispositivo intraoral estudiado, el único grupo que obtiene valores compatibles con precisión clínica es el grupo de 1000 lux (Figura 1).

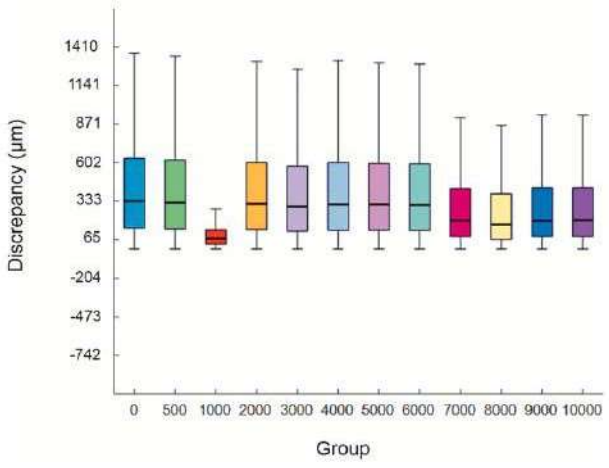

Figura 1. Diagrama de caja y bigotes que ilustra la distribución de los valores de precisión obtenidos con el escáner intraoral (PrimeScan®; Dentsply Sirona) en función de los distintos niveles de iluminación de la luz ambiental.

Existen estudios previos que han analizado el impacto de la luz ambiental sobre la precisión de escáneres intraorales (26-34). Sin embargo, en ninguno de ellos se analizaron los dispositivos bajo 12 condiciones de luz ambientales. Revilla-León y cols (25) publicaron en el año 2020 un estudio en el que analizaron el impacto de la luz ambiental del gabinete sobre 3 dispositivos de escaneado intraoral, siendo éstos: Trios 3; 3Shape, CEREC Omnicam; Dentsply-Sirona e iTero Element; Align Technology. En este estudio, los autores analizaban la precisión de los escáneres intraorales bajo 4 condiciones de luz ambientales: 0 lux (luz apagada), 500 lux (luz apagada del gabinete y entrando luz natural por la ventana), 1000 lux (estándar europeo de iluminación en gabinete) y 10.000 lux (luz del sillón dirigida hacia a la boca del paciente). Los autores encontraron que la máxima precisión de los escáneres Trios 3 e iTero Element se obtenían a 1000 lux con precisiones de 203.86 ± 94.31µm y 191.85 ± 71.97µm respectivamente. En este estudio el escáner CEREC Omnicam obtuvo los mejores valores de precisión con la luz de la habitación apagada (0 lux) obteniendo unos valores de precisión de 279.79 ± 247.06 µm. Sin embargo, la precisión de este escáner bajo unas condiciones de luz ambiental de 1000 lux su precisión fue de 384.74 ± 315.93µm. La condición ambiental de la luz del gabinete claramente influyó en los resultados de precisión de los sistemas de escaneado intraoral estudiados, siendo el escáner intraoral con peores valores de precisión CEREC Omnicam (Dentsply-Sirona). En un estudio posterior Medina-Sotomayor y cols (66) analizaron la relación entre resolución y precisión de 4 sistemas de escaneado intraoral, entre ellos CEREC Ominicam (Dentsply-Sirona). En dicho estudio CEREC Omnicam obtuvo los mejores valores de resolución, 79,82 pts/mm2 (puntos por milímetro cuadrado). Estos autores concluyenron que, a pesar de ser el escáner con la mayor resolución, su baja precisión podía ser debida a errores en la interpolación de la nube de puntos a la hora de reconstruir las mallas 3D Por otra parte, los autores no midieron la condición de luz ambiental ideal para escanear con el escáner intraoral CEREC Omnicam (Dentsply-Sirona). Koseoglu y cols. (31) llevaron a cabo un estudio *in-vivo* con 20 pacientes en el que digitalizaron arcos completos maxilares con el escáner i500 (Medit Corp) utilizando los modos de iluminación blanca y azul del escáner bajo dos condiciones de luz ambiental: 0 luz y 1000 lux. Estos autores midieron exclusivamente la exactitud. En este tranajo, la mejor exactitud se obtuvo a una iluminación de 1000 lux (72.3 µm) escaneado en el modo luz azul, mientras que el peor valor de precisión se obtuvo escaneando a 0 lux en modo lux blanca (88.4 µm). En otro estudio, Wessemann y cols. (31) analizaron 6 escáneres intraorales: Trios 3, Cerec Omnicam, CS3600, iTero Element, GC Advaa, and Planmeca Emerald. Midieron la precisión de estos escáneres intraorales en 4 condiciones de luz ambientales: 100, 500, 1000 y 5000 lux encontrando que existían diferencias estadísticamente significativas entre las 4 condiciones de luz ambientales, siendo el escáner intraoral Trios 3 el que obtuvo menores desviaciones. Hemos encontrado un estudio, el de Jivanescu y cols. (30) que concluyen que la luz ambiental del gabinete no afecta a la precisión de los escáneres intraorales. Esta conclusión puede deberse al escáner intraoral utilizado (Planmeca Emerald®) y al diseño del propio estudio pues se trataba de medir las discrepancias en la preparación de una corona de recubrimiento total realizada *in-vitro* en una fantoma mandibular. En el año 2024, Ma y cols. (142) realizan una revisión sistemática y afirman que la luz ambiental del gabinete afecta a la precisión de los escáneres intraorales. Estos autores encontraron que, en escaneados de arco completo, para la mayoría de dispositivos de escaneado intraoral la condición ideal de luz ambiental es de 1000 lux. Resultados que concuerdan con los

hallados en los estudios de la presente Tesis Doctoral.

Ochoa-López y cols. (32) en un estudio *in-vitro* utilizando el mismo dispositivo de escaneado intraoral que el utilizado en el primer estudio de la presente Tesis Doctoral. Estos autores escanearon bajo 6 condiciones de luz ambientales (0, 100, 500, 1000, 5000 y 10.000 lux) determinando que la mejor condición de luz ambiental para el escáner intraoral PrimeScan® (Dentsply-Sirona) era 10.000 lux con una exactitud de 65.5µm y una fiabilidad de 46.8µm, sin existir diferencias estadísticamente significativas con el grupo de 1000 lux. Los resultados de estos autores difieren de los resultados obtenidos en nuestra investigación. Estas diferencias pueden ser debidas a que estos autores midieron la precisión del escáner intraoral PrimeScan® *in vitro*, sobre un modelo de fantoma edéntulo escaneando *scanbodies* de metal. Además, el protocolo de escaneado realizado en el estudio fue un escaneado en zig-zag, no siendo el protocolo de escaneado recomendado por la casa comercial.

Una vez analizado el impacto de la luz ambiental del gabinete odontológico en la precisión del escáner intraoral PrimeScan®, procedimos al análisis del impacto en los procesos de alineación de diferentes *softwares* CAD 3D, tanto a nivel de precisión como de tiempo de procesamiento. Es necesario entender que uno de los factores clave de la odontología digital se basa en los procesos de alineación para obtener el denominado paciente virtual. A pesar de la importancia de los procesos de alineación, la evidencia científica en cuanto a los protocolos de alineación de mallas, las discrepancias y el tiempo necesario para llevar a cabo dichas alineaciones es limitada. Además, tampoco existe ninguna recomendación por parte de las casas comerciales de *software.*

Para este segundo estudio de análisis de alineación 3D utilizamos uno de los escaneados intraorales del grupo de 1000 lux del primer estudio de esta Tesis Doctoral, ya que era el grupo cuyas mallas 3D presentaban las menores distorsiones. Esto es crucial a la hora de realizar la alineación de mallas 3D. En este estudio analizamos 12 algoritmos de alineación diferentes en 6 *softwares* CAD: B4D (Blender v.3.6.5; B4D, Queensland, Australia), BSP (BlueSkyPlan v.4.13; BlueSkyBio, Illinois, USA), DCA (DentalCAD v.3.2; Exocad, Darmstadt, Germany), MD (Medit Design v.2.1.4; Medit, Seoul, South Korea), NMS (NemoSmile v.24.0.0.3; Nemotec, Madrid, Spain), and MSH (Meshmixer v.3.5.474; Autodesk, California, USA). En la actualidad, los softwares CAD presentan similitudes en cuanto a las operaciones que pueden llevar a cabo con mallas 3D. Sin embargo, existen *softwares* que permiten mayor libertad que otros. Se ha de poner en relieve que, durante el desarrollo de la presente tesis doctoral, y con los *sofwares* CAD empleados, no se ha encontrado que ninguno de los *softwares* anteriormente mencionados pudiera ofrecer al usuario los 12 algoritmos de alineación testados.

En este estudio, los valores promedio de exactitud variaron entre 67 y 162 µm, mientras que los valores de fiabilidad se encontraron en un rango entre 51 y 83 µm. Además, el tiempo promedio de las alineaciones 3D entre los diferentes *softwares* y algoritmos osciló entre 33 y 561 segundos. La hipótesis nula del estudio fue rechazada ya que se encontraron diferencias estadísticamente significativas entre los diferentes algoritmos de alineación y el tiempo de procesamiento. Los mejores resultados se obtuvieron cuando el *software* implementa algoritmos de *best-fit* (BF). Los algoritmos por superficies (SBF), en los que es necesario seleccionar áreas fueron más precisos que los algoritmos de selección por puntos (LBF) (Figura 2). Sin embargo, el tiempo necesario para realizar las alineaciones

SBF fue mayor que con protocolos LBF. En ambos casos, los algoritmos SBF y LBF requieren la intervención humana, lo que supone una introducción a errores. Es por ello, que se recomienda que el *software* utilizado implemente algoritmos BF de segundopaso, para minimizar los errores humanos, ya que es un procedimiento meramente matemático.

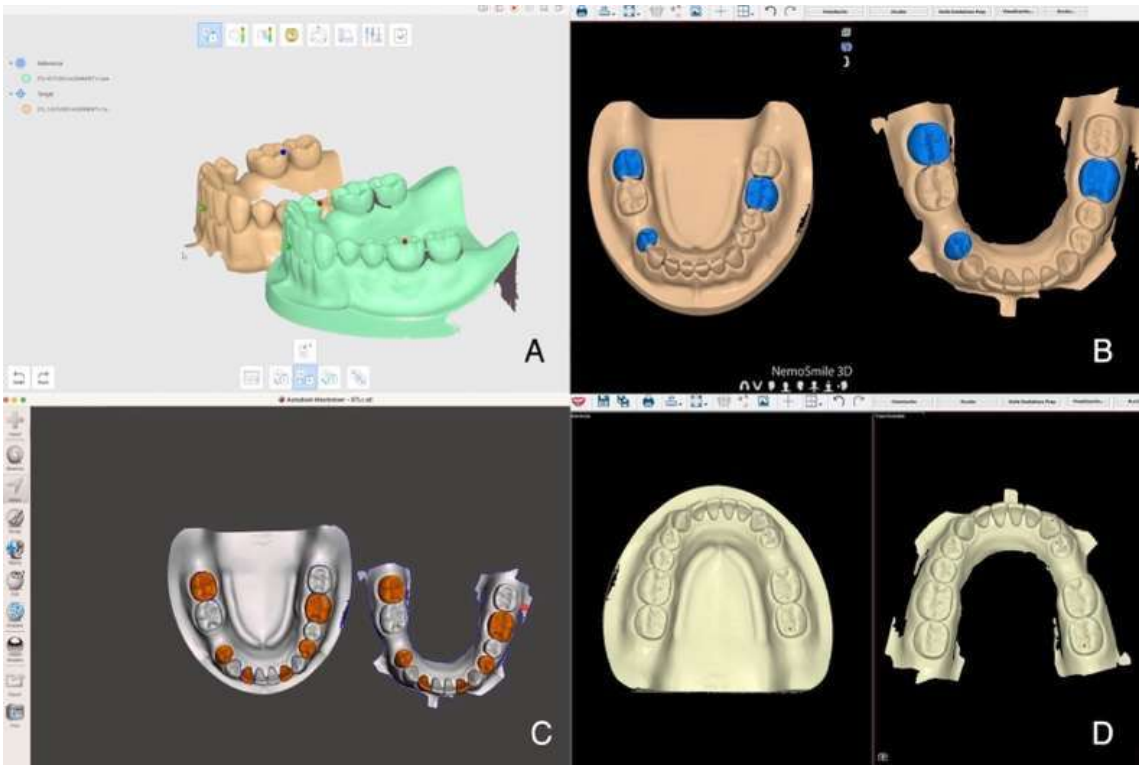

Figura 2A-D. Ejemplos representativos de alineación en diferentes *softwares.* A y D muestran alineación por puntos (LBF), mientras que las figuras B y C muestran alineación por áreas (SBF)

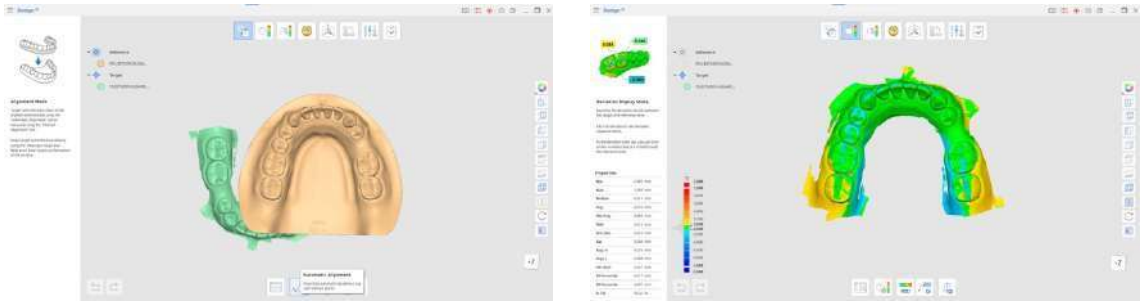

Figura 3A-B. Alineación automática en *software* Medit Design. En la imagen de la izquierda se visualiza la malla de referencia (STL zocalado en escáner de laboratorio) y la malla a alinear (malla sin zócalo) en difernetes ejes de coordenadas -x, -y, -z. Tras seleccionar "Alineación Automática", la malla a alinear se posiciona en el mismo eje de coordenadas que la malla de referencia sin ningún tipo de intervención humana, utilizando un algoritmo de inteligencia artificial y protocolo de alineación *best-fit.*

Es necesario remarcar que no existe en la literatura científica un umbral de referencia para considerar si una malla está correctamente alineada. Un estudio previo de Revilla-León y cols. (138) analizando diferentes protocolos de alineación (BF, 3 puntos LBF, 6 puntos LBF y y 3 áreas SBF) de mallas 3D en un *software* de ingeniería no dental (Geomagic Control X). obtienen valores de exactitud que oscilaban entre 150 y 200 µm y unos valores de fiabilidad en el rango de 1 a 37 µm, encontrando por tanto valores de precisión en alineación que se encontraban entre 149 y 237 µm. Los autores concluyeron que los algoritmos de alineación LBF obtuvieron peores valores de precisión si los comparamos con SBF o BF, hallando además diferencias estadísticamente significativas entre 3 y 6 puntos LBF. Es necesario remarcar que estos autores optaron por tomas 3 o 6 puntos oclusales en sus protocolos LBF, sin embargo, no tuvieron en cuenta que los puntos marcados en protocolos de alineación LBF también se pueden hacer en los diferentes ejes de coordenadas -X, -Y, -Z.

En nuestro estudio, no se obtuvieron diferencias estadísticamente significativas ni en exactitud (p=.056) ni en tiempo de procesamiento (p=.907) entre algoritmos de alineación por 3 y 6 puntos oclusales, pero sí en la fiabilidad (p=.004). Sin embargo, cuando se midieron los valores de exactitud, fiabilidad y tiempo de procesamiento, si se encontraron diferencias estadísticamente significativas si se implementaba en los protocolos de alineación por puntos, seleccionar 3 o 6 puntos en los tres planos -X, -Y, -Z del espacio.

En cuanto a los algoritmos por áreas SBF, no se obtuvieron diferencias significativas en los *softwares* entre seleccionar 3 o 6 áreas, con la excepción del *software* NemoSmile de Nemotec en el que fue necesario seleccionar todos los dientes para obtener los mejores valores de precisión de alineación de mallas (69.92 ± 57.35 µm), siendo necesario invertir un tiempo de 348 segundos. Sin embargo, se puede obtener el mismo nivel de precisión en la alineación de mallas (70.79 ± 56.31 µm) con el *software* Medit Design (Medit Corp) utilizando en primer paso su algoritmo BF, siendo necesario invertir en este caso 33 segundos. Esto supone 10 veces menor tiempo invertido para conseguir la misma alineación entre dos *softwares* diferentes. El impacto ya no es sólo la precisión obtenida en cada protocolo de alineación por *software*, si no el tiempo necesario para llevarlo a cabo, ya que parece constatarse que la intervención humana puede llevar asociada de forma inherente un error.

En relación al *software* Medit Design, Dede y cols. (139) compararon este *software* con Geomagic Control X, un *software de* metrología analizando la desviación de escaneados de estructuras de implantes, no encontraron desviaciones estadísticamente significativas entre ambos *softwares.* Esto es de vital importancia ya que la principal diferencia entre ambos tipos de *softwares* es el precio de la licencia. Mientras que el *software* Medit Design es gratuito o *freemium*, el *software* Geomagic Control X tiene un alto coste por licencia. Es decir, que se puede obtener el mismo grado de alineación indiferentemente del coste de licencia. Los resultados de este estudio son congruentes con los resultados encontrados en nuestra línea de investigación.

Este segundo estudio de la presente Tesis Doctoral puede servir para establecer un

umbral clínico aceptable en los procedimientos de alineación de mallas, así como, para establecer una posible definición de mejor *software* CAD, siendo aquel que, entre otras funcionalidades, sea capaz de obtener los mejores valores de alineación de mallas 3D en el menor tiempo posible.

El tercer y cuarto estudio de la presente Tesis Doctoral están relacionados con la última fase del flujo de trabajo digital en odontología, la fabricación de modelos/ la impresión 3D. El objetivo de estos estudios experimentales fue analizar el efecto en la precisión de impresión 3D del diseño de diferentes tipos de zócalos de modelos (Figura 3) y comprobar si existía o no una interrelación entre el material de impresión 3D utilizado y la tecnología de impresión 3D empleada. Son varios los artículos que analizan la precisión de la impresión 3D (99, 103, 112, 114, 120-150). Sin embargo, existen grandes diferencias entre los protocolos, tecnologías de impresión 3D y resinas de impresión 3D estudiadas dificultando la realización de análisis comparativos entre diferentes materiales e impresoras 3D.

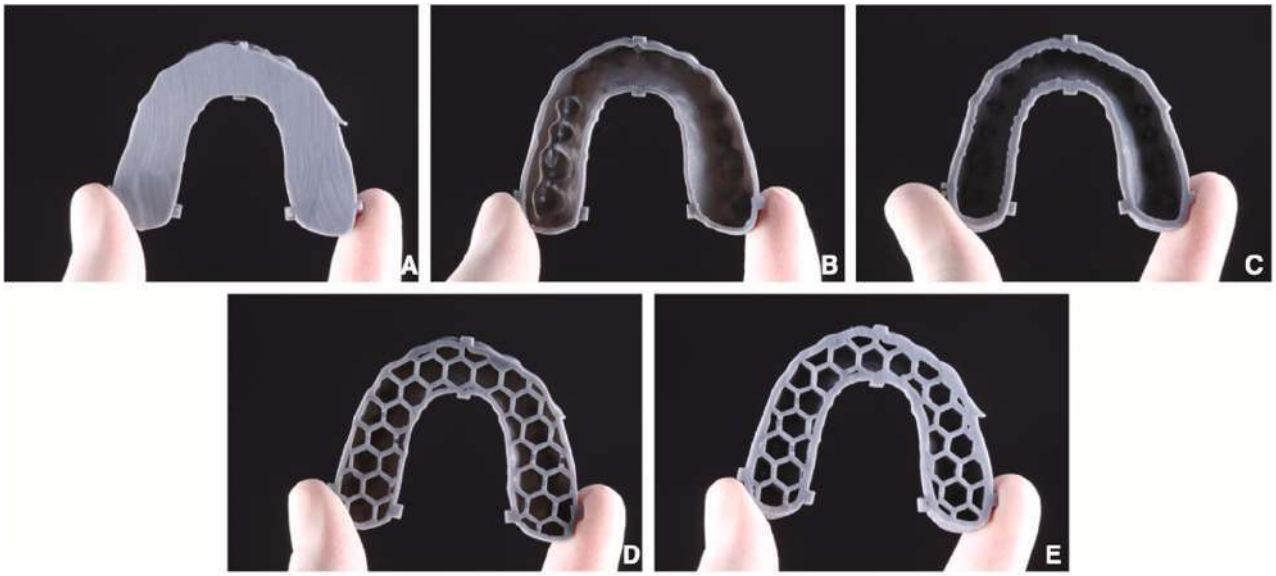

Figura 3. Modelos impresos en 3D con diferentes diseños de zócalos. A) Sólido (S), B) Ahuecado con grosor de pared 1mm (H-1), c) Ahuecado con grosor de pared 2mm (H-2), D) Panal de abejas grosor de pared 1mm (HC-1), E) Panal de abejas grosor de pared 2 mm (HC-2)

En el artículo 3 de esta Tesis Doctoral se analizaron dos impresoras 3D de igual longitud de onda (405nm), siendo una la NextDent 5100 de tecnología DLP y la otra, una impresora Sonic Mini 4K (Phrozen) de tecnología LCD. En ambas impresoras, al compartir la misma longitud de onda se utilizó la misma resina (Model Gray 2.0; NextDent). Además de medir el impacto que puede llegar a tener la tecnología de impresión 3D y el material, también se analizaron 3 diseños de zócalos de modelos odontológicos y dos grosores de pared 8 1mm y 2mm), por lo que se establecieron 5 grupos de estudio, siendo éstos: grupo zócalo sólido

(S), grupo zócalo ahuecado con grosor de pared de 1 mm (H-1), grupo zócalo ahuecado con grosor de pared de 2 mm (H-2), grupo zócalo panal de abejas de grosor de pared de 1 mm (HC-1) y grupo zócalo panal de abejas con grosor de pared de 2 mm (HC-2). Todos los modelos se imprimieron con ambas impresoras y se polimerizaron con la misma polimerizadora, la LC-3DPrint Box de NextDent. Por lo tanto, en este estudio lo único que difiere es el tipo de tecnología de impresión 3D. La hipótesis nula fue rechazada ya que se encontraron diferencias estadísticamente significativas entre los diferentes diseños de zócalos en ambas tecnologías de impresión 3D (LCD y DLP). Entre la impresora NextDent y la Phrozen, fue la impresora NextDent con un diseño de zócalo en panal de abejas con un grosor de pared de 1 mm (HC-1) la que obtuvo el mejor valor de precisión (21.83 ± 18.40 µm), mientras que en el grupo de la impresora Phrozen el mejor valor se obtuvo con un diseño de zócalo ahuecada con grosor de pared de 2 mm (H-2) con una precisión de 45.15 ± 33.51 µm. En nuestro estudio, entre todos los grupos, la exactitud osciló entre 21.83 y 64.51 µm, mientras que la fiabilidad de impresión 3D se situó en un rango entre 17.82 y 48.92 µm. El grupo de la impresora NextDent obtuvo mejores valores de precisión y mayor estabilidad entre grupos que los resultados obtenidos en los grupos de la impresora de Phrozen.

Si comparamos nuestros resultados de impresión 3D con estudios previos de otros autores, nos encontramos con reportes de valores de exactitud en la literatura que varían entre 82 y 289 µm y valores de fiabilidad entre 20 y 284 µm (99, 103, 112, 114, 120-150). Sin embargo, la mayoría de estos estudios no incluyen la información el diseño de zócalo de sus modelos. Existen autores que sí han tenido en cuenta el diseño de base del zócalo, como Rungrojwittayakul y cols. (143) compararon modelos con un zócalo sólido y ahuecado, utilizando dos impresoras DLP, una Carbon M2 y una Sprintray MoonRay S100. Estos autores obtuvieron mejores valores con un diseño de base de zócalo sólido, con valores de exactitud que oscilaban entre 48.y 87µm y valores de fiabilidad que variaban entre 44 y 57 µm. Es necesario remarcar, que con cada impresora 3D utilizaban la resina específica de cada casa comercial, con lo que se introducía una variable no controlada en este estudio que es el material de impresión 3D.

Un trabajo de Revilla-León y cols, (103) en el que se comparten con los estudios de la presente Tesis Doctoral en relación a la impresión 3D el mismo *dataset.* En su estudio, los autores utilizaron la misma impresora NextDent 5100 y la misma resina Model 2.0 de NextDent, así como el mismo protocolo de post-procesado. En su estudio concluyeron que los mejores valores de precisión con la impresora NextDent se obtuvieron con un diseño de zócalos sólido (63.73 ± 45.42 µm), mientras que en nuestra investigación se obtuvieron unos valores de 24.79 ± 20.03 µm para el mismo diseño de zócalo sólido. Sin embargo, como ya se indicó, el mejor valor de precisión con la impresora NextDent 5100 se obtuvo con un diseño de zócalo en panal de abejas con un grosor de pared de 1 mm (21.83 ± 18.40 µm). Esto supone una diferencia utilizando la misma impresora y el mismo diseño de zócalo de 42 µm en exactitud y 27 µm en fiabilidad. Estas diferencias pueden ser claramente debidas a una diferencia en el ángulo orientación de impresión 3D de los modelos y a una diferencia en el diseño de las estructuras de soporte de los modelos. En el estudio de Revilla-León y cols. (103) se utilizaron diseños de estructuras de soportes recomendados por la casa fabricante y se imprimieron los modelos en orientación vertical. Esto hace, que la conclusión de los autores sea que cuanto más ahuecado es un modelo, menor precisión tiene, ya que está claramente influenciado por el ángulo de orientación de

impresión 3D en vertical. Sin embargo, en nuestro estudio utilizamos un ángulo de orientación de impresión 3D a 0º, o lo que es lo mismo, en horizontal. La razón por la que imprimos los modelos en posición completamente horizontal está basado en el estudio de Revilla-León y cols. (159) en el que imprimen llaves de silicona transparente con la resina Ortho IBT de la casa comercial NextDent. Establecen 5 grupos en función del ángulo de orientación de las llaves de silicona en la plataforma de impresión 3D (0º, 25º, 45º, 75º y 90º). Los autores encontraron diferencias estadísticamente significativas entre los grupos, siendo el grupo que obtuvo la menor rugosidad superficial, el grupo de 0º, es decir, aquel grupo en el que las llaves de silicona se imprimieron completamente en horizontal. Estas son las principales razones que pueden explicar por qué una misma impresora, un mismo material y una misma geometría pueden obtener resultados de impresión 3D diferentes.

Maneiro-Lojo y cols. (114) utilizaron una impresora *open-source* (Photon Mono SE; Anycubic) con una resina no específica del sector dental (Aqua Gray 4K; Phrozen). En su estudio compararon 5 ángulos de orientación diferentes (0º, 22. 5º, 45º, 67. 5º y 90º). Determinando que el mejor ángulo de orientación era 22.5º con una precisión de los modelos impresos en el rango de 92 a 131µm. Este estudio presenta claras diferencias con los estudios de impresión 3D de la presente Tesis Doctoral. Las principales diferencias radican en que en nuestras investigaciones imprimimos los modelos completamente en horizontal a un espesor de capa de 50 µm. La precisión obtenida en nuestros estudios con una impresora SLA-LCD y la misma resina se halla en el rango de 4.3 a 43 µm, lo que supone una mejora en términos de precisión de 4.65 veces. Estas diferencias pueden ser explicadas debido a que Maneiro-Lojo y cols (114) no controlaron el diseño de los zócalos para la impresora utilizada, el ángulo de orientación de impresión 3D seleccionado o bien por las diferencias en la metodología de medición. Estos autores escanearon los modelos impresos con un escáner de sobremesa y alinearon estas mallas con la malla de referencia. Durante este procedimiento, y tal y como se ha demostrado en la presente línea de investigación, la acumulación de errores durante las fases de escaneado y alineación pueden introducir desviaciones que afecten a los resultados finales del estudio. Por este motivo en muestro estudio hemos utilizado una máquina de coordenadas (CMM) para eliminar cualquier error durante el proceso de medición.

Hasta la fecha, es de creencia popular que se pueden utilizar resinas de impresión 3D con aquellas impresoras en las que exista una compatibilidad de longitud de onda, como sucede con la resina e impresoras 3D analizadas en nuestra investigación. Sin embargo, nuestros resultados sugieren que no se puede utilizar cualquier resina con cualquier impresora a pesar de su compatibilidad de longitud de onda, ya que ha quedado demostrado que una misma resina, puede obtener valores de precisión diferentes en función de la tecnología de impresión 3D. Las posibles explicaciones a este fenómeno pueden ser que cada impresora tiene una potencia determinada y esto afecta a la polimerización de la resina 3D, que, además, deberá tener una composición y fotoiniciadores determinada y acorde a la potencia de la impresora. La principal limitación de este estudio fue el análisis de una única resina 3D (Model Gray 2.0).

El cuarto y último estudio de esta Tesis Doctoral, (el segundo estudio en relación a la impresión 3D de modelos) se decidió analizar el impacto dos resinas 3D: Model Gray 2.0 (NextDent) y Aqua Gray 4K (Phrozen) utilizando la impresora Sonic Mini 4K de Phrozen, impresora de tecnología LCD. La hipótesis nula de este estudio también fue rechazada ya que se encontraron diferencias estadísticamente significativas entre los modelos impresos

con dos resinas diferentes y la misma tecnología LCD de impresión 3D. Para ambas resinas, los mejores valores se obtuvieron con un diseño de zócalo ahuecado con grosor de pared de 2mm. La resina Aqua Gray 4K, obtuvo una precisión de 24.10 ± 19.80 µm, mientras que la resina Model Gray 2.0 obtuvo una precisión de 44.80 ± 33.50 µm. En este estudio, los modelos impresos con la resina de NextDent se polimerizaron siguiendo el protocolo de la casa fabricante, mientras que los modelos impresos con Aqua Gray 4K, se post-procesaron con la polimerizadora *Curing Station* de la casa comercial Phrozen. Los resultados de esta investigación demostraron que a pesar de que las resinas sean compatibles en cuanto a longitud de onda se refiere con las impresoras 3D, es necesario que exista un alineamiento entre la resina 3D utilizado y la tecnología de impresión 3D utilizada. La principal limitación de este estudio fue el utilizar sólo dos resinas de impresión 3D testadas con una única impresora LCD.

La correlación que hemos encontrado en los estudios de impresión 3D de la presente Tesis Doctoral entre material, tecnología de impresión 3D y diseño de zócalo de modelos es la primera vez que se establece y demuestra en la literatura científica. Una primera aproximación fue llevada a cabo en una revisión narrativa publicada por Piedra-Cascón y cols. (50) en el que establecieron el concepto de *Manufacturing Trinomial*. A través de este concepto, los autores establecieron una posible interrelación entre el material de impresión 3D, la tecnología de impresión y la propia impresora 3D. Sin embargo, en su revisión, los autores no tuvieron en cuenta el posible impacto del diseño de zócalo como hemos demostrado en las investigaciones de la presente Tesis Doctoral. Si se interpretan los resultados de los dos estudios de impresión 3D de esta Tesis Doctoral, se puede llegar a estimar que no existen diferencias estadísticamente significativas entre la tecnología DLP y LCD de impresión 3D, siempre y cuando se adecué la resina y el diseño de zócalo para cada una de ellas

6
CONCLUSIONES

6 CONCLUSIONES

1. La luz ambiental del gabinete afecta a la precisión del escáner intraoral PrimeScan®, obteniendo los mejores valores de precisión bajo una condición de luz ambiental de 1000 lx, y obteniendo los peores valores de precisión en ausencia completa de luz (0 lx).

2. Existen diferencias entre los diferentes algoritmos de alineación de mallas y entre los diferentes *softwares* CAD 3D. El mejor protocolo de alineación de mallas es *best-fit* (BF) seguido de los algoritmos de alineación por áreas (SBF) y finalmente, los algoritmos de alineación por puntos (LBF).

3. Existe una interrelación positiva entre el material de impresión 3D, la tecnología de fabricación aditiva y el diseño de zócalos de modelos, no existiendo diferencias estadísticamente significativas entre impresoras LCD y DLP

4. La tecnología de impresión 3D DLP obtuvo los mejores valores de precisión con un diseño de zócalo en panal de abejas de grosor de pared de 1mm, mientras que la tecnología LCD obtuvo los mejores valores de precisión con un diseño de zócalo ahuecado con grosor de pared de 2mm.

7
REFERENCIAS BIBLIOGRÁFICAS

7 REFERENCIAS

(1) Goldstein RE. Esthetics in Dentistry. Vol 1: Principles, Communication, Treatment Methods, ed 2. Ontario: BC Decker; 1998. p. 3-51.

(2) Chiche GJ, Pinault A. Esthetics of Anterior Fixed Prosthodontics. Chicago: Quintessence; 1996. p. 33-50.

(3) Fradeani M. Esthetic Rehabilitation in Fixed Prosthodontics. Vol 1: Esthetic Analysis: A Systematic Approach to Prosthetic Treatment. Chicago: Quintessence; 2004. p. 22-30.

(4) Rufenacht CR. Fundamentals of Esthetics. Chicago: Quintessence; 1990. p. 205-241.

(5) Spear FM, Kokich VG. A multidisciplinary approach to Esthetic Dentistry. Dent Clin North Am 2007; 51:487-505. doi: 10.1016/j.cden.2006.12.007

(6) Otto T, De Nisco S. Computer-manufactured direct ceramic restorations: a prospective, clinical 10-year study of Cerec CAD-CAM inlays and onlays. Schweiz Monatsschr Zahnmed 2003; 113:156-69. doi: 10.5167/uzh-12825

(7) Luthardt RG, Kuhmstedt P, Walter MH. A new method for the computer- aided evaluation of three-dimensional changes in gypsum materials. Dent Mater 2003; 19:19-24. doi: 10.1016/s0109-5641(02)00013-1

(8) Miyazaki T, Hotta Y. CAD/CAM systems available for the fabrication of crown and bridge restorations. Aust Dent J 2011; 56:97-106. doi: 10.1111/j.1834-7819.2010.01300.x

(9) Singh V. Rapid prototyping, materials for RP and applications of RP. Int J Eng Res Sci 2013; 4:473-48016.

(10) Fahad M, Dickens P, Gilbert M. Novel polymeric support materials for jetting based additive manufacturing processes. Rapid Prototyp J 2013; 19:230-239. doi: 10.1108/13552541311323245

(11) Witkowski S. CAD-/CAM in dental technology. Quintessence Dent Technol 2005; 28:169-184.

(12) Santoro M, Galkin S, Teredesai M, Nicolay OF, Cangialosi TJ. Comparison of measurements made on digital and plaster models. Am J Orthod Dentofacial Orthop 2003; 124:101-5. doi: 10.1016/s0889-5406(03)00152-5

(13) Beuer F, Schweiger J, Edelhoff D. Digital dentistry: an overview of recent developments for CAD/CAM generated restorations. Br Dent J 2008; 204:505-11. doi: 10.1038/sj.bdj.2008.350

(14) Boldt F, Weinzierl C, Hertrich K, Hirschfelder U. Comparison of the spatial landmark scatter of various 3D digitalization methods. J Orofac Orthop 2009; 70:247-63. doi: 10.1007/s00056-009-0902-2

(15) Rosati R, De Menezes M, Rossetti A, Sforza C, Ferrario VF. Digital dental cast placement in 3-dimensional, full-face reconstruction: a technical evaluation. Am J Orthod Dentofacial Orthop 2010; 138:84-8. doi: 10.1016/j.ajodo.2009.10.035

(16) Piedra-Cascón W, Meyer MJ, Methani MM, Revilla-León M. Accuracy of a dual-structured light facial scanner and interexaminer reliability. J Prosthet Dent 2020; 124(5): 567-574. doi: 10.1016/j.prosdent.2019.10.010

(17) Rangel FA, Maal TJ, Bergé SJ, Van Vllijmen OJC, Plooji JM, Schutyser F, Kuijpers-Jagtman AM. Integration of digital dental casts in 3-dimensional facial photographs. Am J Orthod Dentofacial Orthop 2008; 134(6): 820-6. doi: 10.1016/j.ajodo.2007.11.026

(18) Coachman C, Calamita MA, Coachman FG, Coachman RG, Sesma N. Facially generated and cephalometric guided 3D digital design for complete mouth implant rehabilitation: A clinical report. J Prosthet Dent 2017; 117(5): 577-586. doi: 10.1016/j.prosdent.2016.09.005

(19) Hassan, B., M. Greven, and D. Wismeijer. Integrating 3D facial scanning in a digital workflow to CAD/CAM design and fabricate complete dentures for immediate total mouth rehabilitation. J Adv Prosthodont 2017; 9(5): 381-386. doi: 10.4047/jap.2017.9.5.381

(20) Hassan B, González BG, Tahmaseb A, Greven M, Wismeijer D. A digital approach integrating facial scanning in a CAD-CAM workflow for complete-mouth implant-supported rehabilitation of patients with edentulism: A pilot clinical study. J Prosthet Dent 2017; 117(4): 486-492. doi: 10.1016/j.prosdent.2016.07.033

(21) Lee SJ, Gallucci GO. Digital vs. conventional implant impressions: efficiency outcomes. Clin Oral Implants Res 2013; 24:111-5. doi: 10.1111/j.1600-0501.2012.02430.x

(22) Reich S, Kern T, Ritter L. Options in virtual 3D, optical-impression-based planning of dental implants. Int J Comput Dent 2014; 17:101-13.

(23) Jeong ID, Lee JJ, Jeon JH, Kim JH, Kim HY, Kim WC. Accuracy of complete- arch model using an intraoral video scanner: an in vitro study. J Prosthet Dent 2016; 115:755-9. doi: 10.1016/j.prosdent.2015.11.007

(24) Arakida T, Kanazawa M, Iwaki M, Suzuki T, Minakuchi S. Evaluating the influence of ambient light on scanning trueness, precision, and time of intra oral scanner, J Prosthodont. Res 2018; 62:324-329. doi: 10.1016/j.jpor.2017.12.005

(25) Revilla-León M, Jiang P, Sadeghpour M, Piedra-Cascón W, Zandinejad A, Özcan M,

Krishnamurthy VR. Intraoral digital scans-part 1: influence of ambient scanning light conditions on the accuracy (trueness and precision) of different intraoral scanners, J Prosthet Dent 2020; 124:372-378. doi: 0.1016/j.prosdent.2019.06.003

(26) Revilla-León M, Jiang P, Sadeghpour M, Piedra-Cascón W, Zandinejad A, Özcan M, Krishnamurthy VR. Intraoral digital scans: part 2-influence of ambient scanning light conditions on the mesh quality of different intraoral scanners, J Prosthet. Dent 2020; 124:575-580. doi: 10.1016/j.prosdent.2019.06.004

(27) Revilla-León M, Subramanian SG, Özcan M, Krishnamurthy VR. Clinical study of the influence of ambient light scanning conditions on the accuracy (trueness and precision) of an intraoral scanner. J Prosthodont 2020; 29:107-113. doi: 10.1111/jopr.13135

(28) Revilla-León M, Subramanian SG, Att W, Krisnamurthy VR. Analysis of different illuminance of the room lighting condition on the accuracy (trueness and precision) of an intraoral scanner. J Prosthodont 2021; 30:157-162. doi: 10.1111/jopr.13276

(29) Wesemann C, Kienbaum H, Thun M, Spies BC, Beuer F, Bumann A. Does ambient light affect the accuracy and scanning time of intraoral scans? J Prosthet Dent. 2021; 125(6): 924-931. doi: 10.1016/j.prosdent.2020.03.021

(30) Jivanescu A, Faur AB, Rotar RN. Can dental office lighting intensity conditions influence the accuracy of intraoral scanning. Scanning 2021; 27:9980590. doi: 10.1155/2021/9980590

(31) Koseoglu M, Kahramanoglu E, Akin HK. Evaluating the effect of ambient and scanning lights on the trueness of the intraoral scanner. J Prosthodont. 2021; 30:811-816. doi: 10.1111/jopr.13341

(32) Ochoa-López G, Cascos R, Antonaya-Martín JL, Revilla-León M, Gómez-Polo M. Influence of ambient light conditions on the accuracy and scanning time of seven

intraoral scanners in complete-arch implant scans. J Dent 2022; 121:104138. doi: 10.1016/j.jdent.2022.104138

(33) Arunyanak SP, Harris BT, Grant GT, Morton D, Lin WS. Digital approach to planning computer-guided surgery an immediate provisionalization in a partially edentulous patient. J Prosthet Dent 2016; 116:8-14. doi: 10.1016/j.prosdent.2015.11.023

(34) Mangano C, Luongo F, Migliario M, Mortellaro C, Mangano FG. Combining intraoral scans, cone beam computed tomography and face scans: The virtual patient. J Craniofac Surg 2018; 29:2241-6. doi: 10.1097/SCS.0000000000004485

(35) Gibbs CH, Messerman T, Reswick JB, Derda HJ. Functional movements of the mandible. J Prosthet Dent 1971: 26(6): 604-20. doi: 10.1016/0022-3913(71)90085-0

(36) He S, Kau CH, Liao L, Kinderknecht K, Ow A, Saleh TA. The use of a dynamic real-time jaw tracking device and cone beam computed tomography simulation. Ann Maxillofac Surg 2016; 6(1): 113-9. doi: 10.4103/2231-0746.186142

(37) Röhrle O, Waddell JN, Foster KD, Saini H, Pullan AJ. Using a motion-capture system to record dynamic articulation for application in CAD/CAM software. J Prosthodont 2009; 18(8): 703-10. doi: 10.1111/j.1532-849X.2009.00510.x

(38) Park JH, Lee GH, Moon DN, Kim JC, Park M, Lee KM. A digital approach to the evaluation of mandibular position by using a virtual articulator. J Prosthet Dent 2020; 125(6): 849-853. doi: 10.1016/j.prosdent.2020.04.002

(39) Solaberrieta E, Barrenetxea L, Minguez R, Iturrate M, De-Prado I. Registration of mandibular movement for dental diagnosis, planning and treatment. Int J Interact Des Manuf 2018; 12:1027-1038. doi: 10.1007/s12008-017-0438-4

(40) Sójka A, Huber J, Kaczmarek E, Hedzelek W. Evaluation of Mandibular Movement Functions Using Instrumental Ultrasound System. J Prosthodont 2017; 26(2): 123-128.

doi: 10.1111/jopr.12389

(41) Revilla-León M, Agustín-Panadero R, Zeitler JM, Barmak AB, Yilmaz B, Kois JC, Pérez-Barquero JA. Differences in maxillomandibular relationship recorded at centric relation when using a conventional method, four intraoral scanners, and a jaw tracking system: A clinical study. J Prosthet Dent 2024; 132(5): 964-972. doi: 10.1016/j.prosdent.2022.12.007

(42) Piedra-Cascón W, Fountain J, Att W, Revilla-León M. 2D and 3D patient's representation of simulated restorative esthetic outcomes using different computer-aided design software programs. J Esthet Restor Dent 2021; 33(1): 143-151. doi: 10.1111/jerd.12703

(43) Piedra-Cascón W, De-Gopegui JR, Revilla-León M. Facially generated and additively manufactured baseplate and occlusion rim for treatment planning a complete-arch rehabilitation: A dental technique. J Prosthet Dent 2019; 121(5): 741-745. doi: 10.1016/j.prosdent.2018.07.009

(44) Revilla-León M. Pérez-Barquero JA, Barmak BA, Agustín-Panadero R, Fernández-Estevan L, Att W. Facial scanning accuracy depending on the alignment algorithm and digitized surface area location: an in vitro study. J Dent 2021; 110:103680. doi: 10.1016/j.jdent.2021.103680

(45) Revilla-León M, Zandinejad A, Nair MK, Barmak AB, Feilzer AJ, Özcan M. Accuracy of a patient 3-dimensional virtual representation obtained from the superimposition of facial and intraoral scans guided by extraoral and intraoral scanbody systems. J Prosthet Dent 2022; 984-993. doi: 10.1016/j.prosdent.2021.02.023

(46) Son K, Lee WS, Lee KB. Effect of different software programs on the accuracy of dental scanner using three-dimensional analysis. Int J Environ Res Public Health 2021; 18:8449. doi: 10.3390/ijerph18168449

(47) Garikano X, Amezua X, Iturrate M, Solaberrieta E. Evaluation of repeatability of different alignment methods to obtain digital interocclusal records: an in vitro study. J Prosthet Dent 2024; 131:709-717. doi: 10.1016/j.prosdent.2022.07.014

(48) Pérez-Giugovaz MG, Park, SH, Revilla-León M. Three-dimensional virtual representation by superimposing facial and intraoral digital scans with an additively manufactured intraoral scan body. J Prosthet Dent 2021; 126:459- 463. doi: 10.1016/j.prosdent.2020.07.012

(49) Besl PJ, McKay ND. A method for registration of 3-D shapes. IEEE Trans Pattern Anal Mach Intell 1992; 14:239-256.

(50) Piedra-Cascón W, Vinayak KR, Att W, Revilla-León M. 3D printing parameters, supporting structures, slicing, and post-processing procedures of vat-polymerization additive manufacturing technologies: A narrative review. J Dent 2021; 109:10363. doi: 10.1016/j.jdent.2021.103630

(51) Duret F, Duret E, Thermoz C. Apparatus for taking odontological or medical impressions. 1983. US Patent US46611288.

(52) Duret F, Termoz C. Method and apparatus for making a prosthesis, especially a dental prosthesis. 1984. US Patent US4663720.

(53) Brandestini M, Moermann WH. Method and apparatus for the three dimensional registration and display of prepared teeth. US Patent 1989:US4837732.

(54) Zimmermann M, Mehl A, Mörmann WH, Reich S. Intraoral scanning systems.a current overview. Int J Comput Dent 2015; 18:101-129.

(55) Logozzo S, Zanetti EM, Franceschini G, Kilpelä A, Mäkynen A. Recent advances in dental optics - Part I: 3D intraoral scanners for restorative dentistry. Opt Laser Eng

2014; 54:203-221. doi: 10.1016/j.optlaseng.2013.07.017

(56) Richert R, Goujat A, Venet L, Viguie G, Viennot S, Robinson P, Farges JC, Fages M, Ducret M. Intraoral scanner technologies: A review to make a successful impression. J Healthc Eng 2017; 2017:8427595. doi: 10.1155/2017/8427595

(57) Minsky M. Microscopy apparatus. 1961. US Patent 3013467. Available at: https://patents.google.com/patent/US3013467A/en

(58) International Organization for Standardization. ISO 12836: 2012 Dentistry - Digitizing devices for CAD/CAM systems for indirect dental restorations. Test methods for assessing accuracy.

(59) International Organization for Standardization. ISO 5725-1. Accuracy (trueness and precision) of measuring methods and results. Part-I: General principles and definitions. Berlin: International Organization for Standardization; 1994. Available at: https://www.iso.org/standard/11833.html

(60) Ender A, Mehl A. Influence of scanning strategies on the accuracy of digital intraoral scanning systems. Int J Comput Dent 2013; 16:11-21.

(61) Ender A, Zimmermann M, Attin T, Mehl A. In vivo precision of conventional and digital methods for obtaining quadrant dental impressions. Clin Oral Investig 2016; 20:1495- 1504. doi: 10.1007/s00784-015-1641-y

(62) Müller P, Ender A, Joda T, Katsoulis J Impact of digital intraoral scan strategies on the impression accuracy using the TRIOS pod scanner. Quintessence Int 2016; 47:343- 349. doi: 10.3290/j.qi.a35524

(63) Ender A, Mehl A. Accuracy of complete-arch dental impressions: a new method of measuring trueness and precision. J Prosthet Dent 2013; 109:121-128. doi: 10.1016/S0022-3913(13)60028-1

(64) Renne W, Ludlow M, Fryml J, Schurch Z, Mennito A, Kessler R, Lauer A. Evaluation of the accuracy of 7 intraoral scanners: An in vitro analysis based on 3-dimensional comparison. J Prosthet Dent 2017; 118:36-1842. doi: 10.1016/j.prosdent.2016.09.024

(65) Rutkūnas V, Gečiauskaitė A, Jegelevičius D, Vaitiekūnas M. Accuracy of digital implant impressions with intraoral scanners. A systematic review. Eur J Oral Implantol 2017; 0:101-120.

(66) Medina-Sotomayor P, Pascual-Moscardó A, Camps I. Relationship between resolution and accuracy of four intraoral scanners in complete-arch impressions. J Clin Exp Dent 2018; 10:e361-6. doi: 10.4317/jced.54670

(67) Abduo J, Elseyoufi M. Accuracy of intraoral scanners: A systematic review of influencing factors. Eur J Prosthodont Restor Dent 2018; 26:101-121. doi: 10.1922/EJPRD_01752Abduo21

(68) Takeuchi Y, Koizumi H, Furuchi M, Sato Y, Ohkubo C, Matsumura H. Use of digital impression systems with intraoral scanners for fabricating restorations and fixed dental prostheses. J Oral Sci 2018; 60:1-7. doi: 10.2334/josnusd.17-0444

(69) Tomita Y, Uechi J, Konno M, Sasamoto S, Iijima M, Mizoguchi I. Accuracy of digital models generated by conventional impression /plaster-model methods and intraoral scanning. Dent Mater J 2018; 37:628-633. doi: 10.4012/dmj.2017-208

(70) Malik J, Rodriguez J, Weisbloom M, Petridis H. Comparison of accuracy between a conventional and two digital intraoral impression techniques. Int J Prosthodont 2018; 31:107-113. doi: 10.11607/ijp.5643

(71) Nedelcu R, Olsson P, Nyström I, Rydén J, Thor A. Accuracy and precision of 3 intraoral scanners and accuracy of conventional impressions: A novel in vivo analysis method. J Dent 2018; 69:110-118. doi: 10.1016/j.jdent.2017.12.006

(72) Khraishi H, Duane B. Evidence for use of intraoral scanners under clinical conditions for obtaining full-arch digital impressions is insufficient. Evid Based Dent 2017; 18:24- 25. doi: 10.1038/sj.ebd.6401224

(73) Patzelt SB, Emmanouilidi A, Stampf S, Strub JR, Att W. Accuracy of full-arch scans using intraoral scanners. Clin Oral Investig 2014; 18:1687-1694. doi: 10.1007/s00784-013-1132-y

(74) Mennito AS, Evans ZP, Lauer AW, Patel RB, Ludlow ME, Renne WG. Evaluation of the effect scan pattern has on the trueness and precision of six intraoral digital impression systems. J Esthet Restor Dent 2018; 30:113-118. doi: 10.1111/jerd.12371

(75) Shearer BM, Cooke SB, Halenar LB, Reber SL, Plummer JE, Delson E, Tallman. Evaluating causes of error in landmark-based data collection using scanners. PLOS One 2017: 1-37. doi: 10.1371/journal.pone.0187452

(76) Kim J, Park JM, Kim M, Heo SJ, Shin IH, Kim M. Comparison of experience curves between two 3-dimensional intraoral scanners. J Prosthet Dent 2016; 116:221-230. doi: 10.1016/j.prosdent.2015.12.018

(77) Lim JH, Park JM, Kim M, Heo SJ, Myung JY. Comparison of digital intraoral scanner reproducibility and image trueness considering repetitive experience. J Prosthet Dent 2018; 119:225-232. doi: 10.1016/j.prosdent.2017.05.002

(78) Alghazzawi TF, Al-Samadani KH, Lemons J, Liu PR, Essig ME, Bartolucci AA, Janowski GM. Effect of imaging powder and CAD/CAM stone types on the marginal gap of zirconia crowns. J Am Dent Assoc 2015; 146:111-120. doi: 10.1016/j.adaj.2014.10.006

(79) Anh JW, Park JM, Chun YS, Kim M, Kim M. A comparison of the precision of three-dimensional images acquired by two intraoral scanners: effects on tooth irregularities

and scanning direction. Korean J Orthod 2016; 46:3-12. doi: 10.4041/kjod.2016.46.1.3

(80) Park JM. Comparative analysis on reproducibility among 5 intraoral scanners: sectional analysis according to restoration type and preparation outline form. J Adv Prosthodont 2016; 8:354-362. doi: 10.4047/jap.2016.8.5.354

(81) Carbajal Mejía JB, Wakabayashi K, Nakamura T, Yatani H. Influence of abutment tooth geometry on the accuracy of conventional and digital methods of obtaining dental impressions. J Prosthet Dent 2017; 118:392-399. doi: 10.1016/j.prosdent.2016.10.021

(82) Li H, Lyu P, Wang Y, Sun Y. Influence of object translucency on the scanning accuracy of a powder-free intraoral scanner: A laboratory study. J Prosthet Dent 2017; 117:93- 101. doi: 10.1016/j.prosdent.2016.04.008

(83) Güth JF, Runkel C, Beuer F, Stimmelmayr M, Edelhoff D, Keul C. Accuracy of five intraoral scanners compared to indirect digitalization. Clin Oral Investig 2017; 21:1445-1455. doi: 10.1007/s00784-016-1902-4

(84) Gan N, Xiong Y, Jiao T. Accuracy of intraoral digital impressions for whole upper jaws, including full dentitions and palatal soft tissues. PLoS One 2016; 11:e0158800. doi: 10.1371/journal.pone.0158800

(85) Kim MK, Kim JM, Lee YM, Lim YJ, Lee SP. The effect of scanning distance on the accuracy of intra-oral scanners used in dentistry. Clin Anat 2019; 32:430-438. doi: 10.1002/ca.23334

(86) Park JM, Kim RJ, Lee KW. Comparative reproducibility analysis of 6 intraoral scanners used on complex intracoronal preparations. J Prosthet Dent 2020; 123:113-120.

(87) Son K, Lee KB. Effect of tooth types on the accuracy of dental 3D scanners: An in

vitro study. Materials (Basel) 2020; 13:1744.

(88) Nagy Z, Simon B, Mennito A, Evans Z, Renne W, Vág J Comparing the trueness of seven intraoral scanners and a physical impression on dentate human maxilla by a novel method. BMC Oral Health 2020; 20:97.

(89) Winkler J, Gkantidis N. Trueness and precision of intraoral scanners in the maxillary dental arch: an in vivo analysis. Sci Rep 2020; 10:1172.

(90) Roig E, Garza LC, Álvarez-Maldonado N, Maia P, Costa S, Roig M, Espona J In vitro comparison of the accuracy of four intraoral scanners and three conventional impression methods for two neighboring implants. PLoS One 2020; 15:e0228266.

(91) Revilla-León M, Gohil A, Barmak AB, Gómez-Polo M, Pérez-Barquero JA, Att W, Kois JC. Influence of ambient temperature changes on intraoral scanning accuracy. J Prosthet Dent. 2023; 130(5): 755-760.

(92) Agustín-Panadero R, Estada MIC, Pérez-Barquero JA, Zubizarreta-Macho A, Revilla-León M, Gómez-Polo M. Effect of relative humidity on the accuracy, scanning time and number of photograms of dentate complete arch intraoral digital scans. J Prosthet Dent 2025; 133(3): 865-871

(93) Viohl J Dental operating lights and illumination of the dental surgery. Int Dent J 1979; 29:148-63.

(94) European lightening standard EN12464-1. Light and lighting - Lighting of work places - Part 1: Indoor work places; 2011. p. 1-29.

(95) Glossary of digital dental terms, 2nd edition: American College of Prosthodontists and ACP Education Foundation. J Prosthodont. 2021; 30:172-181.

(96) Torabi K, Farjood E, Hamedani S. Rapid prototyping technologies and their

applications in prosthodontics, a review of literature.J Dent Shiraz Univ Med Sci., 2015; 16:1-9.

(97) Strub JR, Rekow ED, Witkowski S. Computer-aided design and fabrication of dental restorations: current systems and future possibilities. J Am Dent Assoc. 2006; 137:1289-1296.

(98) Beuer F, Schweiger J, Edelhoff D. Digital dentistry: an overview of recent developments for CAD/CAM generated restorations. Br Dent J 2008; 204:505-511.

(99) Lebon N, Tapie L, Duret F, et al. Understanding dental CAD/CAM for restorations - dental milling machines from a mechanical engineering viewpoint. Part A: chairside milling machines. Int J Comput Dent. 2016; 19:45-62.

(100) Lebon N, Tapie L, Duret F, et al. Understanding dental CAD/CAM for restorations-dental milling machines from a mechanical engineering viewpoint. Part B: labside milling machines. Int J Comput Dent. 2016; 19:115-134.

(101) International Standardization Organization. ISO/ATSM 52900: 2015 Additive manufacturing - general principles and terminology. https://www.iso.org/standard/69669.html Last Accessed June 2025

(102) International Standardization Organization. ISO 17296-2: 2015 Additive manufacturing - General principles - Part 2: Overview of process categories and feedstock. https://www.iso.org/standard/61626.html?browse=tc Last Accessed June 2025

(103) Revilla-León M, Piedra-Cascón W, Aragoneses R, Sadeghpour M, Barmak BA, Zandinejad A, Raigrodski A. Influence of base design on the manufacturing accuracy of vat-polymerized diagnostic casts: An in vitro study. J Prosthet Dent 2023; 129(1): 166-173. doi: 10.1016/j.prosdent.2021.03.035

(104) Revilla-León M. Meyer MJ, Zandinejad A, Özcan M. Additive manufacturing technologies for processing zirconia in dental applications: A literature review on current status and future perspectives. Int J Comput Dent 2020; 23:27-37. 10.5167/UZH-198906

(105) Methani MM, Revilla-León M, Zandinejad A. The potential of additive manufacturing technologies and their processing parameters for the fabrication of all-ceramic crowns: A review. J Esthet Restor Dent 2020; 32:182-192. doi: 10.1111/jerd.12535

(106) Kodama H. Automatic method for fabricating a three-dimensional plastic model with photo-hardening polymer. Rev Sci Instrum 1981; 52:177. doi: 10.1063/1.1136492

(107) André J C, Mehaute AL, Witte O. Device for producing a model of an industrial part. French Patent 2.567.668. 1986. Available at: https://patents.google.com/patent/FR2567668A1/en

(108) Hull CW. Apparatus for production of three-dimensional objects by stereolithography. US Patent 4575330. 1986. Available at: https://patents.google.com/patent/US4575330A/en

(109) Stereolithography Interface Specification, 3D Systems, Inc. 1988. Valencia, CA.

(110) Hornbeck L. Digital micromirror device 2009. US Patent No. 5061.049. Available at: https://patents.google.com/patent/US5583688A/en

(111) ISO 17296e2. Additive manufacturing general principles part 2: Overview of process categories and feedstock. 2015. Available at: https://www.iso.org/ standard/61626.html?browse=tc.

(112) Holt P.M. Maskless photopolymer exposure process and apparatus 2012. US Patent 8.114.569 B2. Available at: https://patents.google.com/patent/US8114569B2/en

(113) Ambosio L. Biomedical composites. Woodhead Publishing Limited; Oxford Cambridge, New Delhi, 2010, pp. 33-35.

(114) Maneiro-Lojo J, Pérez-Barquero JA, García-Sala BF, Agustín-Panadero R, Yilmaz B, Revilla-León M. Influence of print orientation on the accuracy (trueness and precision) of diagnostic casts manufactured with a daylight polymer printer. J Prosthet Dent 2024; 132(6): 1314-1322. doi: 10.1016/j.prosdent.2023.01.033

(115) Desimone JM, Ermoshkin A, Ermoshkin N, Samulski ET. Continuous liquid interphase printing. Patent WO 2014/126837A2. PCT/US2014/015506. Available at: https://patents.google.com/patent/WO2014126837A2/

(116) Bagheri A, Jin J. Photopolymerization in 3D printing ACS, Appl. Polym. Mater 2019; 1:593-611. doi: 10.1021/acsapm.8b00165

(117) Otsubo Y, Amari, T Watanabe K. Rheological behavior of epoxy acrylate prepolymer during UV curing. J Appl. Polym 1984; 29:4071-4080. doi: 10.1002/app.1984.070291239

(118) Groth C, Kravitz ND, Jones PE. Three-dimensional printing technology. J Clin. Orthod 2014; 48:475-485.

(119) Braian M, Jimbo R, Wennerberg A. Production tolerance of additive manufactured polymeric objects for clinical applications. Dent Mater 2016; 32:853-861. doi: 10.1016/j.dental.2016.03.020

(120) Unkovskiy A, Bui PH, Schille C, Geis-Gerstorfer J, Huettig F, Spintzyk S. Objects build orientation, positioning, and curing influence dimensional accuracy and flexural properties of stereolithographically printed resin. Dent Mater 2018; 34:e324-e333. doi: 10.1016/j.dental.2018.09.011

(121) Alharbi N, Osman R, Wismeijer D. Effect of build direction on the mechanical

properties of 3D printed complete coverage interim dental restorations. J Prosthet Dent 2016; 155:760-767. doi: 10.1016/j.prosdent.2015.12.002

(122) Revilla-León M, Jordan D, Methani MM, Piedra-Cascón W, Özcan M, Zandinejad A. Influence of printing angulation on the surface roughness of additive manufactured clear silicon indices: An in vitro study. J Prosthet Dent 2021; 125(3): 462-468. doi: 10.1016/j.prosdent.2020.02.008

(123) Reymus M, Fabritius R, Kebler A, Hickel R, Edelhoff D, Stawarczyk B. Fracture load of 3D-printed fixed dental prostheses compared with milled and conventionally fabricated ones: the impact of resin material, build orientation, postcuring and artificial aging - an in vitro study. Clin Oral Investig 2020; 24:701-710. doi: 10.1007/s00784-019-02952-7

(124) Ide Y, Nayar S, Logan H, Gallagher B, Wolfaardt J The effect of the angle of acuteness of additive manufactured models and the direction of printing on the dimensional fidelity: clinical implications. Odontology 2017; 105:108-115. doi: 10.1007/s10266-016-0239-4

(125) Wu D, Zhao Z, Zhang Q, Qi HJ, Fang D. Mechanics of shape distortion of DLP 3D printed structures during UV post-curing. Soft Matter 2019; 15:6151-6159. doi: 10.1039/c9sm00725c

(126) Cho HS, Park WS, Choi BW, Leu MC. Determining optimal parameters for stereolithography processes via genetic algorithm. J Manuf 2000; 19:18-27. doi: 10.1016/S0278-6125(00)88887-1

(127) Alharbi N, Osman RB, Wismeijer D. Factors influencing the dimensional accuracy of 3D-printed full-coverage dental restorations using stereolithography technology. Int J Prosthodont 2016; 29:503-510. doi: 10.11607/ijp.4835

(128) Reymus M, Lümkemann N, Stawarczyk B. 3D printed material for temporary

restorations: impact of print layer thickness and post-curing methods on the degree of conversion. Int J Comput Dent 2019; 22:231-237.

(129) Park GS, Kim SK, Heo SJ, Koak JY, Seo DG. Effects of printing parameters on the fit of implant-supported 3D printing resin prosthetics. Materials (Basel) 2019; 12:2533. doi: 10.3390/ma12162533

(130) Allen S, Dutta D. On the computation of part orientation using support structures in layered manufacturing. Austin, TX, Proceedings of the Solid Freeform Fabrication Symposium,1994, pp. 259-269. Available at: http://hdl.handle.net/2152/68653

(131) Zhang ZC, Li PL, Chu FT, Shen G. Influence of the three-dimensional printing technique and printing layer thickness on model accuracy. J Orofac Ortho 2019; 80:194-204. doi: 10.1007/s00056-019-00180-y

(132) Loflin WA,English JD,Borders C, Harris LM, Moon A, Holland JN, Kasper FK. Effect of print layer height on the assessment of 3D-printed models. Am J Orthod Dentofacial Orthop 2019; 156:283-289. doi: 10.1016/j.ajodo.2019.02.013

(133) Arnold C, Monsees D, Hey J, Schweyen R. Surface quality of 3D-printed models as a function of various printing parameters. Materials (Basel) 2019; 19; 12. doi: 10.3390/ma12121970

(134) Chockalingam K, Jawahar N, Chandrasekhar U. Influence of layer thickness on mechanical properties in stereolithography. Rapid Prototyp J 2006; 12:106-113. doi: 10.1108/13552540610652456

(135) Favero CS, English JD, Cozad BE, Wirthlin JO, Short MM Kasper FK. Effect of print layer height and printer type on the accuracy of 3-dimensional printed orthodontic models. Am J Orthod Dentofacial Orthop 2017; 152:557-565. doi: 10.1016/j.ajodo.2017.06.012

(136) Tahayeri A, Morgan M, Fugolin AP, Bompolaki D, Athirasala A, Pfeifer CS, Ferracane JL, Bertassoni LE. 3D printed versus conventionally cured provisional crown and bridge dental materials. Dent Mater 2018; 34:192-200. doi: 10.1016/j.dental.2017.10.003

(137) Mostafavi D, Metahni MM, Piedra-Cascón W, Zandinejad A, Att W, Revilla-León M. Influence of polymerization postprocessing procedures on the accuracy of additvely manufactured dental model material. Int J Prosthodont 2023; 36(4): 479-485. doi: 10.11607/ijp.7349

(138) Revilla-León M, Gohil A, Barmak AB, Zandinejad A, Raigrodski, AJ, Pérez-Barquero AJ. Best-fit algorithm influences on virtual cast alignment discrepancies, J Prosthodont 2023; 32:331-339. doi: 10.1111/jopr.13537

(139) Dede G, Çakmak G, Donmez MB, Küçükekenci AS, Lu WE, Ni AA, Yilmaz B. Effect of analysis software program on measuring deviation in complete arch implant-supported framework scans. J Prosthet Dent 2023; 16:S0022-391. doi: 10.1016/j.prosdent.2023.06.028

(140) The Joint Committee for Guides in Metrology. JCGM 200: 2012. International vocabulary of metrology: basic and general concepts and associated terms (VIM). 3rd Ed. Available at: https://www.bipm.org/utils/common/documents/jcgm/JCGM_200_2012.pdf

(141) Deutsches Institut für Normung. DIN 55350-13: 1987-07. Concepts in quality and statistics: concepts relating to the accuracy of methods of determination and of results of determination. Available at: https://infostore.saiglobal.com/en-us/Standards/DIN-55350-13-1987-07-447439_SAIG_DIN_DIN_1009173/

(142) Ma Y, Guo YQ, Saleh MQ, Yu H. Influence of ambient light conditions on intraoral scanning: A systematic review. J Prosthodont Res 2024; 8; 68(2): 237-245. doi: 10.2186/jpr.JPR_D_23_00098

(143) Rungrojwittayakul O, Kan JY, Shiozaki K, et al. Accuracy of 3D printed models created by two technologies of printers with different designs of model base. J Prosthodont. 2020; 29:124-128. doi: 10.1111/jopr.13107

(144) Etemad-Shahidi Y, Qallandar OB, Evenden J, Alifui-Segbaya F, Ahmed KE. Accuracy of 3-dimensionally printed full-arch dental models: a systematic Review. J Clin Med 2020; 9:3357. doi: 10.3390/jcm9103357

(145) Kim SY, Shin YS, Jung HD, Hwang CJ, Baik HS, Cha JY. Precision and trueness of dental models manufactured with different 3-dimensional printing techniques. Am J Orthod Dentofacial Orthop 2018; 153:144-53. doi: 10.1016/j.ajodo.2017.05.025

(146) Brown GB, Currier GF, Kadioglu O, Kierl JP. Accuracy of 3-dimensional printed dental models reconstructed from digital intraoral impressions. Am J Orthod Dentofacial Orthop 2018; 154:733-9. doi: 10.1016/j.ajodo.2018.06.009

(147) Park ME, Shin SY. Three-dimensional comparative study on the accuracy and reproducibility of dental casts fabricated by 3D printers. J Prosthet Dent 2018; 119:861.e1-7. doi: 10.1016/j.prosdent.2017.08.020

(148) Camardella LT, Vilella ODV, Breuning H. Accuracy of printed dental models made with 2 prototype technologies and different designs of model bases. Am J Orthod Dentofacial Orthop 2017; 151:1178-87. doi: 10.1016/j.ajodo.2017.03.012

(149) Dietrich CA, Ender A, Baumgartner S, Mehl A. A validation study of reconstructed rapid prototyping models produced by two technologies. Angle Orthod 2017; 87:782-7. doi: 10.2319/01091-727.1

(150) Rossini G, Parrini S, Castroflorio T, Deregibus A, Debernardi CL. Diagnostic accuracy and measurement sensitivity of digital models for orthodontic pur- poses: a systematic review. Am J Orthod Dentofacial Orthop 2016; 149:161-70. doi:

10.1016/j.ajodo.2015.06.029

8

ANEXOS

8.1 AUTORIZACIONES DE LAS REVISTAS

Dear Wenceslao Piedra-Cascón,

Thank you for your query.

Please note that, as one of the authors of these articles, you retain the right to reuse it in your thesis/dissertation. You do not require formal permission to do so. You are permitted to post this Elsevier articles online if it is embedded within your thesis.

Please feel free to contact me if you have any queries.

Kind regards,
Kaveri Thakuria
Customer Relationship Specialist
ELSEVIER | HCM - Health Content Management

From: Administrator
Date: Monday, July 28, 2025 03:56 PM GMT

Dear Customer

Thank you for contacting Elsevier's Permissions Helpdesk.

This is an automated acknowledgement to confirm we have received your query. Ticket number 250728-024322 has been opened on your behalf and we aim to respond within two business days.

Regards,

Permissions Helpdesk

From: Wenceslao Piedra-Cascón
Date: Monday, July 28, 2025 03:56 PM GMT

Dear Elsevier Permissions Team,

My name is Dr. Wenceslao Piedra, and I am currently completing my PhD in Digital Dentistry. As part of the requirements for the submission of my doctoral thesis, I would like to request permission to include the full text of the following peer-reviewed articles published under Elsevier journals in which I am the corresponding author:

Piedra W, et al. Accuracy assessment (trueness and precision) of a confocal based intraoral scanner under twelve different ambient lighting conditions. Journal of Dentistry. 2023; 134:104530. DOI: 10.1016/j.jdent.2023.104530

Piedra W, et al. Evaluation of the accuracy (trueness, precision) and processing time of different 3-dimensional CAD software programs and algorithms for virtual cast alignment. Journal of Dentistry. 2025; 155:105619. DOI: 10.1016/j.jdent.2025.105619

Piedra W, et al. Impact of 3D resin and base designs on the accuracy of additively manufactured casts using a stereolithography technology. The Journal of Prosthetic Dentistry. 2025; 14:S0022-3913(25)00282-3. DOI: 10.1016/j.prosden rntmarker_41840

Piedra W, et al. Influence of base designs on the manufacturing accuracy of vat-polymerized diagnostic casts using two different technologies. The Journal of Prosthetic Dentistry. 2024; 132(2):453.e1-e9. DOI: 10.1016/j.prosdent.2024.04.009

These articles are intended to be included in my thesis as individual chapters and will be submitted to my university's institutional repository for academic purposes only, without any commercial use.

I would be grateful if you could confirm whether this use is covered by Elsevier's standard permissions policy for thesis reproduction or if explicit permission is required.

Thank you very much in advance for your attention to this request. I look forward to your response.

Best regards,
Dr. Wenceslao Piedra-Cascón
University of Santiago de Compostela

8.2 BECAS DE INVESTIGACIÓN

SEPES
Sociedad Española de Prótesis Estomatológica y Estética

Estimado Dr. Wenceslao Piedra Cascón,

En nombre de la Junta Directiva de SEPES es un placer comunicarle que su protocolo de investigación *""Precisión, en términos de exactitud y fiabilidad, de una impresora dental en comparación con una impresora Open-Source en función del diseño del zócalo del modelo: Estudio in vitro"*, ha sido premiado con una BECA SEPES DE INVESTIGACIÓN EN PRÓTESIS Y ESTÉTICA 2022.

La dotación del premio es de 6.000 € para gastos de investigación que serán abonados contra factura de gasto informado a SEPES previamente.

El fallo se comunicará oficialmente en la Asamblea General Ordinaria de SEPES que tendrá lugar el jueves 13 de octubre en el próximo congreso de Gran Canaria. En el caso de que usted vaya a asistir al congreso comuníquenoslo para convocarle a la ceremonia de entrega de premios que tendrá lugar el sábado 15 en el congreso y así poder recoger en mano el certificado acreditativo. No siendo así, le enviaremos por correo dicho certificado.

Reiterando nuevamente nuestra felicitación, le enviamos un cordial saludo.

Prof. Guillermo Pradíes Ramiro
Presidente de SEPES

Prof. Rafael Martínez de Fuentes
Coordinador de premios y becas SEPES

WENCESLAO PIEDRA CASCÓN

El flujo de trabajo digital en Odontología comprende tres fases: digitalización, diseño y fabricación. Esta tesis doctoral evaluó de forma sistemática los factores que afectan a cada una de estas faces para estabcler la precisión global del proceso, mediante cuatro estudios experimentales *in vitro*.

En la fase de digitalización se analizó la influencia de la iluminación ambiental sobre la exactitud de los escáneres intraorales, demostrando que el sistema PrimeScan® alcanza sus mejores resultados en torno a 1000 lux. En la fase de diseño se compararon diferentes softwares y algoritmos de alineación de mallas 3D, constatándose que los algoritmos de tipo *best-fit* ofrecen una mayor precisión y eficiencia en comparación a otros métodos de alineación. En la fase de fabricación se estudió el impacto del "*trinomial manufacturing*", confirmando que la precisión depende de la interacción entre estos la tecnología de impresión 3D, la resina y el diseño del objeto a imprimir.

Los resultados de esta investigación ponen de manifiesto el carácter multifactorial del flujo digital aplicado a la odontología y la necesidad de protocolos estandarizados que garanticen resultados clínicos fiables y reproducibles. Esta tesis aporta evidencia científica para la correcta selección de equipos, softwares y materiales, contribuyendo al desarrollo de una Odontología Digital más precisa, segura y eficiente.